Electron Tunneling in Solid-State Electron-Transfer Reactions

KURT V. MIKKELSEN and MARK A. RATNER*

Department of Chemistry and Materials Research Center, Northwestern University, Evanston, Illinois 60201

Received April 16, 1986 (Revised Manuscript Received August 11, 1986)

Contents

Kurt Mikkelsen was born in Århus, Denmark, in 1959 and obtained his cand. Scient. degree in Theoretical Chemistry at the University of Århus. He is presently a postdoctoral fellow at Northwestern University. His research interests include electron transfer in various media, molecular dynamics, effects of solvent structure and dynamics on molecular properties and chemical reactions, electrochemistry, and soccer.

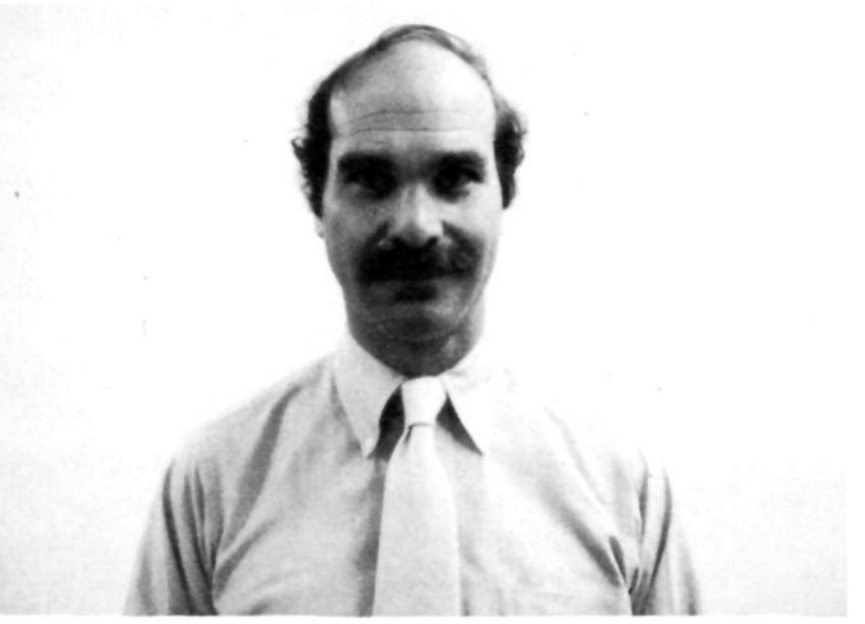

Mark Ratner (A.B. Harvard, 1964; Ph.D. Northwestern, 1969) is in the Department of Chemistry at Northwestern. His interest in electron transfer began during postdoctoral work with Jan Linderberg in Århus, and increased substantially during his time on the faculty at NYU (1970–1975) and since his coming to Northwestern (1976). His other research interests include energy transfer and molecular dynamics, solid electrolytes, molecular metals, molecular electronic devices, nonlinear optics, and Denmark.

I. Introduction

Electron transfer is clearly one of the most fundamental and important chemical processes. The group of processes collectively known as electron transfer is crucially important to chemical reactions on timescales from femtoseconds to seconds, at distance scales from less than 1 Å to more than 20 Å, in physical, chemical, biological, and materials systems and in all of the usual subdivisions of the discipline of chemistry. Electron transfer (ET) is important in reaction mechanisms and photosynthesis, in disease control and energy transduction, in catalysis and copy machines. This ubiquity

0009-2665/87/0787-0113$06.50/0

and importance have led to a vast amount of research on ET processes and reactions, research which crystallized in a series of great advances in the 1950s. The experimental work of Taube and the theoretical efforts of Marcus constitute high points of this period of research, though critical insights were contributed by many others, notably Libby, Hush, Dogonadze, and Levich. In the 3 decades following this early understanding of ET processes, research on ET has extended throughout chemistry and sister disciplines (especially biochemistry, materials science, and physics). While a great deal of understanding has been achieved, there remain substantial questions, both experimental and theoretical, whose answers are not at all clear.

The purpose of this article is to examine a particular class of electron-transfer reactions, which comprises reactions occurring via electron tunneling in the solid phase. This has, historically, not been an area of major focus in the study of electron transfer. Most of the early experimental and theoretical efforts were devoted to reactions occurring in solution, reactions which generally followed second-order chemical kinetics (first-order in both oxidant and reductant), and in which the diffusion together of the reactants to form a precursor complex and the separation of the product of the actual electron transfer were important steps in the overall mechanism. Such reactions have long been a staple of transition-metal chemistry; their systematic experimental investigation and theoretical explication have, indeed, provided most of the current understanding and vocabulary of ET, and the very exciting and young area of single-electron-transfer mechanisms in organic chemistry shows clearly how important and challenging such reactions remain. The study of ET processes in solids is far more incomplete than it is in solution; some of the mechanistic steps are entirely different, as are often the experimental means needed to study the reactions. Our major purposes here are to indicate these differences, to review just what can be adapted from solution-phase ET reactions to help in the description of ET in solids, to review some of the recent progress in solid-state ET, to indicate some novel avenues both theoretical and experimental which are being explored and, finally, to suggest some areas in which huge challenges remain and substantial progress may fairly be expected.

The outline of the article is clearly dictated by its aims. Section II sketches the essential differences between solid-phase and liquid-phase ET processes. Section III is devoted to a survey of the various types of ET in solids, from the viewpoint of macroscopic and mechanistic classification. Section IV sketches the theory of liquid-state ET process, emphasizing mechanistic regularities and the standard theoretical descriptions. Section V presents the crucial concepts for discussing solid-state ET, both for extended systems and for local donor/acceptor pairs. In Section VI the experimental situation of molecular ET in solids is described. Finally, Section VII discusses several outstanding problems in the field, and some possible approaches to their understanding.

In keeping with its importance in chemistry and the extent of research in this area, electron transfer has been reviewed many times.[1-21] Most of these reviews are quite general in their overall presentations, but when specific systems are discussed, they are almost all taken from liquid-state transfers. For example, Cannon's 1980 survey,[9] 351 pages in length, devotes only 17 pages to solid-state ET. Since so many excellent reviews of ET already exist, several of which are very new, it seems appropriate to limit severely our discussion of liquid-state ET and even of much of the standard theory; thus section IV, which is in fact devoted to the area in which most progress has been made, is deliberately very abbreviated in its presentation. Solid-state ET is a far less explored field for the chemist, but with the current renaissance in solid-state chemistry and the development of elegant new experimental methods for the direct study of ET in solids, substantial progress in this field can fairly be anticipated.

From the perspective of solid-state physics, of course, conductivity or photoconductivity in metals or semiconductors is, quite simply, an electron-transfer process. Indeed, there are very marked resemblances between the polaron model used for discussion of conductivity in narrow-band conductors and the standard vibronic models used for nonadiabatic electron transfer. Since electron mobility in metals and semiconductors is a vast field of its own, we restrict ourselves in this discussion to those aspects of the (long range) conductivity process which most usefully illuminate the (short-range) ET processes of primary interest to chemists. Such areas of current interest as inelastic electron tunneling spectroscopy, chemical field-effect transistors, conductive polymers, mixed valency, solid-state electrochemistry, surface-modified electrodes, photoelectrochemistry, and photovoltaics present situations in which solid-state ET processes are indeed of vital importance to chemists. We hope that this review will provide a convenient link between the usual ideas of ET in chemistry and the phenomenon of tunneling in solid-state electron-transfer reactions.

II. Electron-Transfer Reactions in Solids and in Liquid Solution: Significant Differences

Electron-transfer reactions, rather than electron transfer in general, is the theme of our discussion. We can define an ET reaction as having occurred if the localized electronic charge in an atomic, molecular, or solid-state system has been observed to change in time, while the nuclear coordinates have evolved only slightly. Electron transfer can also be understood as describing the equilibrium state which occurs as the end result of ET reactions; thus Pauling[22] uses the term electron transfer to describe the changes in atomic charges when, for example, Al and Fe atoms are brought together to form the ordered intermetallic compound $AlFe_3$. The usual focus, however, is on electron-transfer kinetics, meaning the dynamics of ET reactions, and we will limit our discussion to kinetics.

To describe any problem in chemical kinetics, it is first necessary to define the reactants and the products. In the case of a homogeneous, liquid-phase bimolecular reaction such as

$$Co(OOCCH_2COO)_3^{3-} + Fe(CN)_6^{4-} \rightarrow Co(OOCCH_2COO)_3^{4-} + Fe(CN)_6^{3-} \quad (1)$$

the measurement of reactant and product is quite clear, and by monitoring, say, the appearance of the Fe^{III}

absorption spectrum one can follow the reaction rate. For precisely this same situation in a frozen (solid) solvent, however, the situation becomes more complex. The ET event will occur with significant probability only if the two species are fairly close together (<10 Å or so). But it is often difficult to prepare such a system. In liquids, the oxidant (the Co^{III} species in (1)) and reductant (Fe^{II} species in (1)) may be prepared separately, after which the solutions may be mixed and the species permitted to diffuse toward one another (This is precisely what is done in a stopped-flow measurement). In solids, such mutual interdiffusion occurs with diffusion coefficients $D \lesssim 10^{-12}$ cm^2/sec, so that the reactants, if originally prepared far apart, can essentially never diffuse close enough together to react ("never" meaning on any convenient experimental time scale). This simple fact of experimental observability lies at the root of the most significant differences between solid-state and liquid-state bimolecular ET reactions: to study ET kinetics in solids, the reactants must be prepared in some rather special way; simple mutual interdiffusion of oxidant and reductant is inadequate. (Note that intramolecular ET reactions in liquids occur at closely fixed values of the relative reductant and oxidant geometries; thus, they are far more similar to ET reactions in solids than are bimolecular liquid-state ET processes).

The simple fact of near-zero molecular diffusion constitutes the greatest single difference between bimolecular liquid-state and solid-state ET reactions. There are several other significant differences, both in the experimental study and in the theoretical analysis. These include:

A. In nearly all solutions (a possible exception may be found in highly concentrated alkali metal/ammonia solutions), the electronic states are localized to within (at most) a few angstroms, whereas in such solids as metals, photoconductive materials, and conductive polymers the states are often best described as delocalized. The mechanism of ET will be very different for the delocalized class than for the localized one. In mixed-valency chemistry this issue is described in terms of the Robin/Day classification,[11,23,24] which ranges from Robin/Day I (localized electronic states, as in $Cu_3(NH_3)_4Br_4$) to Robin/Day III (averaged valency, fully delocalized sites as in $K_2Pt(CN)_4Br_{0.3}\cdot 3H_2O$). In metals and semiconductors, the Mott transition[25] from insulators (localized electronic state) to metals (delocalized electronic state) crucially depends on this difference. Thus the class of ET processes in solids is larger than in liquids.

B. While all liquids are thermally and spatially disordered, solids may be ordered (crystal) or disordered (glass). The higher symmetry of ordered solids introduces new conserved quantities, notably the quasimomentum or wave vector. In ordered solids, processes must conserve quasimomentum as well as energy, and this ordinarily means that the electron/vibration interaction in crystalline materials is most easily expressed in terms of phonons, rather than local vibrations. This in turn limits the vibrations which can effectively couple with the electrons, and renders localization more difficult.

C. In solution ET, it is generally fairly straightforward to distinguish an inner sphere of nuclei from an outer sphere around the ET sites: the inner-sphere nuclei are usually taken either as those covalently bonded to the redox sites or as those on which the electronic states among which ET occurs have some amplitude, while the outer-sphere nuclei are those of the solvent. For solids this distinction may become more difficult. For example, in photoexcited germanium, it is hard to distinguish inner-sphere from outer-sphere nuclei.

D. Because in solids diffusion is so slow, intrinsic ET may be observed on very long time scales, up to the order of seconds. This means that very weak interactions may cause observable ET in solids, whereas in solution the actual ET process (as opposed to formation of the precursor complex) is generally very fast. This means that such interactions as bridge-assisted tunneling and superexchange may be far more important in solids than in liquids.

E. Many solids, from an electronic structure viewpoint, are multiply connected; each site is linked indirectly to many ($\sim 10^{23}$) others. This means that many electronic states lie very close to one another, so that any substantial change in the electronic energy (say by an exoergic ET process) must ineluctably involve many electronic states. This can be a considerable complication compared to isolated-pair ET in liquids, where only a few (generally two) electronic states are usually involved.

F. Vibrational relaxation processes are generally more efficient in liquids than in solids. This is clearly manifested in phosphorescence phenomena: phosphorescence in liquids is far less common than in solids, because nonradiative relaxation routes are more efficient in the liquid. This in turn might well have important effects on ET: the actual dynamics, rather than simply the energetics, of the solvent cage might be more important in solids, and very recent work, both experimental[26,27] and theoretical,[28-33] has begun to examine the short-time dynamics of ET. Correlations among vibrations of the solvent should be more important in solids than in liquids; such correlations, again, are of intense current interest.

G. Solids can support shear waves and exhibit well-defined phonon spectra, whereas liquids have no static shear and exhibit damped vibrational modes. In addition to implying stronger memory effects in solids (point F above), this might well mean larger reorganization energies in the outer sphere upon ET, due to a combination of a larger number of coupled vibrations and higher vibrational frequencies. This, in turn, will mean slower ET in the solid than in the liquid, at least in the so-called "normal" regime[16] in which the reorganization energy is greater than the exoergicity. There have been relatively few experiments in which ET rates were studied, as a function of temperature, through the melting point of the solvent. The best-documented cases have shown no sharp change in rate at the melting point (compare Figure 1). These reactions may not be the best test cases, however, since they occurred in large biological systems, in which a "solvent cage" of lipid intervenes between the inner-sphere around the transition metal and the actual solvent, so that the solvent contact with the inner sphere is very attenuated. Indeed, when the protein itself undergoes a phase-transition-like conformational change (at ~250 K, in Figure

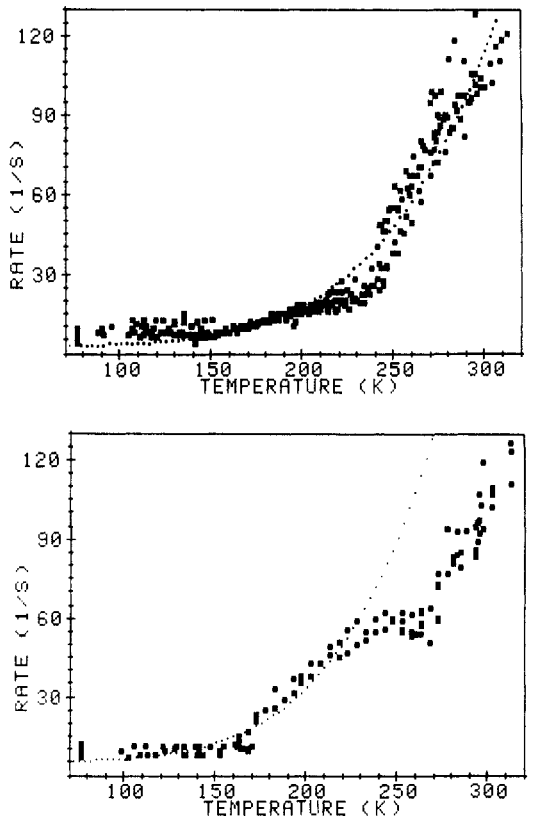

Figure 1. Temperature dependence of the electron-transfer rate for Zn-substituted hemoglobins. The rate refers to transfer from photoexcited ^{3}ZnP to $Fe^{III}P$ (P = porphyrin). The reaction is exoergic by ~0.8 eV. Part A shows the results for the [α(Zn), $\beta(Fe^{III}H_2O)$] hybrid, part B shows the [$\alpha(Fe^{III})$, β(Zn)]. The dotted curve is a fit to the small-polaron-type theoretical model of Jortner [Jortner, J. *J. Chem. Phys.* **1976**, *64*, 4860]. The switch in the data near 250 K in part B is attributed to a change in axial ligation. Reprinted with permission from: Peterson-Kennedy, S. E.; McGourty, J. L.; Kalweit, J. A.; Hoffman, B. M. *J. Am. Chem. Soc.* **1986**, *108*, 1739. Copyright 1986, American Chemical *Society*.

1b) there *is* a sudden change in ET rate.

H. Perhaps most importantly, experimental techniques for the study of ET in liquids and in solids are often very different. In liquids, many ET reactions can be studied by following, either chemically or spectroscopically, the time-dependent formation of products following the mutual interdiffusion of reactants. In solids, each of these three may become difficult: mutual interdiffusion, as discussed above, is too slow to matter. Chemical observation of product formation again normally depends on reactions, which depend on diffusion, so that such standard schemes as examining dissociation products of labile Co^{II} formed by ET, which are often used to follow ET rates in solution, are not useful in solids. Even spectroscopic study may be difficult in such solids as metals, in which the spectroscopic probe does not penetrate, or glasses and other amorphous solids, which may simply scatter all of the light. Thus differing methods for both preparation and detection of ET processes are required to study ET in solids, and we can now turn to some of these.

III. Electron-Transfer Reactions In Solids: Classification and Examples

The usual chemist's notion of electron-transfer reactions as occurring between isolated molecular oxidants and reductants must be considerably amplified when examining ET in solids. To begin, however, we might first cite some isolated molecular ET reactions in solids which are in fact similar to those in liquids.

The most obvious way to circumvent the limitation that diffusion cannot conveniently be used to prepare the "precursor complex" of oxidant (Ox) and reductant (Red) reactants for an ET reactions is to prepare Ox and/or Red by means of an externally supplied pulse. Most commonly, the external pulse is simply a photon, and the photoexcited state is used as Ox and/or as Red. For example, Leland et al.[34] studied the ET from a photoexcited zinc porphyrin linked via a rigid sigma-type covalent bridge to a quinone (species **A**). They suggest a rate constant of $\sim 10^{10}$ s^{-1} at 77 K in frozen methyltetrahydrofuran. This is quite typical of the *molecular* solid-state ET events which have been studied; most of them involve excited-state reactants, and as such are expected to behave quite differently from the ET reactions between ground state Ox and Red which are most commonly studied in liquid solutions. There are two essential reasons for this difference. The first is that after excitation with an optical photon of more than one eV in energy, the wave function of the optically-excited reactant will be extended quite considerably compared to its ground-state shape; this physical extension will cause the rate of ET to increase, and its dependence on distance to change. The second effect of reactant excitation is to change the exoergicity of any putative ET reaction. For example,[35] the very popular reductant $Ru(bpy)_3^{2+}$ (bpy = 2,2′-bipyridyl) when promoted to its first optically excited state at 2.10 eV above the ground state, becomes a very strong oxidant as well as a strong reductant. The very substantial exoergicities associated with this ET relaxation (eq 2), mean that enough energy is available

$$\begin{gathered} Ru^*(bpy)_3^{2+} + e^- \rightarrow Ru^+(bpy)_3 \\ \Delta E^\circ(\text{NHE}) = .84 \text{ V} \\ Ru^*(bpy)_3^{2+} \rightarrow Ru^{3+}(bpy)_3 + e^- \\ \Delta E^\circ(\text{NHE}) = .84 \text{ V} \end{gathered} \tag{2}$$

in general, to populate more than one electronic state of the products. While this complication can also occur for ground-state ET reactions, especially in the highly exoergic or "abnormal" regime, its possible role in photoexcited ET processes is even greater (there is a great deal more energy to be disposed of), and therefore it is even more important that analysis of the kinetics include the possibility of initial, rate-determining formation of photoexcited products, as in eq 3. Indeed,

$$\begin{gathered} Ox^* + Red \xrightarrow{k_1} Ox^{*-} + Red^+ \xrightarrow{k_2} Ox^- + Red^+ \\ k_1 \ll k_2 \end{gathered} \tag{3}$$

just such excited-state formation has been suggested[36,37] as one possible explanation for the observed nearly-constant rate of ET with increasing exoergicity for many highly exoergic electron-transfer quenching experiments.

An alternative technique for preparing the reactants for study of a solid-state ET reaction involves adding an electron, rather than a photon. This method has been developed very extensively by Miller and his colleagues,[37,38] who have studied intermolecular ET in a series of frozen glasses. In their work, a glass containing the parent (neutral) donor and acceptor species

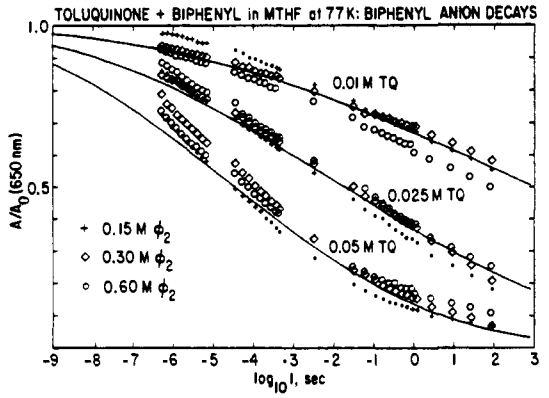

Figure 2. Kinetics of electron tunneling from biphenyl ions to toluquinone at 77 K in methyltetrahydrofuran glass. A and A_0 are the absorbance of biphenyl with or without added toluquinone. The solid lines are simulations as described in section VI.B. The center-to-center-tunneling distances vary from 13 Å at 10^{-6} s to 30 Å at 100 s. Reprinted with permission from: Beitz, J. V.; Miller, J. R. *Radiation Research, Proceedings International Congress, 6th*, 1979; Okada, S., Ed.; Toppan: Japan, 1979; p 301. Copyright 1979, Toppan Publishing Co.

is subjected to short (4–20 ns) pulses of 15 MeV electrons. The electrons become thermalized, eventually forming either molecular anions or stable trapped electrons; via hole transfer, positive ions can also be produced (eq 4). The ET event is then monitored

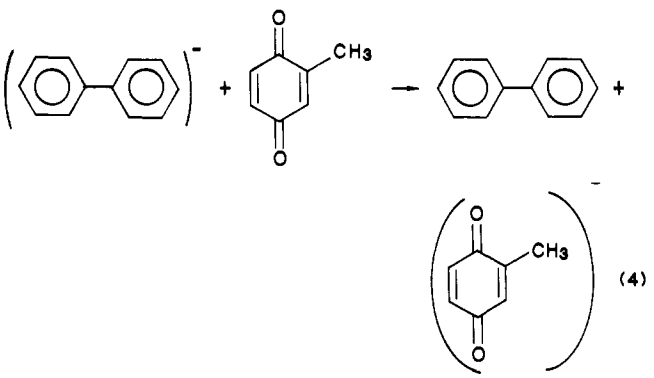

(4)

optically. Figure 2 shows some of their early data[39] for the reaction. The analysis of these data is a bit complicated, involving both statistical considerations concerning the mutual distributions of donor and acceptors and fits to some simple theoretical forms for the ET rate; further discussion is given in section VI.

As these examples have shown, both optically-induced and electron-capture-induced ET in solids can be studied for either intramolecular or intermolecular processes. In solution, considerable simplification results upon studying intramolecular cases.[40] This simplification occurs because the oxidant and reductant are already assembled at a fixed (and, in principle, known from structural work) relative geometry, and because there is no work term required to bring together the (generally charged) Ox and Red species in solution. The elegant work of Taube[11,40] and his students in studying intramolecular ET in bridged bimetallic species was designed to take advantage of these special features. In solid-state ET, the advantage of no work terms arising from diffusion is irrelevant since, once again, no meaningful mutual diffusion of Ox and Red can occur. The advantage of known geometry remains, however, and much of the most exciting recent work on molecular solid-state ET has involved intramolecular transfer.

These two classes of reaction (photoinduced excited-state ET, either intermolecular or intramolecular, and ET in radicals prepared by electron or hole capture, again either intramolecular or intermolecular) comprise nearly all of the well-characterized experimental studies of solid-state ET reactions between (or within) molecules. There are many other processes in solids in which ET processes occurs, and which might, therefore, be considered as cases of ET tunneling reactions in the solid state. These processes include

A. Extended systems
1. Conductivity in good metals
2. Conductivity in narrow-band metals
3. Conductivity and photoconductivity in reduced-dimensionality species including conductive stacks and polymers
4. Semiconductor and doped semiconductor systems, conduction and photoconduction
5. Impurity conduction, in species such as mixed crystals or photoexcited rare-gas matrices
6. Amorphous conductors, including conductive glasses.

B. Intermediate sizes
1. Quantum multiwell structures
2. Inelastic electron tunneling spectroscopy and scanning tunneling microscopy
3. Surface-modified electrodes, interfacial ET, microstructures, photoconverters. Ordered molecular/metal/semiconductor arrays.

C. Localized species
1. Donor/acceptor pairs in solid hosts
2. Intramolecular ET species in solid hosts
3. Mixed-valency situations
4. Biological units and subunits

Clearly this classification scheme is arbitrary, inexact, and selective. It does serve, however, to show how extensive and variegated solid-state ET phenomena are. In section V we present some detailed theoretical ideas on the description of these processes. But at a very qualitative level, we can suggest the general scheme which all of these processes will follow. In each case, the ET reaction involves motion of an electronic charge density from one site in the solid to another. Since the solid is composed of discrete subunits (atomic, ionic, or molecular), we can discuss the transfer as involving electronic motion among these subunits. At zero temperature and ignoring both zero-point vibrational motion and electron-electron repulsions, the electronic behavior can be characterized in terms of electron localization upon and motion among a set of orbitals located on the sites (crystalline or amorphous) of the solid. We can denote this set of localized basis orbitals by u_i, $i = 1,2,3...$. In metallic lithium, for example, the u_i would be the Li 2s atomic orbitals, one on each Li. For chain material

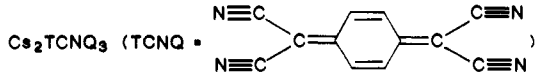

they would be the LUMO molecular orbitals of the TCNQ species, which are pi orbitals of b_{1u} symmetry[41] and are empty in the isolated molecule but become partly full in the solid due to partial charge transfer (.67 electrons per TCNQ) from Cs. For the mixed crystals such as anthracene in durene, there can be both hole and electron transfers, and so the set u_i must include

HOMO and LUMO orbitals on both host (durene) and guest (anthracene) species. For isolated pairs such as those in reactions (2–4), the orbitals u_i must again include whichever molecular orbitals (HOMO and/or LUMO) might change population as the electrons move.

Formally, we can write the hamiltonian operator for these electrons moving among clamped nuclei in the simple form

$$H_{el} = \sum_i \sum_j \sum_{\mu=\alpha,\beta} t_{ij} a_{i\mu}^{+} a_{j\mu} \quad (5)$$

Here the operator $a_{i\mu}^{+}$ creates an electron in the basis orbital u_i with spin μ, while the operator $a_{j\mu}$ destroys an electron of spin μ in basis orbital u_j. Thus the operator product $a_{i\mu}^{+} a_{j\mu}$ moves an electron of spin μ from orbital u_j to orbital u_i, while the product $a_{i\mu}^{+} a_{i\mu}$ simply counts the number of μ-spin electrons in orbital u_i. The quantity t_{ij} in (5) is usually called an electron-tunneling matrix element. Formally, it is just $\langle u_i | H_{el} | u_j \rangle$, and it measures a transition amplitude for electron tunneling from u_i to u_j. In (5) the sums on i,j run over all of the orbitals in the set (u_i, i = 1,2,...). Once we have chosen a set of u_i and defined the values for all of the t_{ij}, we have defined a model hamiltonian[42] for description of electronic motions. Several concrete examples of (5) might be mentioned. For isolated π-electron molecules, if u_i are restricted to one 2pπ function on each carbon and t_{ij} is restricted to a value β if i and j are neighbors, α if $i = j$ and zero otherwise, the Hückel model[43] is recovered. If this is extended such that $\{u_i\}$ includes valence orbitals on all atoms, we have the extended Hückel picture. For metals, restriction of the u_i to a single orbital on each atom and limitation of the sums such that i,j must be nearest neighbors defines the tight-binding model, which is just the Hückel model for metals. For isolated pairs such as those of eq 4, the u_i will include HOMO and LUMO on Red and on Ox.

The electronic motion implied by (5) is simple: the electrons can remain on their original sites, or can tunnel from site j to site i. If first-order perturbation theory is used, the transfer probability from u_i to u_j is proportional to t_{ij}^2, so that the electrons can move between sites i and j only if those sites are directly "bonded"; that is, only if t_{ij} is not zero. Expansion to second order in t_{ij} yields a form (if $t_{ij} = 0$)

$$w_{i \to j} \sim \sum_{k \neq j} \frac{t_{ik}^2 t_{kj}^2}{(t_{kk} - t_{jj})^2} \quad (6)$$

corresponding to motion from orbital u_j to u_i via orbital u_k; this path involves an energy penalty (denominator) corresponding to the energy to promote the electron from site j with site energy t_{jj} to site k with energy t_{kk}. Thus the motion of the electrons from any initial site to any final site may be followed; the structure of the t_{ij} elements provides a roadmap to just which routes the electrons can travel.

No real solid can be measured at $T = 0$, and in any material zero-point vibrations in fact are present. Thus any proper description of ET phenomena must involve vibrations. As electrons or holes move in the material (solid or liquid, molecules or atoms or crystals or glasses), the vibrational displacement and vibrational frequencies will change. For example, in the self-exchange reaction between $Ru(NH_3)_6^{3+}$ and $Ru(NH_3)_6^{2+}$, the Ru–N distance will change[44] by .02 Å, since the Ru^{3+} will hold its lone-pair NH_3 ligand more tightly than will the Ru^{2+}. For this particular case the frequency change is quite small[44] (roughly 40 cm^{-1} out of 474 cm^{-1} for the a_{1g} fully symmetric stretch mode), because of very slight covalency in the Ru–N bond. The rearrangement of the ligands about the redox centers requires an energy; this is normally called the reorganization energy,[1-21] and is denoted as λ in Figure 3. For such a self-exchange reaction in any phase there is no change in energy, entropy, or free energy attendant on the ET process. Then the activation energy $\Delta E^{\ddagger}$ or E_A is simply equal to one-fourth of the reorganization energy λ. The equivalence $E_A^{th} = {}^1/_4 E_A^{op}$, where E_a^{th} and E_A^{op} are thermal and optical ET activation energies was first noted by Hush.[45] In fact, electronic splitting somewhat increases the numerical factor 4. More generally, the reorganization free energy λ is related to the actual physical parameters of rearrangement, namely the changes in displacement and in frequency when an electron transfer occurs. If the frequencies do not change, then there is no entropy (disorder) change, and λ becomes equal both to the free energy and to the energy of reorganization.[46]

Activation barriers such as that in Figure 3 are found for nearly all ET reactions. They arise from several sources, and will, generally, depend nonmonotonically on the reaction exoergicity $\Delta E°$ and on the reorganization free energy λ. To a very good approximation, the activation energy is given by[1-21]

$$E_A = \Delta E^{\ddagger} = (\lambda + \Delta E°)^2/4\lambda \quad (7)$$

if there are no frequency changes, and by

$$\Delta G^{\ddagger} = (\lambda + \Delta G°)^2/4\lambda \quad (8)$$

if there are changes in frequency. ET reactions for which $\lambda > |\Delta G°|$ are often referred to as lying in the normal regime, while those for which $\lambda < |\Delta G°|$ are said to lie in the abnormal regime, and those for which $\Delta G° > 0$ do not occur. This nomenclature is illustrated in Figure 3, and will be discussed at length in sections IV and V.

The nomenclature in the last paragraph is drawn from standard ET theory for molecules in solution. For our more general discussion here, the important point is that the presence of nuclear motions (vibrations, librations, internal and hindered rotations) means that the rate of ET processes is fixed not only by the electronic motion in the clamped-nuclei situation described in eq 5, but also by the interactions between electronic and nuclear motion and by the motions of the nuclei themselves. In liquid-state molecular ET reactions, these interactions are manifested in the appearance of an activation energy for ET and in the reorganization process and energy. In extended systems such as those listed under A above, ET is manifested as electronic conductivity. For conduction in a good metal such as copper, the electron/vibration interactions are responsible for the resistivity, which arises partly from scattering of the conduction electrons by the vibrations of the Cu nuclei. For a narrow-band metal or semiconductor such as Ni phthalocyanine iodide[47-50] or Ni phthalocyanine, respectively, the conductivity is again limited by scattering of carriers of current (electrons or holes) by motions of molecular or atomic nuclei.[51-53] For good metals, there is very little reorganization required as the electrons move, so that the reorganization

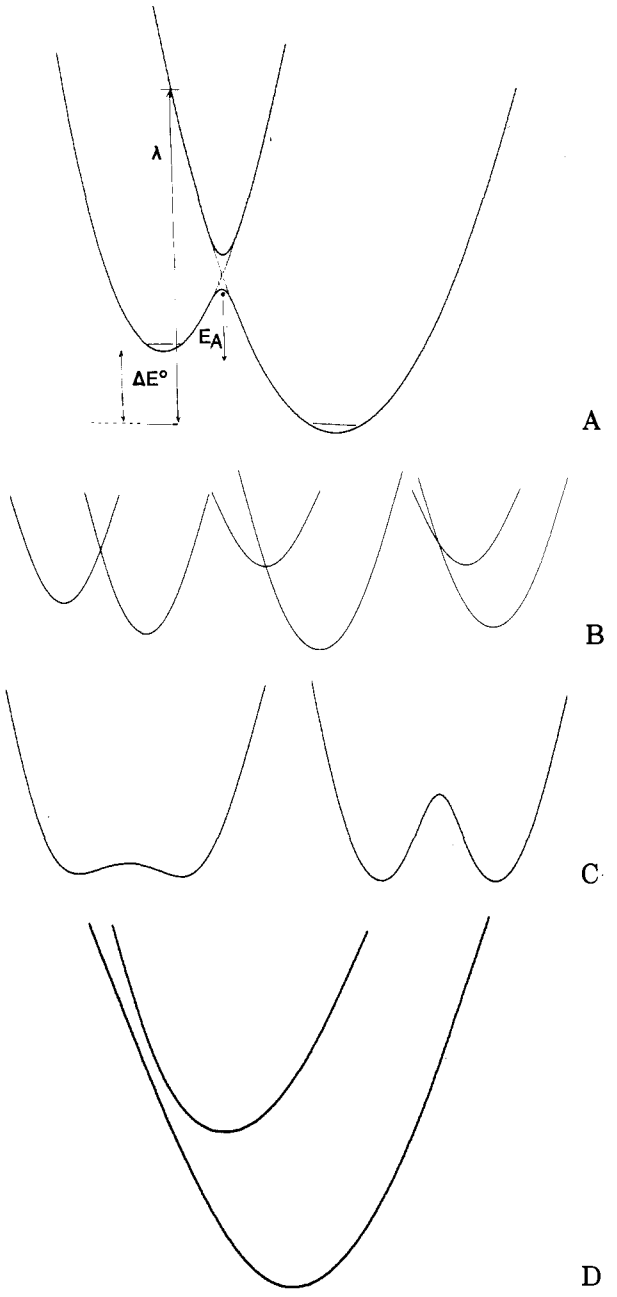

Figure 3. Schematic potential curves for two-site electron transfer. The abscissa is a reaction coordinate, which is, for example, the difference in the displacements of the two diatomics in the molecular crystal model of section V.A. The ordinate is the electronic potential energy. Part A defines the reorganization energy λ, the activation energy E_A, and the exoergicity $\Delta E°$. The solid lines are the adiabatic surfaces; the dotted lines are the diabatic curves. Part B sketches diabatic curves for the normal region ($\lambda > |\Delta E°|$), the barrier-free case ($\lambda = \Delta E_0$), and the abnormal regime ($\lambda < \Delta E_0$), respectively. Part C shows the lower adiabatic surface for self-exchange in a mixed-valency species; the left and right curves represent Robin/Day III (delocalized) and I (localized) behavior. Part D shows the adiabatic curves for transfer in the abnormal regime.

energy is small and the electron/vibrational coupling is weak, the scattering is also weak, and the conductivity is high. For narrow-band metals or semiconductors, the reorganization energy and electron/vibrational coupling are larger, the scattering is stronger and the conductivity is smaller.

From a formal viewpoint, the full dynamics of ET processes requires consideration of a hamiltonian of the form

$$H = H_{el} + H_{nuc} + H_{el\text{-}nuc} \quad (9)$$

where H_{nuc} is the hamiltonian for nuclear motion and $H_{el\text{-}nuc}$ is the interaction between electronic and nuclear motion which is responsible for resistivity in metals, for Jahn–Teller distortions in degenerate-state molecules and for reorganization energies in ET. All of the ET-type processes listed under A-C above may be understood[54-59] on the basis of eq 9, whose structure is suggested theoretically by the Born–Oppenheimer separation of electronic and nuclear motions, and experimentally by our wish to focus on the electron transfer phenomenon which is principally induced by H_{el} of eq 5. While the details of just how to handle H of (9) are quite complex and depend upon the relative magnitudes of the electron delocalization terms (t_{ij} of (5)) and the electron/vibration couplings, still all cases of ET can be discussed by the use of (9).

Often it is convenient to separate the nuclear motions involved in ET events into two sets.[16] The inner sphere of nuclei comprises those which directly neighbor the site at which the orbital u_i is located. For transition-metal complexes, this is usually taken as the inner coordination sphere, and for π-electron systems, it can be taken to include those nuclei in which π-density is found in molecular orbital u_i. More inclusively, we can take the inner sphere as including the nuclei which are covalently or datively bonded to the atoms on which the electron population changes in an ET event. For molecular ET in a solvent, it is usually simply taken to be the molecules themselves. The outer sphere then includes all the rest of the nuclei, which usually simply means the solvent. Then the reorganization free energy λ will be written as

$$\lambda = \lambda_i + \lambda_o \quad (10)$$

where the terms are, respectively, an inner-sphere and an outer-sphere contribution. The inner-sphere, or molecular, vibrations are generally described quantum mechanically (as a set of phonons), while the outer-sphere is treated either quantum mechanically or classically (as a continuous dielectric medium).

Understanding, then, that ET processes generally involve both electronic and nuclear motions, we require one more piece of nomenclature before exemplifying situations such as those listed above under A–C. Consider for a moment a two-site problem, in which ET can occur from orbital u_i to (spatially distinct) orbital u_j. There will exist some reorganization free energy λ for this transfer, which is due to the third term in eq 9, and there will also be a transfer amplitude t_{ij} in eq 5. When t_{ij} becomes large enough, the electronic states are so strongly mixed that further increase in t_{ij} will not change the ET rate, which will be determined essentially solely by nuclear motions described by λ; this situation is referred to as adiabatic electron transfer. Conversely, for small t_{ij}, the electron states on i and j mix so weakly that even for favorable nuclear geometries, for which the Franck–Condon requirements for ET[60] are satisfied, weak mixing may not permit the electron to jump; in this situation increasing t_{ij} will increase the ET rate, and this is called nonadiabatic ET (further discussion is found in section VA).

It is helpful to exemplify the ET-type phenomena listed under (A–C) above, to see how these concepts of adiabatic and nonadiabatic transfer, activated processes,

reorganization and tunneling, vibronic coupling and normal and abnormal regimes can be used to classify and understand them.

[A1,2,3] In good metals the simplest and most common description of the electronic structure is in terms of the nearly free electron model.[61] An alternative picture which is more useful for our purposes (although not usually used for quantitative studies of metals) is called the tight-binding scheme.[43,61] The local atomic functions u_i of eq 5 can be combined into a delocalized set of functions corresponding to the molecular orbitals of the entire metal. When this is done, eq 5 can be rewritten

$$H_{el} = \sum_{\vec{k}} \sum_{\mu} w_{\vec{k}} a_{\vec{k},\mu}^{+} a_{\vec{k},\mu} \qquad (11)$$

where $w_{\vec{k}}$, referred to as the energy of a band state labelled by quasimomentum $\vec{k}$ as well as spin μ, is analogous to a molecular orbital energy. The $a_{\vec{k},\mu}^{+}$ are just linear combinations of the $a_{i\mu}^{+}$ of eq 5, and create an electron in the band eigenstate labeled by $\vec{k}$ and μ (if each unit cell contains more than one basis function, the $a_{\vec{k},\mu}$ obtains more labels, describing the contribution from these different basis functions). The energy spectrum of the band states (or molecular orbitals) of the metal is determined by the set of $w_{\vec{k}}$. In a one-dimensional tight-binding (Hückel-like) model of a good metal, the energy difference between the largest and smallest w_k is called the bandwidth; it is exactly $4t$ for the one-dimensional band, and, generally, is proportional to the nearest-neighbor tunneling integral $t_{i,i+1}$. Good metals such as Cu or Au or Na have large bandwidths, because of very effective overlap of the partly full s orbitals.

The number of $\vec{k}$ states in eq 11 is precisely the same as the number of basis states labeled by i in eq 5 since the number of MO's in an LCAO approximation is the same as the number of AO basis functions. In a metal like Na, where the outermost orbital (3s, corresponding to a HOMO) is only half full, only half of the $\vec{k}$ states (or MO's) will be full. Since the energy levels $w_{\vec{k}}$ form a continuum, an electron can be excited from a full state to an empty state in the metal with only an infinitesimal energy addition. Thus applied electric fields can cause electrons to move, and the metal is a good conductor. If the highest energy orbital is full (as it is in He), then the bands will be full, excitation from the highest-energy full orbital (Fermi level) of the solid will require a finite amount of energy to get to the next band (the 2s band, for He) and the material should be either an insulator (large gap between bands) or a semiconductor (small gap between bands).

The quantum number $\vec{k}$, which corresponds to a quasimomentum, is a good quantum number if the third term of eq 9 is ignored, since (11) is a diagonal expression, just the sum of number operators $a_k^{+}a_k$ times energies w_k. The electron/vibration interaction (last term of (9)) destroys this behavior, and permits the electrons to exchange energy with the nuclear vibrations. This leads to changes in the electronic momentum due to absorption or emission of phonons (the quanta of collective oscillations of the nuclei). For wide-band metals or quasi-free electron metals the conductivity may be estimated rather well using the Drude model,[61] in which the scattering of conduction electrons by phonons leads to a scattering or relaxation time, and this scattering time determines the conductivity. Thus in good metals conductivity is fixed by scattering events due to electron/vibration coupling (and to impurity scattering and electron–electron scattering). The conductivity is proportional to the Drude scattering time, or to the mean free path, and is determined by the behavior of the electrons in the immediate vicinity of the Fermi surface. More efficient electron/phonon coupling decreases scattering time, mean free path, and conductivity,[61] and since the scattering arises from vibrations, and since mean square vibrational amplitude is proportional to temperature (from the equipartition theorem), we expect, for good metals, that conductivity is proportional to T^{-1}. From the viewpoint of the ET concepts we have discussed, conduction in good metals is an example of adiabatic ET, since further increases in bandwidth (equivalently, in t_{ij}) will not further increase conductivity σ, which is fixed by the electrons near the Fermi surface. Moreover, the barrier of Figure 3a for a two-site model will disappear, because the so-called tunneling splitting indicated in Figure 3c is so large (this tunneling splitting is proportional to $2t_{12}$ for the two-site case, and the activation barrier will disappear when $\lambda/4 \sim t_{12}$). Thus the transfer rate is not activated, and indeed the long-distance transfer (conductivity) drops with increasing temperature.

This picture of nearly free electrons in good metals becomes modified in polar conductors or in narrow-band metals or semiconductors. Materials of the latter classes include not only such standard samples as NiO and ferrites, but also many of the molecular metals, or synthetic metals,[47,62] which have been of major importance to chemists in the past two decades; these materials include charge-transfer salts based on π-electron donors and/or acceptors. One of the clearest examples is the linear-chain material[48-50] NiPcI (pc = phthalocyanine), in which nearly planar (phthalocyaninato)Ni macrocycles are stacked like poker chips directly above one another, and I_3^- anions are distributed lengthwise in channels between the stacks. The formal charge dictates that 0.33 electrons per macrocycle have transferred to the I_3^-. Thus the band, which in this case can be thought of as a one-dimensional tight-binding band whose basis[51,52,63] consists of the nondegenerate a_{1u} π-electron HOMO on each Nipc, is 5/6 full. If the band were very wide, as it is in a metal like Al or Ag, this would mean nearly-free electron behavior and high conductivity. For NiPcI, however, the situation is more interesting. The width of the one-dimensional tight-binding band is precisely $4t$, where t is the nearest-neighbor tunneling integral on the Nipc chain (eq 5). The bandwidth may be obtained[63] from optical reflectance spectroscopy of the chain material, or from the splitting ($2t$) of the levels of a dimeric subunit of the conductive chain, which in turn may be deduced either from photoemission spectra[64] or from electronic structure calculation. For the Nipc case, all three indicate[63] a bandwidth $4t$ of roughly 0.70 eV. This is a very narrow band and as such will be even more sensitive to electron/vibration interaction.

The vibrations on the Nipc chain are of two kinds. The intramolecular vibrations, which cause changes in shape or size of the individual Nipc units, may be distinguished from the intermolecular vibrations, in which

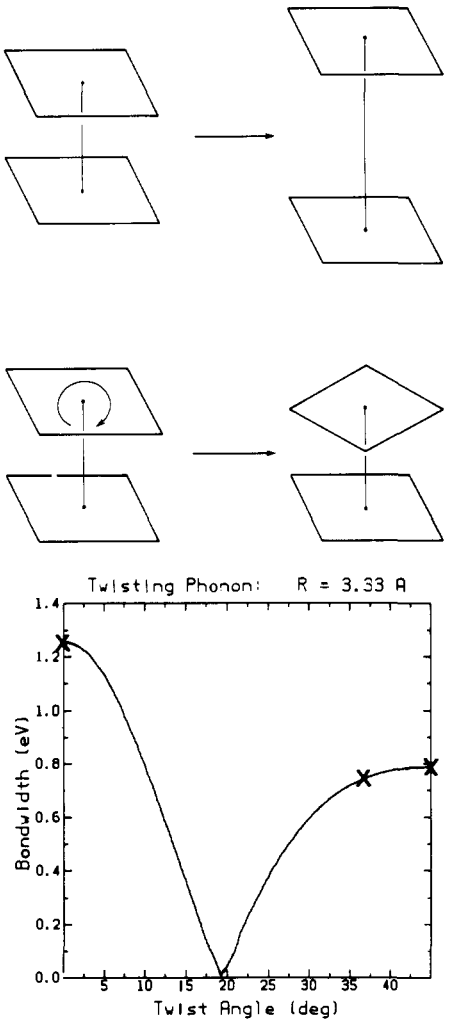

Figure 4. Molecular motions which produce resistivity in phthalocyanine-based molecular metals. Part A shows the phonon (translation) and librational (twisting) motions of two coplanar phthalocyanine macrocycles (each represented as a square). Part B shows the calculated variation in bandwidth (or, equivalently, of the tunneling integral t) as the relative orientational angle is varied. Reprinted with permission from: Pietro, W. J.; Ellis, D. E.; Marks, T. J.; Ratner, M. A. *Mol. Cryst. Liq. Cryst.* **1984**, *105*, 273. Pietro, W. J.; Marks, T. J.; Ratner, M. A. *J. Am. Chem. Soc.* **1985**, *107*, 5387. Hale, P. D.; Ratner, M. A. *J. Chem. Phys.* **1985**, *83*, 5277.

the individual macrocycles move rigidly with respect to one another. The intramolecular vibrations will modulate principally the diagonal terms t_{ii} of eq 5, corresponding to changes of the basis function energies upon molecular distortion, whereas the intermolecular vibrations will modulate chiefly the tunneling transfer integral $t_{i,i+1}$ of eq 5, corresponding to variation of the tunneling integral as the local basis functions change their distance and/or orientation with respect to one another. For the particular case of NiPcI, the observed temperature dependence of the conductivity ($\sigma \sim T^{-1.4}$) indicates that while the material is metallic, in agreement with its optical properties, the expected $\sigma \sim T^{-1}$ behavior of good metals is not seen. It has been shown[51-53] from first-principles electronic-structure calculations of $t_{i,i+1}$ and its derivatives that the observed T-dependence of σ arises from roughly equal admixtures of longitudinal phonons (accordion mode) and twisting of the macrocycles around the stacking (z) axis; compare Figures 4 and 5. In the particular case of this macrocycle, the partly full HOMO a_{1u} π-electron level

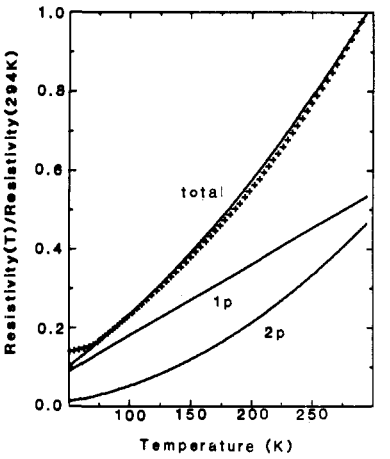

Figure 5. Resistivity of NipcI (pc = phthalocyanine). The crosses are experimental data (Ogawa, M.; Hoffman, B. M., manuscript in preparation), and the solid lines are first-principles theoretical calculations. The total resistivity is the sum of the librational part (curved lower line, $\rho \sim T^2$) and a vibrational part ($\rho \sim T$), which arise from the motions of Figure 4. Reprinted with permission from: Hale, P. D.; Ratner, M. A. *J. Chem. Phys.* **1985**, *83*, 5277. Copyright 1985, American Institute of Physics.

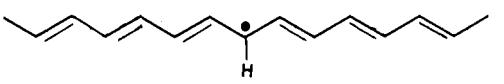

Figure 6. A schematic representation of the orientational "soliton" defect in polyacetylene. The defect is uncharged, but carries spin of one-half, and is centered at the dot.

contains mainly 2pπ carbon atomic orbitals, and is therefore not very much changed by intramolecular motions.

This behavior (metallic-like resistivity dominated by coupling to intermolecular motions in rigid subunits) is not common to all molecular metals. More usual, particularly in conductive polymers[47-62] such as poly(acetylene) or poly(pyrrole) or poly(thiophene) or poly(*p*-phenylene), is a situation in which there is an extremely strong coupling of the charge carrier (electron or hole) to an *intramolecular* (or, since a polymer is really one giant molecule, an intrasite) vibrational motion. This corresponds exactly to the reorganization process responsible for the occurrence of the free energy term denoted by λ_i for ordinary molecular ET reactions. In some conductive polymers such as $(-CH-CH-)_x$, the coupling, or reorganization energy or Stokes shift, is so large that the charge carrier motion may become linked to a local polarization, leading to defect motion. Probably the best known example of such a defect is the localized radical which occurs in poly(acetylene) when the alternating (formal) single and double bonds are out of phase by one bond (Figure 6). Such a localized defect was first discussed for π systems by Pople and Walmsley;[65] Su, Schrieffer, and Heeger[66] proposed that such defects, which they called solitons, were important charge carriers in poly(acetylene). The soliton in Figure 6 is neutral (seven valence electrons around triply-bonded carbon), but it can become a charged soliton upon capture or loss of one electron. The soliton literature is now enormous,[62,67] and although we are aware of no direct proof that they are the charge-carrying species in $(CH)_x$ and related species, such as assumption seems reasonable.

The soliton defect arises from trapping of an electronic species (hole, spin, or electron pair for positive,

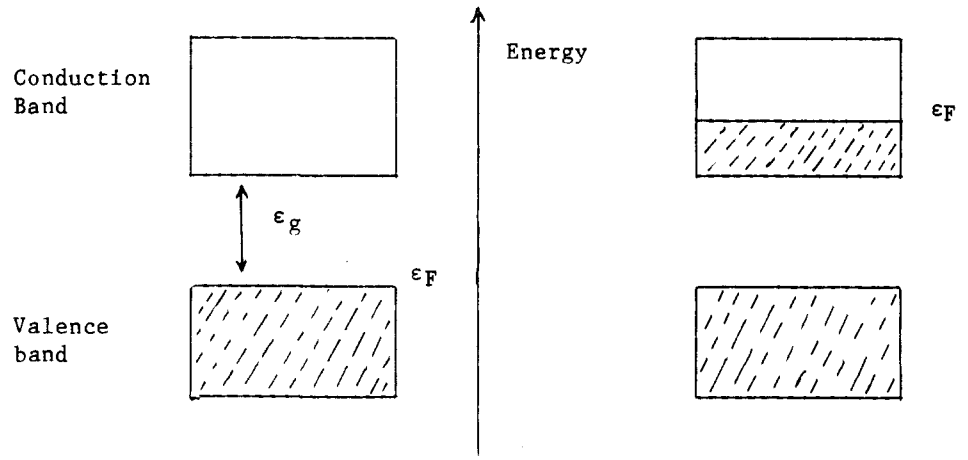

Figure 7. Schematic band structure diagram for a semiconductor (left) and a metal (right). The shading represents filled energy levels for the electrons. In the semiconductor (to the left), the gap ϵ_g must be overcome to promote electrons into the conduction band while in the metal (right), the conduction band is partly filled and the electrons can be accelerated by an applied field. The Fermi (highest filled) energy level is denoted ϵ_F.

neutral, and negative solitons, respectively) by a localized distortion of the nuclear framework. In defect-free all-trans or all-cis poly(acetylene), all C–C bonds exist in a bond-alternating structure, with alternating C–C links corresponding to formally single and double C–C bonds, respectively, and with the bond lengths differing[68] by 0.08 Å. Around a soliton, the C–C bond distances are rearranged. Both experimental and calculational evidence[67,68] suggests that the bond lengths near a soliton are substantially different from their values in the parent poly(acetylene) materials. This behavior is very similar to the rearrangement processes accompanying ET in molecular systems and sketched in Figure 3 for a two-site model. The geometry about the oxidant and/or the reductant changes when the ET process occurs. The transfer cannot occur unless this rearrangement does, and the electron is closely coupled to the nuclear displacements. Note that in both ET and soliton motion the primary coupling is to a number of intrasite vibrations, which in the $(-CH-)_x$ case are simply C–C bond length changes.

Neutral solitons correspond to uncharged localized spin radicals; as such, they have spin and can be seen in epr studies. A second sort of defect can also occur due to trapping and localization of a carrier arising from interaction with lattice distortions (bond stretches). If the trapped species is a charged particle, in particular if it is a localized electron, the composite entity of the electron and the associated lattice distortion is referred to as a polaron,[69] and if the localization is such that the electron is essentially restricted to one lattice site, it is called a small polaron.[70,71] The small polaron model is important both in electronic hopping conduction (A.5,6 below) and in molecular ET (sections IV and V).

The cases of NipcI and $(-CH-)_x$ represent situations in which electronic motion, or conductivity, takes place in a one-dimensional chain. In both cases, the electronic motion occurs in a band whose width is determined by the local overlap of site basis functions (carbon $p\pi$ orbitals in poly(acetylene), macrocycle π HOMO's in NipcI). In both cases, however, the bandwidth is not the determining factor in conductivity; in this sense, they correspond to adiabatic ET between molecules. The intermolecular orientational motions which modulate the tunneling integral and dominate the resistivity in the phthalocyanine conductor[53] should certainly be important in some ET reactions, though only in the case of nonadiabatic transfer, since for fully adiabatic ET the size of the tunneling integral is unimportant for determining the rate, once that integral is big enough to be sure that the ET reaction lies in the adiabatic regime. The intrasite electron/vibrational coupling which is responsible for the formation of solitons (and other defects such as polarons and bipolarons) in $(-CH-)_x$ and related polymers is exactly analogous to the rearrangement process in molecular ET reactions, and there are close analogies between soliton motion and adiabatic ET reactions.

[A.4] To a very rough approximation, the difference between a conductor and a photoconductor is simply the location of the Fermi surface (highest filled level). Figure 7 illustrates this point in a highly schematic way. The gap in energy (no states available) occurs right at the Fermi energy ϵ_F for a semiconductor. To move an electron in a metal, only an infinitesimal energy from an applied field is needed, since empty levels lie right above full ones. For a semiconductor, however, the gap must be overcome. Electrons can be placed into the conduction band, where they can contribute to a current. This can occur by thermal excitation if the gap is not too much greater than k_BT, or, for larger gaps, by semiconductor doping, or photoexcitation with a frequency equal to or greater than $\epsilon_{gap}/\hbar$. This photoexcited carrier will then move in the conduction band very much as any other carrier would; photoconductivity, like ordinary electronic conductivity, is limited by scattering from defects, other electrons or holes, spins, and nuclear vibration.

In fact, the situation is slightly more complicated than in metals, since the formation by photoexcitation of an electron in the conduction band will leave behind a hole in the valence band, and the residual Coulomb attraction between hole and electron can result in formation of an exciton,[25] which is a mutually-trapped electron/hole pair, or even in recombination to form the original electronic occupation plus heat in the lattice vibrations. The general area of photoconductivity has been enormously active for the past 2 decades, due partly to interest in solar photoconversion, in photocopying machines, and in photosynthesis, and largely

to intrinsic scientific interest. In both photosynthesis and photoconversion devices, it is necessary to separate the electron and hole formed through photoconversion, and this can be done in several ways,[72] including band bending at surfaces (used widely in photoconversion devices),[73] charge separation at interfaces (used in micellar and microemulsion systems),[74] dissemination of one carrier into a continuum (metallic or semiconductor electrode conversion),[75] or rapid ET or hole transfer away from the original exciton geometry (one of the tricks in photosynthesis).[76]

Once the charges are effectively separated, they move by a generalized sort of ET, which, in crystalline systems such as Ge with wide conduction bands, can be quite similar to charge carrier motion in good metals. Many photoconductors of current interest, however, including hydrogenated amorphous silicon (a-SiH) and the chemically fascinating polysilanes (systems isoelectronic to alkanes which nevertheless show very large electron delocalization effects and good photoconductivity)[77] are highly disordered, and the charge carrier motion is usually controlled by defect scattering or trapping of the carrier. In all these materials, once again, the width of the relevant conduction band is large, and from an ET point of view the transfer can be classed as adiabatic, with the rate determined by factors (scatter from vibrations or defects or impurities) other than the size of the tunneling matrix elements t_{ij} of (5).

[A.5,6] Electrical conductivity in metals is largely a coherent process—the current-carrying states are of nearly free-electron or of wide-band type, and are delocalized throughout the crystal; resistivity occurs because these coherent states are scattered by impurities or vibrations. Now if the bands become very narrow, the total energy gain upon delocalization of the band electrons decreases. If electrons can lower their total energy by means of an elastic relaxation or polarization of the solid, then there will be a competition between the electronic band energy, which favors delocalization, and the polarization energy which favors localization of the electron. Under these conditions, raising the temperature (therefore the vibrational amplitude) can result in electron localization. This is the essence of the small polaron picture of conduction.[70,71,78] While there are few materials for which small polaron transport behavior has been conclusively demonstrated, the model is important conceptually for solids. More significantly for our purposes, the standard vibronic models for understanding both ET reactions and mixed valency behavior (as well as radiationless transitions, luminescence, Jahn–Teller distortions, and a host of other vibronic phenomena) is based on a small-polaron-type model. Therefore it seems appropriate to summarize the essential ideas of small polaron theory and to discuss its relationship to electronic conductivity; we can then refer to these when discussing ET formalisms in sections IV–VII.

The simplest picture to describe small polarons is the molecular crystal model of Holstein.[71] In this model, each site in the crystal consists of an electronic state and a local vibration (chemically, we might think of a chain of H_2^+ species). Then the total energy will include the vibrational energies, the electronic energies, and the polarization energies which result when an electron is trapped on a site. This last term arises from the change in geometry (bond lengths) and/or frequency when an extra (carrier) electron is placed onto the molecule at any given site. This model will be discussed at some length in sections IV and V in connection with the two-site ET problem. The important point here is that when the temperature is quite low, the vibrational amplitudes are small, the vibration/electron coupling is still fairly weak, and the electronic motion is still dominated by the (small) tunneling terms between near-neighbor sites. In this regime, the motion remains coherent (like a metal), and the electron/vibration scattering provides a metal-like conductivity ($\sigma \sim T^{-1}$). As temperature increases, the coupling term comes to dominate the band term. Then the localized states of the electron are (variationally) better zero-order states than are the delocalized band states. They are still not eigenstates, however, and the residual tunneling interactions result in motion of the electrons from site to site. This motion can either involve jumps between equivalent configurations, which involve no gain or loss of vibrational energy, or jumps between inequivalent local geometries, which then involve gain or loss of vibrational quanta. These latter processes are dominant at high temperatures (about roughly half the Debye temperature), and describe incoherent hopping motion of the electrons (or polarons). Now the conduction is activated ($\sigma \sim e^{-E_A/k_BT}$), and increases with temperature.

The small polaron model thus predicts that $\sigma(T)$, the conductivity, starts out band-like at low temperatures ($\sigma \sim T^{-1}$), and then reaches a minimum at some temperature related to the electron/vibrational coupling strength before becoming activated (hopping) at high temperatures. As we have already discussed, good metals and some conductive chains follow the $T \rightarrow 0$ behavior of a polaron. We now discuss very briefly hopping electronic conductors, in which the high-T limit of the small polaron behavior is seen.

Hopping conduction is of great interest in conducting glasses, amorphous conductors, certain mixed crystals, mixed-valency solids, and some conductive charge-transport polymers.[78] All of these systems contain localized, rather than bandlike, electronic states. Chemically, perhaps the most interesting of them are the redox conductive polymers or ion-exchange polymers filled with electroactive counterions.[79] Just as small-polaron semiconductors differ from metals, these hopping electroactive polymers differ from the conjugated, bandlike conductive chains and polymers such as those based on poly(*p*-phenylene) or NipcI.[62] A typical[79] hopping type electroactive polymer is poly[M-(bpy)$_2$(vpy)$_2$(ClO$_4$)$_x$], with M = Os or Ru, bpy and vpy being 2,2′-bipyridyl and 4-vinylpyridine, respectively, and x = 0–3. The self-exchange, hopping reaction between, say, neighboring Os(bpy)$_2$(vpy)$_2$(ClO$_4$)$_x$ sites can be written

$$Os^{III} + Os^{II} \xrightarrow{k} Os^{II} + Os^{III} \qquad (12)$$

where k is a self-exchange rate constant. By a series of such hops, charges can be transported down the redox polymer chain. The local behavior in this case (high temperature) is of hopping type and is activated. It can occur only under conditions of "mixed valency"—that is, it is necessary that some of the Os be present in one

valence state (here Os^{II}) and others in another valency (Os^{III}). The mixed-valent state may be prepared either by chemical oxidation or, more commonly, by application of an external potential (electrochemically).

The use of these redox polymers has been beautifully developed by several groups.[79-82] These groups have constructed such microstructures as array electrodes and ion-gate electrodes based on the use of these redox polymers in connection with microfabrication techniques. These microstructures are of great promise in energy conversion, sensing, display, and energy storage devices, as well as in electrochemical synthesis applications, and several reviews of this work have appeared.[79-82] Indeed, the effective combination of surface fabrication and lithography techniques with chemical derivatization and chemical synthesis is well on its way toward defining a new area of macromolecular electronics.[79] Insofar as ET is concerned, nearly all of these systems are based on site-to-site hopping behavior of localized electrons. Exceptions occur when delocalized polymers such as polypyrrole are used, and these in fact provide higher conduction[80] (at convenient temperatures) than do the mixed-valent hopping redox conductors, largely because the activation barriers for hopping in such systems as Ru^{III}/Ru^{II} or Os^{I}/Os^{0} are quite large with delocalized chelate ligands such as bpy.

A final example of hopping electron transfer involves randomly oriented and spaced ET centers in a solid matrix. For example, Domingue and Fayer[83] have recently investigated ET quenching of excited pentacene by ground-state duroquinone in a sucrose octaacetate glass. The pentacene is excited using a doubled Nd:YAG laser line at 532 nm, and the pentacene decay is then monitored. They observe that for short times (<100 ps), the transfer is dependent on the relative orientation angle of the donor and acceptor, but that at longer times this angular dependence can be averaged. The essential behavior found in their work (and in many other experimental and theoretical studies of this sort of electron or exciton hopping among localized sites in rigid systems) can be understood from a theoretical model developed by Inokuti and Hirayama,[84] based on earlier work by Dexter[85] and by Förster.[86] It really depends on use of simple rate theory: if the relative probability at time t after excitation for observing an excited donor is $\rho(t)$, then one can write

$$\rho(t) = \exp\left\{-t \times \left[\frac{1}{\tau_0} + \sum k(R_k)\right]\right\} \qquad (13)$$

where $k(R_k)$ is the rate constant for transfer to an acceptor at position R_k and τ_0 is the lifetime, including radiative and nonradiative parts, in the absence of quenching. The constant $k(R_k)$ is in turn taken to be the simple golden rule form

$$k(R_k) = \frac{2\pi}{\hbar} T_{DA}^{2} \times \{FC\} \qquad (14)$$

which is appropriate for nonadiabatic electron transfer (compare sections IV and V). Here T_{DA} is the electron tunneling or transfer matrix element (the one called $t_{i,i+1}$, for the periodic chain in eq 5) and {FC} is a vibrational overlap factor, which is a density-weighted Franck–Condon sum (again, compare sections IV and V). Thus these quenching processes are solid-state ET reactions which proceed via electron tunneling.

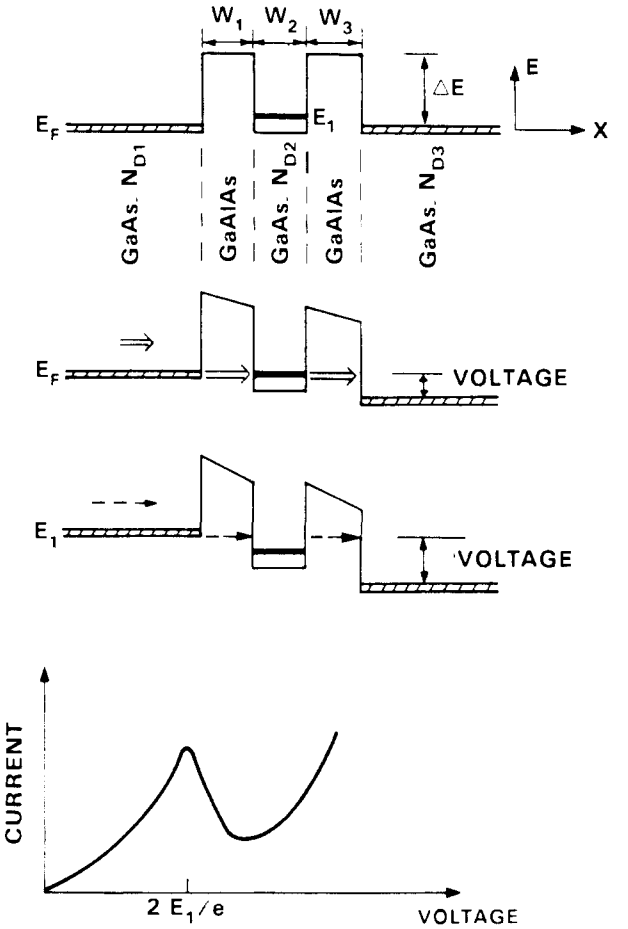

Figure 8. A quantum well heterostructure showing electron energy as a function of position. The thickness $W_1 = W_2 = W_3 = 50$ Å, and the level E_1 occurs above the bottom of the bulk conduction band because of electron confinement in the x-direction. The second figure shows resonant tunneling, corresponding to the peak in the I/V curve, while the third sketch shows inefficient nonresonant tunneling. The bottom figure shows the observed I/V characteristic at 25 K. Note "abnormal regime" behavior, with rate decreasing with increasing exoergicity, to right of peak. Reprinted with permission from: Sollner, T. C. L. G.; Tannewald, P. E.; Peck, D. D.; Goodhue, W. D. *Appl. Phys. Lett.* **1984**, *45*, 1319. Sollner, T. C. L. G.; Goodhue, W. D.; Tannewald, P. E.; Parker, C. D.; Peck, D. D. *Appl. Phys. Lett.* **1983**, *43*, 580.

Except for the relatively fast timescale, these studies are similar to many other measurements in which quenching via ET reactions is studied. These experiments are properly discussed in terms of transfer between isolated molecular pairs, and as such provide a link between motion in the solids (metals, semiconductors, polymers, glasses) which we have been considering thus far and the molecular ET reactions which are the traditional domain of liquid-state ET reactions. They are discussed in detail in section VI.A.

[B.1] Some of the most novel and direct observations on ET in solids have been reported in so-called quantum well heterostructures.[87-89a] These are materials consisting of thin layers (~100 Å or so thick) of two or more different components (generally metals or semiconductors). The layers are generally prepared either by molecular-beam epitaxy (MBE) or by chemical vapor deposition (CVD). Figure 8 schematically sketches such a quantum-well heterostructure. They can be prepared with nearly any number of layers of material, and the dimensions and compositions of the individual layers may be very carefully controlled. By the placement of

electrodes on the top and bottom layers, currents passing through the heterostructure may be measured and voltages applied across the heterostructure may be controlled. In addition, by variation of the atomic composition of the layers themselves, energy levels and electron densities may be varied over a wide range.

Sollner et al. measured[88] the current/voltage characteristic across a single quantum-well structure (Figure 8) consisting of three layers, each 50 Å thick. The outermost two layers consisted of $Ga_{0.75}Al_{0.25}As$, and the inner well of GaAs. The substrate on which the structure was deposited was GaAs, and a 5000-Å-thick layer of GaAs was deposited on top of the three-layer heterostructure. In field-free conditions, the energy levels in the central GaAs layer are higher than those in the thicker layers because of kinetic-energy confinement (the energy levels of a particle-in-a-box rise as the box becomes smaller). When a voltage was applied across the structure, resonant tunneling was observed when the voltage drop across the GaAlAs barrier was equal to the energy E_1 (Figure 8) arising from the localization within the 50-Å middle region of GaAs. From an applications viewpoint, such tunneling phenomena may be useful as millimeter and submillimeter amplifiers or oscillators. From our perspective, the I/V characteristic of Figure 8 is important for several reasons. Firstly, the rapid falloff with voltage away from the resonance case ($V_{res} = 2E_1/e$ in Figure 8) constitutes one of the best marked cases of the "inverted" or "abnormal regime" in nonadiabatic ET:[1-18] as V is increased above V_{res}, the rate of tunneling (and therefore the current) decreases quite markedly. This decrease of rate with exoergicity above a threshold region is the signature of abnormal-regime ET; such energy-gap behavior is also seen in vibrational energy transfer and in nonradiative decay, but for ET itself we are aware of no well-defined molecular example which shows so clear an abnormal region as in Figure 8.

One reason for this behavior is suggested by Figure 9, which shows a measurement on resonance ET in a different quantum multiwell structure.[89] In this case, there were 70 separate layers, each 139 Å thick, and consisting alternately of $Ga_{0.47}In_{0.53}As$ and $Al_{0.48}In_{0.52}As$. As the voltage drop across the heterostructure is increased, a first resonance is observed at an applied potential equal to the energy difference between the ground state and the first excited state of the quantum wells, roughly at $V \cong 2.1$ eV in Figure 9. With further increase in applied field, the current first drops (abnormal regime), but then increases again toward a second resonance near 6.5 volts, where the potential energy drop across the superlattice period is equal to the excitation energy to the second excited state of the well. The discrete multipeak structure progressively washes out with increasing temperature, as side features due to absorption or emission of phonons broaden each individual resonance peak. More importantly, if the resonances occur fairly close together, then the falloff from one peak will not be seen before the current rise starts for the next resonance. Then the overall shape of the I/V characteristic might rise at low voltage until the first resonance is reached, and then remain sensibly constant with rising voltage as one resonance dies out but another is reached. With microstructures such as these layered ones, such behavior cannot persist indefinitely, because the energy gaps between the resonance states rise sharply with quantum number (proportional to n^2 for particle-in-a-box levels). For molecules, however, we might expect a large number of open-shell electronic states of the Red^+–Ox^- system to appear fairly close to the first excited state.[36,37] More such states will become energetically available as the exoergicity increases (compare eq 3), and therefore one might expect, again, a sensibly flat rate for ET as exoergicity is increased beyond threshold. Such behavior has been seen in many studies of ET quenching of optically excited donor/acceptor pairs,[90] and the formation of excited product states has been put forward as one possible explanation of this unexpected behavior.[38,39]

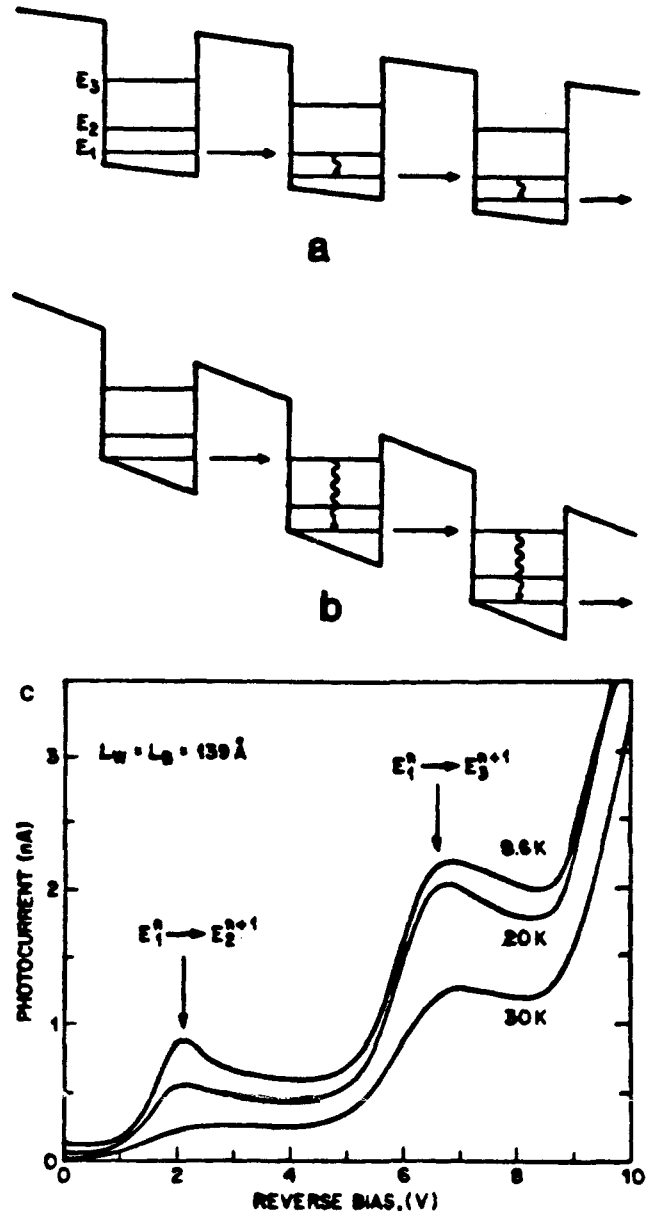

Figure 9. Sequential resonant tunneling through a 1-μm-thick superlattice at low temperature. The superlattice consists of alternating $Al_{0.48}In_{0.52}As$ and $Ga_{0.47}In_{0.53}As$ layers, each 139 Å thick. Parts A and B show resonant tunneling through the first and second excited states, while part C shows the observed current, with peaks due to both of these resonant events. Reprinted with permission from: Capasso, F.; Mohammed, K.; Cho, A. Y. *I.E.D. Meeting of IEEE*; IEEE: Washington, DC, 1985; p 764. Copyright 1985, IEEE.

The second aspect of these measurements which is of real importance for understanding ET is the time

scale of transfer. Sollner et al. showed[88] that the I/V characteristic at 2.5×10^{12} Hz is sensibly the same as that at dc, and used this observation to argue that the "charge transport mechanism is at least as fast as the angular period of 2.5 Thz; i.e., $\tau = 6 \times 10^{-14}$ s." An alternative estimate arising from the time/energy uncertainty relationship also yields $\tau \simeq 10^{-13}$ s. The barrier height is deduced from optical measurements as[88] roughly 0.23 eV in the GaAlAs barrier, whose width was 50 Å. Molecular ET reactions in frozen solution over far shorter distances (e.g., 24 Å or so) exhibit characteristic times, or inverse rate constants, *12 orders of magnitude slower* (cf. section VI). These huge rate differences might arise in several ways, but clearly the most obvious ones, assuming that ET in the microstructures is a fairly similar physical phenomenon to molecular ET, are either from the isoenergetic (resonance tunneling) feature or by very large differences either in the tunneling matrix elements or in the density-of-state-weighted Franck–Condon factor, that represents the vibronic part of the rate. Given the quite low barrier height of the microstructures (0.23 eV in ref 88), and the prediction from simple tunneling theory (section V.B) that the transfer tunneling matrix element should scale like $\exp\{-\sqrt{E_B}\,R\}$, where E_B is barrier height in volts and R is separation in Å, the far lower barrier height in the microstructures suggests that it is the substantially enhanced electronic tunneling probability which provides some of the rate enhancement, and that the other major acceleration is due to the resonant nature of the transfer. If so, it would be of great interest, from an ET viewpoint, to examine systematically the I/V characteristic, and thus the transfer time, as the barrier height E_B and the tunneling distance (layer thickness), as well as the applied voltage (exoergicity) are varied.

[B.2] Tunneling in solid-state ET processes serves as the basis for two quite new and powerful analytical spectroscopies. The first of these, inelastic electron tunneling spectroscopy or IETS, is a sensitive technique for measuring vibrational spectra and, in a less precise manner, molecular orientation.[91] The technique was first discussed by Jaklevic and Lambe[92] 20 years ago. It is based on the observations that a tunneling current can pass between two metallic electrodes when a potential is applied, that such a current will also flow if molecular species are introduced into the area between the electrodes, and that electron/vibrational interaction can cause the electrons in this tunneling current to lose energy to the vibrations. Thus the tunneling current will have both elastic and inelastic (energy loss) components. If the second derivative of the tunneling current is plotted as a function of applied voltage, peaks will be observed whenever the applied voltage V_{app} achieves a resonance energy $V_{app} = h\nu/e$, where e is the electron charge and ν is the vibrational frequency. This peak arises because the overall increase of flowing current will show a jump whenever the applied voltage provides enough extra potential energy to excite the molecular vibration of energy $h\nu$.

The IETS field has developed quite rapidly. Experimentally, microlithographic and microstructural techniques are used to assemble the tunneling junction consisting of a flat strip of metal, a thin layer of the molecule to be measured, and an upper metallic electrode. Normally the spectra are run at liquid He temperatures, and often Pb is the metal of choice for the top electrode, since it is superconducting in this temperature range. The IETS technique has several very significant advantages:

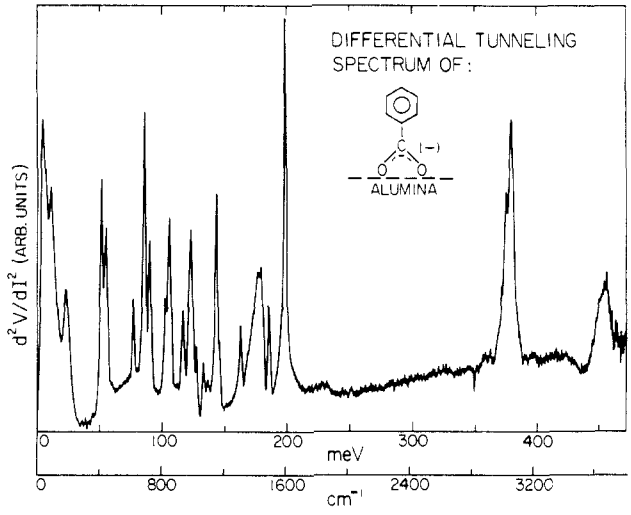

Figure 10. Scanning tunneling microscopy spectrum of benzoate anion adsorbed on alumina. Note very high resolution of the ion's vibrational spectrum. The ordinate is second derivative of voltage with respect to current. Reprinted with permission from: *Tunneling Spectroscopy: Capabilities, Applications and New Techniques*; Hansma, P. K., Ed.; Plenum: New York, 1982. Copyright 1982, Plenum Press.

The spectral range extends from 0 to well beyond 4000 cm^{-1}; compare Figure 10, the IETS spectrum of benzoate ions on alumina. The ability to see quite easily vibrations in the very far IR (below 200 cm^{-1}) may be of real value in many studies, for example of hindered vibrations or librations.

Sensitivity. Ordinarily the thickness of the molecular tunneling structure is just one monolayer. Given that the junctions themselves can be less than 1 mm on a side, this means that subnanomolar amounts can be measured.

Selection rules. There are no strong selection rules. Like inelastic neutron scattering, IETS appears to detect vibrations of all symmetries.

Theoretically, IETS is generally described[91] using a golden-rule expression for the transition rate per unit time, with the matrix element fixed by interactions of the tunneling electron with the molecular dipole and its image charge as well as with the molecular polarizability. These simple pictures work qualitatively; more complex theoretical models have also been developed. The IETS phenomenon differs from the ET reactions usually studied in that the energy dependence of the tunneling process, rather than the time dependence, is of dominant interest; it yields the spectrum of Figure 10.

The second new analytical technique based on tunneling in solid-state ET reactions is called scanning tunneling microscopy, or STM.[93,94] Here a metallic point probe, generally made of tungsten, is scanned along (x,y) coordinates just above a surface to be studied. The tunneling current between the conductive surface and the tip, when a potential difference is applied, will depend strongly on the distances, essentially because the overlap of wave functions on the surface and the tip falls off exponentially with tip-to-surface

separation. The technique is both exquisitely sensitive and exquisitely delicate. In the usual mode of operation, the tip-to-surface distance is kept constant (to within 0.1 Å) using piezoelectric expansion materials. By monitoring the variations in z-coordinate of the tip as (x,y) coordinates are scanned, and maintaining the tunneling current at a constant value, precise mapping of surface heights can be obtained. This technique is only 5 years old (it was developed at IBM Zurich in 1981),[93] but it has already been used to study several surface structure problems of real importance. For example, recent work from the Zurich laboratory demonstrates directly the hexagonal carbon ring structure of the graphite surface, and also shows that the six carbons are inequivalent, since only three of them have neighboring atoms in the layer directly below the surface.[94] The technique's sensitivity is roughly 0.1 Å in surface height. Since the STM is sensitive to the surface electronic states (which are the source of the tunneling current), it can sense changes in electron density even when no atomic changes occur. Recently[95] this has been used to detect charge-density waves in $TaSe_2$ and $TiSe_2$ by measurement of the STM image of their surface; a hexagonal structure with a spacing roughly 3.5 times that of the surface atoms is observed, which is due to the charge-density waves.

Most recently,[94] the voltage dependence of STM has been used to study the spatial dependence of the surface electronic states of solids. Since elastic tunneling is seen in the STM experiment the electronic states on the surface and the tip must be degenerate. By a change in the potential the energies of the surface electronic states may be monitored. Feenstra et al.[95] have recently used variable-potential STM to observe energy gaps at the Si(111) surface. Scanning tunneling microscopy provides a strongly surface-structure-sensitive technique, which can in principle be used to map out defects, adsorbate islands and clustering, oxidative or reductive chemistry or phase separation at surfaces. In principle, STM could be used to study inelastic as well as elastic tunneling, and thereby provide spatially resolved vibrational spectra of surfaces, but the experimental requirements, especially for geometric stability of the scanning tip, are quite severe, and we are not aware of any completed studies of this type.

[B.3] Molecular and macromolecular assemblies[72,79-82] can involve extended systems (and therefore have been discussed under A.5 above) or intermediate sizes, from monolayers to macromaterials. The unifying principle of these synthetic organized systems involves the use of chemical techniques such as surface derivatization or cross-linking in connection with physical techniques such as photolithography to prepare heterostructures of well-defined chemical constituency and physical dimension. Much of the attention in such systems has been focused on control of ET processes of one sort or another. In particular, polymer-coated electrodes have been actively investigated for suppression of corrosion in electrochemical processing, electrocatalysis has been studied at chemically modified semiconductor electrodes for improved analytical performance, and photoelectrochemical cells for direct conversion of sunlight to electricity have been actively investigated. In each case, the ET phenomenon at the interface has been substantially changed by chemical modification.

A fairly typical example is offered by some relatively early work[97] on oxidation of reductants in solution via holes generated in semiconductor photoelectrodes. This process is useful as a means of charge separation in photovoltaic conversion, but is plagued by several serious experimental complications, including surface decay of the n-type semiconductor surface, which is in contact with the electrolyte, via photoanodic decomposition. By coating the electrode with a conductive polymer, the desired electron transfer between the solution redox couple (such as I_2/I_3^- or Fe^{III}/Fe^{II}) and the semiconductor electrode can proceed without competitive decomposition, since the solvent contacts the conductive polymer,[97,98] which is the effective redox site, rather than the electrode itself. An ideal conductive polymer for this purpose is poly(pyrrole), which can be placed on the silicon photoanode either via[99] simple anodic growth (eq 15) or via a preliminary surface de-

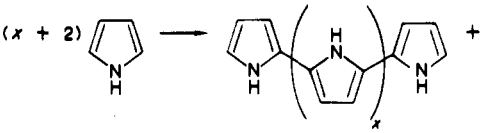

$$(2x + 2)H^+ + (2x + 2)e^- \quad (15)$$

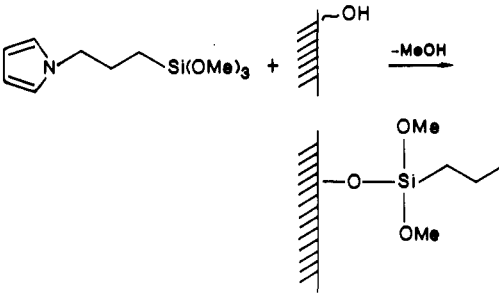

(16)

rivatization with a siloxy reagent (eq 16). The second scheme leads to far better adhesion of the polypyrrole film to the surface,[80,98] as it should, since it is held in place by covalent linkages.

These surface-modified and polymer-coated electrodes are of substantial current interest as useful reagents and offer real potential in device applications. Indeed, a new sort of molecular or macromolecular electronics is beginning to develop, based largely upon the preparation of molecular/surface species of controlled electrochemical behavior, chemical properties, and geometry. It is the control of the energetics and the rate of the ET process which makes these substances of interest.

[C.1-4] These molecular solid-state ET processes are closest to those of ordinary solution ET. We have discussed some of the best examples of these ET events at the beginning of this section, and will describe some others in detail in section VI, after setting out theoretical approaches to ET phenomena in solutions and in solids in the next two sections.

IV. Rate Theory for Electron-Transfer Reactions In Solution

A. General-Rate-Theory Approach

Several recent reviews, notably those by Newton and Sutin[16] and by Marcus and Sutin,[14] deal quite extensively with theoretical approaches to ET reactions in

solution. Treatises by Ulstrup[8] and by Cristov,[17] as well as a number both of newer and of older but still very helpful review articles[1-19] also consider solution ET in some detail, and therefore we will limit the discussion here to a very brief sketch, which outlines the three standard approaches (classical, quantum, and semiclassical[16,46,103]) to the problem. It also introduces some important concepts and nomenclature. In chapter V, we will present some variant theoretical approaches, ones which are in some cases more appropriate for discussion of solid-state ET.

We will consider transfer of an electron from a selected donor to a selected acceptor

$$D^- + A \rightarrow D + A^- \tag{17}$$

The observed rate constant can be expressed as[16]

$$\frac{1}{k_{obs}} = \frac{1}{k_{diff}} + \frac{1}{k_{act}} \tag{18}$$

where k_{diff} is the diffusion-controlled rate constant for the formation of an encounter complex (a complex consisting of the selected acceptor and donor molecules). Usually the encounter complex is comprised of one acceptor and one donor species, and we neglect other types. The acceptor and donor molecules can be more or less solvated depending on the properties of the medium and the molecules. When the complex is formed, the rate of ET from the donor to the acceptor is given by the activated complex rate constant k_{act}, which is expressed as an integral over orientations and time as[100]

$$k_{act} = \int_v d\vec{r} \int_0^\infty d\epsilon\, j(\vec{r},\epsilon) \int_0^\infty dt\, g(t) k_{el}(\vec{r},\epsilon,t) \tag{19}$$

Here $j(\vec{r},\epsilon)$ is a distribution function for the reactive complex, defined as the number of encounters per unit energy and volume with relative orientation between $\vec{r}$ and $\vec{r} + d\vec{r}$ and energy between ϵ and $\epsilon + d\epsilon$. The distribution $g(t)$ is the probability per unit time for the encounter complex to exist for one interval t called the interaction period. Separation of the encounter complex takes place after the time t. Since $g(t)$ is a probability, it is normalized by

$$\int_0^\infty g(t)\, dt = 1 \tag{20}$$

The microscopic, first-order ("intramolecular") rate constant $k_{el}(\vec{r},\epsilon,t)$ is the rate of transfer at time t for an encounter complex with relative orientation between $\vec{r}$ and $\vec{r} + d\vec{r}$ and energy between ϵ and $\epsilon + d\epsilon$.

The usual approximate expression for k_{act} is given as[3,16,101-105]

$$k_{act} = \int_0^\infty 4\pi r^2 j(r) k_{el}(r)\, dr \tag{21}$$

$$j(r) = \exp(-\beta u(r)) \tag{22}$$

$$\beta = (k_B T)^{-1} \tag{23}$$

where $u(r)$ is the interaction potential between the two compounds at the separation distance r. In eq 21 the angular dependence of the rate constant is either neglected or approximated in some way.[103,106] The time integral is performed by assuming that k_{el} is independent of time and is given by its value at the interaction time equals zero. The energy integration is contained in $k_{el}(r)$. From eq 21 it is seen that k_{act} has two major contributions, namely the radial distribution of the reactive compound and the rate of electron transfer for a given separation r of the reactive compound. The rate constant $k_{el}(r)$ involves the quantum and statistical mechanics associated with the atomic and electronic motion in the reactive compounds, and $j(r)$ involves all the statistical mechanical aspects of solutions.

If the integrand in eq 21 is large over a small range of r values and approximately zero elsewhere, eq 21 can be expressed as[16,103,107,108]

$$k_{act} = 4\pi r^2 u(r_m) k_{el}(r_m) \delta r \tag{24}$$

$r_m \equiv$ distance at which integrand in (21) is maximal (25)

where δr is the range of r-values over which the integrand is taken to be non-zero. The value of δr depends on the specified reaction but some values of δr have been proposed.[16]

B. Consideration in Terms of States and Energies

The reaction system which we consider consists of the more-or-less solvated acceptor and donor compounds and the surrounding solvent. This entire system is described by a multidimensional energy surface and is usually considered as a solvent surrounding a supermolecule, which is itself an encounter complex consisting of the solvated acceptor and donor.[8,104,105,109,110] The solvent can be represented in several ways,[111-117] but in ET theory the most common representations are the continuum model[111-113] and the multiphonon representation.[3,8,116,118] The degrees of freedom for the system are divided into a set of electronic degrees of freedom, r, for the solvated donor and acceptor and a second set of coordinates describing the nuclear degrees of freedom of the solvated acceptor and donor compounds. A third set of coordinates is needed for describing the solvent, and this set is usually constructed from the Fourier transformed polarization vector.[3,8,116,118] The entire set of nuclear coordinates (both molecular and solvent subsystems) is represented by Q. Using the Born–Oppenheimer approximation the hamiltonian for the system may be represented as

$$H_{sys}(r,Q) = H(r,Q) + T(Q) \tag{26}$$

where $H(r,Q)$ is the electronic hamiltonian for a given configuration Q and $T(Q)$ is the kinetic energy operator for the Q-coordinate. The vibronic wave functions are represented as[3,8,16,102-105,109,110]

$$\Psi(r,Q,t) = \sum \phi_i(r,Q,t)\chi_i(Q,t) \tag{27}$$

where ϕ_i is the electronic wavefunction describing the electronic subsystem and χ_i is the wavefunction for the subsystem described by the coordinate set Q.

In molecular ET theory[3,8,16,102-105,109,110,119] the expansion in eq 27 is generally limited to two static electronic states. These two are an initial state representing the reactants surrounded by the solvent and a final state representing the products surrounded by the solvent. This means that eq 27 is truncated to two terms:[16]

$$\Psi(r,Q,t) = \phi_{in}(r,Q)\chi_{in}(Q,t) + \phi_{fi}(r,Q)\chi_{fi}(Q,t) \tag{28}$$

where ϕ_α is the electronic wave function associated with

$H(r,Q)$ for the configuration described by Q_α. Since the ET reaction is a time-dependent phenomenon, we have to employ the time-dependent Schrödinger equation. In the following it is assumed that the overlap between the two electronic states is zero. This orthonormality condition can be attained in a straightforward manner.[103,120] Then we have

$$i\hbar\frac{\partial}{\partial t}\Psi(r,Q,t) = \{H(r,Q) + T(Q)\}\Psi(r,Q,t) \quad (29)$$

Using eq 28 in eq 29,

$$i\hbar\frac{\partial}{\partial t}\chi_\alpha(Q,t) = \{H_{\alpha\alpha} + T_{\alpha\alpha} + T(Q)\}\chi_\alpha(Q,t) + \{H_{\alpha\beta} + T_{\alpha\beta}\}\chi_\beta(Q,t) \quad (30)$$

where $\alpha \neq \beta$ and $(\alpha,\beta) = (in,fi)$, and $H_{\alpha\alpha}$, $H_{\alpha\beta}$, $T_{\alpha\alpha}$, $T_{\alpha\beta}$ are defined as

$$H_{\alpha\alpha} = \langle\phi_\alpha(r,Q)|H(r,Q)|\phi_\alpha(r,Q)\rangle \quad (31)$$

$$H_{\alpha\beta} = \langle\phi_\alpha(r,Q)|H(r,Q)|\phi_\beta(r,Q)\rangle \quad (32)$$

$$T_{\alpha\beta} = \left\langle \phi_\alpha(r,Q)\middle|\left(-\sum_Q \frac{\hbar^2}{2M_Q}\nabla_Q^2\right)\middle|\phi_\beta(r,Q)\right\rangle + \left\langle \phi_\alpha(r,Q)\middle|\left(-\sum_Q \frac{\hbar^2}{M_Q}\nabla_Q\right)\middle|\phi_\beta(r,Q)\right\rangle \times \nabla_Q \quad (33)$$

$$T_{\alpha\alpha} = \left\langle \phi_\alpha(r,Q)\middle|\left\{-\sum_Q \frac{\hbar^2}{2M_Q}\nabla_Q^2|\phi_\alpha(r,Q)\right\rangle - \sum_Q \frac{\hbar^2}{M_Q}\nabla_Q|\phi_\alpha(r,Q)\rangle \times \nabla_Q\right\} \quad (34)$$

Here $\langle||\rangle$ denotes integration over the electronic coordinates. $H_{\alpha\alpha}$ defines the Born–Oppenheimer potential energy surface associated with the electronic state ϕ_α. M_Q is the effective mass associated with the Qth coordinate. The nuclear wavefunction $\chi_\alpha(Q,t)$ can be expanded as

$$\chi_\alpha(Q,t) = \sum_\upsilon C_{\alpha\upsilon}(t)\chi_{\alpha\upsilon}^\circ(Q)\exp(-itE_{\alpha\upsilon}/\hbar) \quad (35)$$

where $\chi_{\alpha\upsilon}^\circ, E_{\alpha\upsilon}$ are solutions to

$$E_{\alpha\upsilon}\chi_{\alpha\upsilon}^\circ(Q) = \{H_{\alpha\alpha} + T_{\alpha\alpha} + T(Q)\}\chi_{\alpha\upsilon}^\circ(Q) \quad (36)$$

Adding the diagonal nonadiabatic correction $T_{\alpha\alpha}$ to $H_{\alpha\alpha}$ would simply constitute an improvement of the potential energy surface associated with the electronic state ϕ_α.

The coupling of the simple vibronic products arises from the second term on the rhs of eq 30, and this term determines whether the reaction is going to take place. The $T_{\alpha\alpha}$ and $T_{\alpha\beta}$ terms are frequently called the nuclear coupling terms, the terms of the Born–Oppenheimer breakdown-operators, or the nonadiabaticity operators. The $H_{\alpha\beta}$ term is generally called the electronic coupling matrix element between the two electronic states ϕ_α and ϕ_β.

The kind of electronic wave functions which are used for this reaction are either a set that does not diagonalize the electronic hamiltonian or a set that does. The first basis set can be identified as the valence bond structure of the reactants ϕ_r and of the products ϕ_p, and the electronic states are generally[8,16,105] designated "diabatic". The electronic basis set $\{\phi_1,\phi_2\}$ which diagonalizes the electronic hamiltonian is designated "adiabatic"; in this representation, only $T_{\alpha\beta}$ couples the states. These adiabatic states are easier to define since the condition for these states is the diagonalization of the electronic hamiltonian. Figure 3 compares diabatic and adiabatic states.

It is generally expected that the dependence of the "diabatic" electronic wave functions on Q is small.[16,102,103] So for the diabatic basis the $T_{\alpha\alpha}$ and $T_{\alpha\beta}$ terms are neglected, which reduces eq 30 to

$$i\hbar\,\dot{\chi}_\alpha(Q,t) = \{H_{\alpha\alpha} + T(Q)\}\chi_\alpha(Q,t) + H_{\alpha\beta}\chi_\beta(Q,t) \quad (37)$$

where $\alpha \neq \beta$ and $\alpha,\beta = r,p$. When this diabatic basis set is used, the ET process is essentially the following transition

$$\phi_r(r,Q_r^\circ) \rightarrow \phi_p(r,Q_p^\circ)$$

where Q_r° or Q_p° denotes the equilibrium configuration of the encounter complex for the reactants or products.

Alternatively (and more commonly), one can describe ET using the adiabatic electronic basis set $\{\phi_1,\phi_2\}$. Then the following expression is obtained from eq 30.

$$i\hbar\frac{d\chi_\alpha}{dt}(Q,t) = [T(Q) + H_{\alpha\alpha} + T_{\alpha\alpha}]\chi_\alpha(Q,T) + T_{\alpha\beta}\chi_\beta(Q,t) \quad (38)$$

$\alpha \neq \beta$ and $\alpha,\beta = 1,2$. In this basis set, $H_{12} = 0$ and the mixing comes from the nuclear kinetic energy operator. In this case the reaction is essentially described either by

$$\phi_1(r,Q_r^\circ) \rightarrow \phi_1(r,Q_p^\circ) \quad \text{(normal region)}$$

or by

$$\phi_1(r,Q_r^\circ) \rightarrow \phi_2(r,Q_p^\circ) \quad \text{(abnormal region)}$$

The two different ways of representing the ET system are shown in Figure 3, which shows the diabatic potential energy surfaces H_{rr} and H_{pp} and the adiabatic potential energy surfaces H_{11} and H_{22}. For the symmetric case, the splitting of the two adiabatic surfaces at the point of avoided crossing Q^* is $2H_{rp}$. The nuclear configuration corresponding to Q^* can lie between the two configurations Q_r° and Q_p° (this case is referred to as the normal region); the situation when Q^* does not lie between Q_r° and Q_p° is referred to either as the inverted region or as the abnormal[9,12,14-16,18,113] region (cf. Figure 3). Energetically, as mentioned in section III, the "abnormal" regime involves situations in which the total reorganization free energy λ is smaller than the standard free energy change $|\Delta G^\circ|$, while for the normal regime $|\Delta G^\circ| < \lambda$. Often ET reactions are classified as being either "adiabatic" or "nonadiabatic". These terms are related to the strength of the coupling element H_{pr}. When this coupling element is large (small), the ET is classified as being an adiabatic (nonadiabatic) reaction. For the "adiabatic" situation the ET can be analyzed in terms of the potential energy surface H_{11}. For "nonadiabatic" ET it is necessary to analyze the ET reaction in terms of two potential energy surfaces; more detail is given in section VA.

C. The Classical Description of Electron Transfer

The classical descriptions of ET are mainly due to Marcus[1,113] and Hush.[45,121] In these models the tran-

sition state theory is used, with the transition state corresponding to the configuration at Q^*. The electronic coupling is assumed to be so large that it is reasonable just to use one potential energy surface, so that the ET is adiabatic. For the classical model the ET rate constant is given as[8,45,113,121,122]

$$k_{et} = \frac{k_B T}{h} \exp(-\Delta G^*/k_B T) \tag{39}$$

ΔG^* is the activation free energy associated with the ET reaction of the solvated acceptor and donor compound existing as an encounter complex. This expression does not take quantum effects into account, and is based on the assumptions that: (i) the transition conserves energy, and activated states of the reactants and the products have the same energy; (ii) the Franck–Condon principle is valid, so that the actual electronic-state change occurs at fixed nuclear momentum and position; (iii) the electronic coupling is assumed large enough so that the reactants are converted into products with unit probability in the region of Q^*. On the other hand it is assumed small enough to be neglected in calculating the amount of energy to reach the region of Q^*. Thus no transmission coefficient appears in the activated complex theory expression (39).

By assuming a quadratic Q dependence of the potential energy surfaces eq 39 can be expressed as[1,16,102,103,123]

$$k_{el} = \nu_{\text{eff}} \exp(-E_A/RT) \tag{40}$$

where

$$E_A = (E_\lambda + \Delta E_0)^2/4E_\lambda \tag{41}$$

Note that we use ΔE_0 and E_λ here, while ΔG_0 and λ (free energy) were used above in section B; the latter takes entropy effects into account and is preferable. They become the same for zero activation entropy. ΔE_0 is the net energy change for the reaction and E_λ is the reorganization energy, in turn given as

$$E_\lambda = \frac{1}{2}\sum_\mu \bar{f}_\mu[(Q_\mu^\circ)_r - (Q_\mu^\circ)_p]^2 \equiv \sum_\mu E_\mu \tag{42}$$

$(Q_\mu^\circ)_r$ and $(Q_\mu^\circ)_p$ are respectively the equilibrium value of the μth Q-coordinate for the reactant or product complex, and $\bar{f}_\mu$ is an average force constant for each Q_μ

$$\bar{f}_\mu = \frac{2 f_\mu^r f_\mu^p}{f_\mu^r + f_\mu^p} \tag{43}$$

This approximation to $\bar{f}_\mu$ is generally believed to be reasonable. The weighted average frequency ν_{eff} for the Q-coordinates is fixed by

$$\nu_{\text{eff}}^2 = \frac{\sum_\mu \nu_\mu^2 E_\mu}{\sum_\mu E_\mu} \tag{44}$$

where ν_μ is the frequency for the μth normal vibrational mode. The reorganization energy is conveniently divided into two contributions,[1-18] one from coordinates of the encounter complex itself (inner shell or inner sphere) and the other from Q-coordinates of the solvent (outer shell or outer sphere). The first contribution is given by

$$E_{\text{in}} = \lambda_{\text{in}} = \frac{1}{2}\sum_\mu \bar{f}_\mu[(Q_\mu^\circ)_r - (Q_\mu^\circ)_p]^2 \tag{45}$$

On the basis of the dielectric continuum approximation, the solvent contribution is given by[1,18,24]

$$E_{\text{out}} = \lambda_{\text{out}} = \frac{e^2}{8\pi}\left(\frac{1}{D_{op}} - \frac{1}{D_s}\right)\int_v (\vec{D}_p - \vec{D}_r)^2 \, dV \tag{46}$$

where D_{op} and D_s are the optical and static dielectric constants of the medium and $\vec{D}_r$ and $\vec{D}_p$ are, respectively, the electric displacement vectors associated with the charge distribution of the encounter complex of the reactants and the products. The volume V is the dielectric medium excluding the cavities which contain the solvated donor and acceptor compounds. Actual calculations of λ_{out} have been carried out in several ways.[1,8,111-117]

D. The Quantum Mechanical Description of Electron Transfer

To describe ET when the electronic coupling is small (a nonadiabatic ET) or when nuclear tunneling is important, it is necessary to approach the problem quantum mechanically. The description is based on a first-order time-dependent perturbation treatment of eq 37 resulting in a Fermi-golden-rule expression. This expression gives the probability per unit time that a system in an initial vibronic state $\phi_r(r,Q)\chi_{rv}(Q,t)$ will pass to a set of final vibronic states $\phi_p(r,Q)\chi_{pw}(Q,t)$ (ϕ_r and ϕ_p are the only electronic states considered). The use of the Fermi golden rule assumes that the interaction time goes to infinity, the existence of a continuum set of final states and energy conservation in the ET. The initial vibronic states are assumed to be Boltzmann distributed. The result for k_{el} is given as[3,8,16,104,105,125-128]

$$k_{el} = \frac{2\pi}{\hbar} Z^{-1} \sum_w \sum_v \exp(-\beta E_{rv}) \tag{47}$$
$$|(\chi_{rv}^\circ|\langle\phi_r|H|\phi_p\rangle|\chi_{pw}^\circ)|^2$$
$$\delta(E_{rv} - E_{pw})$$

By use of the Franck–Condon approximation, eq 47 becomes (with Z denoting the vibrational partition function)

$$k_{el} = \frac{2\pi}{\hbar} H_{rp}^2 \, Z^{-1} \sum_v \sum_w \exp(-\beta E_{rv}) \tag{48}$$
$$|(\chi_{rv}^\circ|\chi_{pw}^\circ)|^2 \delta(E_{rv} - E_{pw})$$
$$= \frac{2\pi}{\hbar} H_{rp}^2 \{FC\}$$

$$\{\text{FC}\} = (Z)^{-1} \sum_w \sum_v |(\chi_{rv}^\circ|\chi_{pw}^\circ)|^2 \tag{49}$$
$$\delta(E_{rv} - E_{pw})\exp(-\beta E_{rv})$$

For the diabatic electronic states the use of the Franck–Condon approximation is expected to be reasonably accurate, though there have been attempts to go beyond it.[129,130] The matrix element H_{rp} is usually determined at the Q^*-configuration, where it has its maximum value.[8,16,17,101] To obtain an expression for the energy-weighted Franck–Condon product {FC}, the vibrational modes of the system are separated[8,16,104,105]

into two categories: (i) discrete high-frequency modes characterizing the vibrations of the solvated acceptor and donor compounds. These modes are characterized by the coordinates Q_c and the vibrational frequncies ω_c. These modes do not necessarily have the same frequencies and equilibrium positions in the two electronic states. These modes have $\omega_c \gg k_B T/\hbar$ at room temperature and are treated by quantum mechanics. (ii) The modes of the solvent which are considered as low-frequency modes are characterized by the normal modes q_k and the corresponding frequencies ω_k. These low-frequency modes are described by the use of classical mechanics. The multidimensional potential energy surfaces for the initial (U_r) and final (U_p) state are approximated as

$$U_r(q_k,Q) = U_r^D(Q_r^D) + U_r^A(Q_r^A) + U_r^{sol}(q_k) \quad (50)$$

$$U_p(q_k,Q) = U_p^D(Q_p^D) + U_p^A(Q_p^A) + U_p^{sol}(q_k) + \Delta E \quad (51)$$

The solvent contribution to the potential energy surface is represented in the harmonic approximation as

$$U_r^{sol}(q_k) = \frac{1}{2}\sum_k M_k\omega_k^2\, q_k^2 \quad (52)$$

$$U_p^{sol}(q_k) = \frac{1}{2}\sum M_k\omega_k^2\,(q_k - q_k^0)^2 \quad (53)$$

q_k is the displacement of the kth solvent mode and q_k^0 is the change of the position of minima for the initial and final potential energy surface of the solvent. ΔE is the energetic difference between the minima of U_r and U_p. U_r^D and U_r^A are the potential energy surfaces for the selected donor and acceptor compounds in the reactant states. Due to the assumed harmonic structure of the approximate potential energy surfaces the wave functions χ_r and χ_p are factorized according to the separable potentials.

Using the approximation that the solvent modes can be treated classically (that is $\hbar\,\omega_k \ll kT$), {FC} is expressed as:

$$\{FC\} = \left(\frac{\pi\beta}{E_s}\right)^{1/2}(\prod_I Z_I)^{-1}\sum_{\epsilon_r^I\epsilon_p^I}\exp(-\beta\sum_I \epsilon_r^I)\prod_I S_I(\epsilon_r^I,\epsilon_p^I) \quad (54)$$

$$\exp[-\beta\{E_s + \Delta E + \sum_I(\epsilon_p^I - \epsilon_r^I)\}^2/4E_s]$$

$$I = A, D$$

$$Z_I = \sum_{\epsilon_r^I}\exp(-\beta\epsilon_r^I) \quad (55)$$

$$S_I(\epsilon_r^I,\epsilon_p^I) = |(\chi_r^I(Q_r^I;\epsilon_r^I)|\chi_p^I(Q_p^I;\epsilon_p^I))|^2$$

The potential energy surfaces for the solvated acceptor and donor compound can be selected in any arbitrary way. Ulstrup and Jortner[104] have concluded by the use of numerical calculations that changes in frequencies, displacements, and anharmonicity effects for the modes of the encounter complex can be important for the determination of the activation energy. In many cases the evaluation of the {FC} factor in eq 49 and 54 is determined by the steepest descent method,[109,121,132] thereby achieving an analytical expression for k_{el}, and also describing the actual flow of energy (exoergicity) into the various vibrational modes.

E. Semiclassical Description of Electron Transfer

These methods are simple approximate procedures for extending the validity of the classical models. Generally k_{el} is for this kind of description written as[1,8,15,16,103,123]

$$k_{el} = \kappa_{el}\Gamma_n k_{el}^{class} \quad (56)$$

where κ_{el} is the electronic transmission factor, Γ_n is the nuclear tunneling factor for the high frequency modes, and k_{el}^{class} is the classical rate constant of eq 39. By use of the two-state Landau–Zener[16,17,133,134] model, κ_{el} can be expressed as (in the limit of weak electronic coupling)

$$\kappa_{el} = \frac{2H_{rp}^2}{h\,\nu_{eff}}\left[\frac{\pi^3}{(E_{in} + E_{sol})\,k_B T}\right]^{1/2} \quad (57)$$

κ_{el} is the probability that a system starting in the diabatic state ϕ_A (and with energy in excess of E_A) will undergo a transition to the diabatic state ϕ_B. The nuclear tunneling factor Γ_n describes corrections which are only important for the internal modes; it is defined by the ratio of the rate constant determined by the Q-modes to the rate constant in the classical limit[103,123]

$$\Gamma_n = \frac{k_{in}(T)}{k_{class}} = e^{-(4\Delta G^*(T)-E_{in})/4k_B T} \quad (58)$$

There are several expressions[8,14-16,123] for Γ_n most of which have a restricted range of validity. However, the activation parameters for the semiclassical model agree well with the activation parameters from the previous section.[123] Semiclassical expressions are of great value in fitting experimental temperature dependence, and in extensions of the theory to consider friction effects (section V.C).

This *very* brief survey of standard ET theories in solution points out the key roles of Franck–Condon restrictions and of activated processes in fixing such ET rates. These considerations remain important in solid-state ET.

V. Molecular Electron-Transfer Reactions in Solids: Theoretical Approaches

Three decades of intense theoretical and experimental effort have led to a fairly satisfactory understanding of ET reactions in homogeneous solution. Most such ET reactions occur by means of diffusion-controlled formation of a precursor complex, which then undergoes the ET event following first-order kinetics. Most such reactions are electronically adiabatic, and the Marcus formulation describes them well. There are some fairly well-understood exceptions, such as spin intercombination transitions which are electronically nonadiabatic. There are also certain unresolved issues, such as the exact conditions under which the "abnormal" behavior (rate decrease with increasing exoergicity) will be observed, or how solvent dynamics, as opposed to mere energetics, is to be included, or the precise quantitative values of λ_i and λ_o, but in general the formulations of section IV have been very successful.

For solid-state ET, the situation is more complex. In section III, we have discussed some of the very special features which are found in ET in solids, including extended systems, hopping conductors, metals and

semiconductors, heterostructures and polymers, inelastic tunneling spectroscopy, and scanning tunneling microscopy. We also indicated some of the principal molecular studies which have been carried out in solids. The remainder of this article will focus on molecular ET in solids, but some of the other systems discussed in section III serve as a reminder that other techniques and problems are very important in solid-state ET.

Because molecular diffusion in solids is so slow as to be essentially unimportant for ET, solid-state ET reactions will occur at relative Ox/Red geometries which are fixed by the preparation of the sample. In general, this will mean that the distances are larger than those typically found in precursor complexes in solution-phase ET, and therefore that Ox/Red electronic overlap is far smaller. This in turn has several important implications for theoretical discussion: the transfer is likely to be nonadiabatic and therefore sensitive to the electronic structures both of the redox species and of any intervening matter. Thus ET theory in solids is most often formulated in a purely quantum-mechanical fashion, and electronic structure calculations can be very useful in understanding ET rates and their dependence on energetics and composition. We will briefly outline some approaches which have been used for discussing molecular ET in solids, each of which has some obvious strengths and weaknesses.

A. Vibronic Approaches: Small-Polaron-Type Models

This approach is a direct generalization of the vibronic ET theory in liquids, which had been developed by several authors[8,16,104,105,109,110] in the early 1970s. It is really modeled after treatments of other vibronic coupling phenomena, notably radiationless transitions,[135,136] in the chemical literature, though treatments of ET using polaron-type models have been in the physics literature[70,71,132,137] since the 1950s. Although more elegant formulations based on time-dependent correlation functions have been given,[135] the essential idea can be presented in simple golden-rule form.

For simplicity, consider a two-site transfer situation in which the two sites are simple parallel diatomics (perhaps Li_2^+ and Na_2), with rigid relative orientation. Then the Holstein molecular crystal model[71] can be used (section III.A.5), and the total Hamiltonian of eq 9 can be written

$$H = H_{el} + H_{nuc} + H_{el\text{-}vib}$$

$$H_{el} = \epsilon_l a_l^+ a_l + \epsilon_r a_r^+ a_r + t(a_l^+ a_r + a_r^+ a_l) \quad (59)$$

$$H_{vib} = (b_l^+ b_l + 1/2)\hbar\omega + (b_r^+ b_r + 1/2)\hbar\omega \quad (60)$$

$$H_{el\text{-}vib} = H_{int} = (b_l^+ + b_l)g_l\hbar\omega(a_l^+ a_l - a_r^+ a_r) + (b_r^+ + b_r)g_r\hbar\omega(a_r^+ a_r - a_l^+ a_l) \quad (61)$$

Here $a_l^+ a_l$ is the number of electrons on the left diatomic, where the one-electron energy is ϵ_l. The operator $a_l^+ a_r$ moves an electron from the right to the left diatomic. We have assumed that each diatomic is a harmonic oscillator, with frequency ω taken to be the same for both diatomics. The b^+,b are the usual creation and destruction operators for vibrational quanta. Thus H_{el} describes electrons tunneling between or sitting on the two-diatomics (it is the two-site Hückel hamiltonian), H_{vib} is the energy of the two-bond stretch vibrations. The electron/vibration coupling term of (61) describes the displaced-oscillator situation of eq 53; when an electron is removed to the right from the left diatomic, the latter's bond length lengthens by $2g_lQ_l^{00}$ (Q_l^{00} is the zero-point displacement). We assume for simplicity that the bond length changes upon reorganization are identical for the two diatomics. Then we can write

$$H_{int} = g_l\hbar\omega(a_l^+ a_l - a_r^+ a_r)(b_l^+ + b_l - b_r^+ - b_r) \quad (62)$$

which simply couples a change in population to a change in bond length. We can define sum and difference vibrations by $\sqrt{2}\, b_\pm \equiv (b_r \pm b_l)$ and $g \equiv \sqrt{2}\, g_l$ and then rewrite H as

$$H = \hbar\omega(b_+^+ b_+ + b_-^+ b_- + 1) + g\hbar\omega(b_-^+ + b_-) \times (a_r^+ a_r - a_l^+ a_l) + \epsilon_l a_l^+ a_l + \epsilon_r a_r^+ a_r + t(a_r^+ a_l + a_l^+ a_r) \quad (63)$$

In (59–61), we have omitted the coupling of the electron-tunneling term $a_l^+ a_r$ to the vibrational displacement ($b^+ + b$). Such terms are important in formal small-polaron theory[71,138] ("phonon-assisted hops") and dominate the T-dependence of conductivity in some molecular metals (section III.A.3), but they are generally ignored in molecular ET theory.

Because the vibronic coupling term (proportional to g) may be larger than the tunneling term (proportional to t), the vibronic term, written second in (63), is not suitable for perturbative treatment, whereas the tunneling term is. Formally, then, an operator transformation[135,139] corresponding to state-dependent displacement of the oscillator is performed, after which H can be written as

$$\tilde{H} = \hbar\omega(b_+^+ b_+ + b_-^+ b_- + 1) + (\epsilon_l - g^2\hbar\omega)a_l^+ a_l + (\epsilon_r - g^2\hbar\omega)a_r^+ a_r + t[a_r^+ B_r^+ B_l a_l + \text{C.C.}] \quad (64)$$

Here the on-site energies are relaxed by a value $g^2\hbar\omega$ on each site; this is just the reorganization energy λ, as sketched in Figure 3. The operators B_l and B_r describe the polarization of the nuclei, in this case the change in bondlength, due to the electronic population change. Formally,

$$B_l = \exp\{-g(b_-^+ - b_-)\} = B_r^+ \quad (65)$$

notice from (64) that only the b_- vibration, which describes the difference in displacement between the molecule on the left and that on the right, enters into the polarization.

Equation 64 can be treated using either linear response theory[135] or simple golden-rule. In either case, we obtain for the transition rate

$$w_{l\to r} = \frac{2\pi}{\hbar}\, t^2\, \{FC\} \quad (66)$$

with the generalized Franck–Condon factor {FC} simply[109,135]

$$\{FC\} = \hbar^{-1}\int_{-\infty}^{\infty} e^{it(\epsilon_l - \epsilon_r)}\exp\{g^2(n_- + 1)(e^{+i\omega t} - 1) + g^2 n_-(e^{-i\omega t} - 1)\}\, dt \quad (67)$$

Here $n_- = [\exp(\hbar\omega/kt)-1]^{-1}$ is the Bose population of difference vibrations between left and right. In the low-temperature limit, $\{FC\}$ becomes a sum of energy-conserving δ functions, corresponding to the balancing of electronic energy change $\epsilon_l - \epsilon_r$ by m quanta of ω,

CHART I

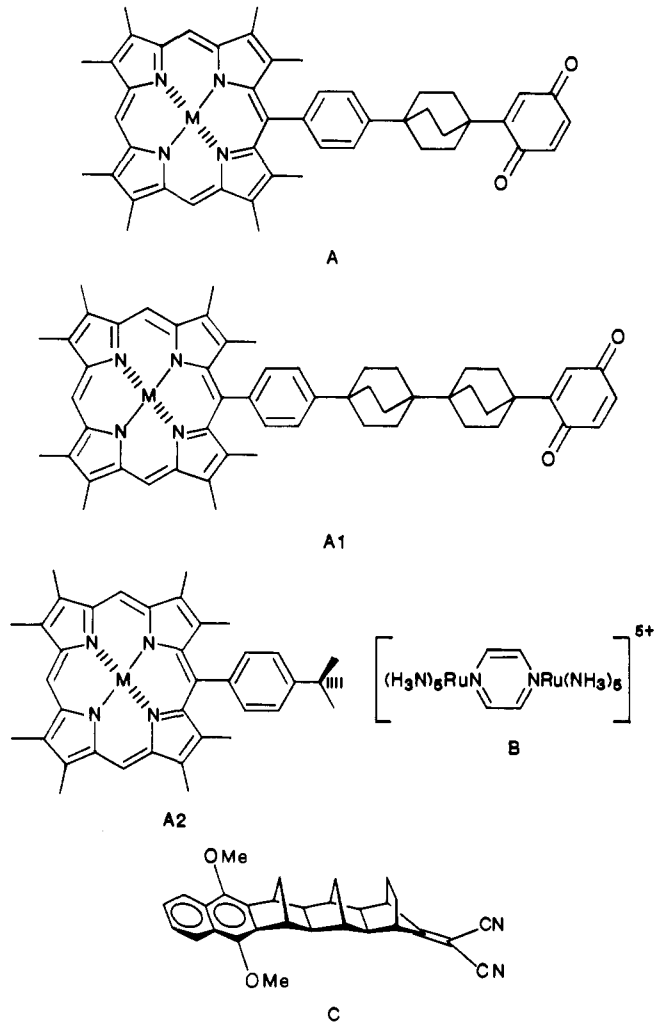

weighted by a factor $g^{2m}/m!$ which is characteristic of harmonic oscillator overlaps. The slope of $w_{l\to r}$ for $kT \ll \omega\hbar$ is flat, as is observed experimentally (Figure 1) for a number of molecular ET processes in proteins. As temperature increases, the process becomes activated, again in agreement with the experiments. The flat T-dependence at low temperatures can be explained on the basis of nuclear tunneling, in which the nuclear wave functions within the left parabolic minimum of the adiabatic potential surface (Figure 3) have a classically forbidden probability of tunneling through the activation barrier. As the temperature increases, so do the n_- terms in (67), and the system is activated to vibrational levels which lie above the barrier, or intersection point. Then the ET is activated, and the motion does not have an important *nuclear* tunneling component. The *electronic* tunneling, however,[14,16] is still important, since the transfer is nonadiabatic and, from (66), the transfer probability is proportional to t^2, the square of the electronic tunneling matrix element.

Insight into the various energy terms which determine the nature of the vibronic ET in solids can be gained by consideration of the problem of mixed valency,[11,23,24,45] which was referred to in section III. Mixed valency occurs in f-block elements where it is of interest in systems such as samarium chalcogenides. Molecular systems which focus on mixed valency have mostly centered on transition metal dimers such as the celebrated Creutz–Taube ion B.[140,141] (See Chart I). Formally, this species contains either Ru^{2+} and Ru^{3+} (mixed valency) or two $Ru^{2.5+}$ (averaged valency). In their pioneering discussions of these species, Robin and Day[24] distinguished fully delocalized species (such as I_3^-) as class III, and fully localized systems (such as $(NH_4)_2SbBr_6$ in which individual Sb^{3+} and Sb^{5+} may be seen crystallographically) as class I, with class II describing intermediate cases. Classification of any given species will depend upon the environment in which it is found, since both strong ion pairing and solvent polarization, like the polarization of the bonds within the molecule described by the inner-sphere reorganization energy, will favor localization of the charge, resulting in class II or I, rather than III, behavior. The criteria for mixed valency (Robin/Day II or I) as opposed to average valency (Robin/Day III) relate closely both to the nature of the transport (coherent or diffusive) and to the type[55,58,142] of ET observed (adiabatic or nonadiabatic).

In 1966, Goodenough introduced[143] a criterion for distinguishing these cases, based upon the overlap of the atomic wave functions at each electron localization center: if the wave function overlap exceeded some critical value, the charge would be delocalized and averaged valency (now denoted Robin/Day III) would be found. In fact, the electronic terms *alone* do not fix the ET process or the Robin/Day classification.

The nature of vibronic ET in the case of two electronic states is fixed by the energy quantities corresponding to electron tunneling, thermal energy, reorganization energy, vibrational energy, and exoergicity which are denoted t, k_BT, $\lambda = g^2\hbar\omega$, $\hbar\omega$, and $\Delta E°$, respectively. We can then define four smallness parameters[55,58,132,142]

$$\eta_1 = t/g^2\omega\hbar \tag{68}$$

$$\eta_2 = t^2/\hbar\omega[k_BTg^2\hbar\omega]^{1/2} \tag{69}$$

$$\eta_3 = \frac{k_BT}{\hbar\omega} \tag{70}$$

$$\eta_4 = \frac{|\Delta E°|}{g^2\hbar\omega} \tag{71}$$

which characterize the ET, as depicted in Chart II. The parameters η_1 and η_2 relate to electron dynamics; η_1 is the ratio of the electron delocalization energy t to the "polaron shift" energy $\hbar g^2\omega$; this latter is simply the amount by which the potential energy is lowered due to change in equilibrium displacement along q, when the transfer electron is localized; it is the reorganization energy. For degenerate systems, when $\eta_1 \ll 1$, the lowering of potential energy upon electron localization more than overcomes the gain in electronic delocalization energy; thus the states are largely localized, and the situation corresponds to Robin–Day I [Figure 3(c)]. If $\eta_1 \gg 1$, the opposite situation holds; the variational principle then favors the delocalized electron, and the system is best described as Robin–Day III [Figure 3(d)]. The parameter η_2 is the square of the ratio of the time during which the nuclear configuration is equivalent on sites l,r to the time associated with electronic tunneling from l to r. If $\eta_1 \gg 1$, the transfer rate is irrelevant, since the states are delocalized. If $\eta_1 \ll 1$, however, the nature of the motion between the minima in Figure 3(a) is determined by the size of η_2. If $\eta_2 \ll 1$, the system

CHART II

	$\eta_1 << 1$	$\eta_1 > 1$
$\eta_2 << 1$	localized states nonadiabatic ET electron tunneling (Robin/Day I, II) $\eta_3 << 1$: nuclear tunneling, rate weakly T-dependent $\eta_3 > 1$: activated rate, nuclear tunneling unimportant	delocalized states (Robin/Day III)
$\eta_2 >> 1$	localized states adiabatic ET no role for electron tunneling (Robin/Day I, II) $\eta_3 << 1$: nuclear tunneling, rate weakly T-dependent $\eta_3 > 1$: activated rate, nuclear tunneling unimportant	delocalized states

will have equivalent geometries (called a "coincidence event") for long times before the electron hops; in this case, the hopping rate is determined by t, and the transfer is nonadiabatic. If, however, $\eta_2 \gg 1$, the electron will jump each time a "coincidence event" occurs,[78] and thus the rate of transfer will depend only on the "event" frequency, and will be independent of t; this is the limit of adiabatic electron transfer. In this case, at high temperatures, the occurrence probability of a "coincidence event" is then $\exp(-E_A/k_BT)$, where the activation energy E_A[257] is roughly $(\Delta E^\circ + \lambda)^2/4\lambda$ – t, where $\lambda = g^2\hbar\omega$. This activated behavior is characteristic of standard adiabatic electron-transfer theories.

The parameters η_3 and η_4 relate to the nuclear dynamics. When the exoergicity $-\Delta E^\circ$ exceeds the reorganization energy λ (which is just $g^2\hbar\omega$ for this simple two-mode example) so that $\eta_4 > 1$, there is a bottleneck in the vibrational energy flow which reduces the transfer rate. This arises, essentially, because the vibrations are forced to accept more energy than will optimize the Franck–Condon factors, and the rate should then decrease as the exoergicity increases. This is the abnormal regime or Marcus inverted region. For either ΔE° or λ fixed, the rate should maximize when the value of the other (λ or ΔE°) is such that $\eta_4 = 1$, which is where the intersection in Figure 3b occurs at the minimum of the upper parabola. As explained in sections III and VI, the inverted region may be difficult to observe experimentally because of the intervention of electronically excited product states. The parameter η_3 characterizes the nuclear tunneling contribution to the rates: when $\eta_3 \ll 1$, there is very little thermal excitation, n_- in (67) is essentially zero, and the allowed nuclear displacements are limited to $Q^{00} = (\hbar/2m\omega)^{1/2}$. Then if the activation energy E_A exceeds the zero-point energy $\hbar\omega/2$, the system will not show much contribution from motion over the activation barrier, but rather from nuclear tunneling under it. As the temperature and η_3 increase, activation over the barrier becomes more probable, and nuclear tunneling makes a smaller contribution to the rate (compare Figure 1).

The two-mode system described here captures the essence of the small-polaron description of ET processes, which is based on the simple displaced-harmonic-oscillator model, of eq 59–61. For real systems, the set of vibrational modes should include not only all the vibrational modes of the molecule itself, but also the modes (phonons) of the host; these are responsible, respectively, for λ_i and λ_o, the inner-sphere and outer-sphere reorganization energies. Formally, inclusion of other harmonic modes with no frequency changes simply involves summing the terms involving Q or ω in eq 59–61 over all modes so that, for instance,[16,109]

$$\lambda_i = \hbar \sum_v g_v^2 \omega_v \tag{72}$$

For most ET systems, such analyses are incomplete, largely due to lack of detailed vibrational data (all q_v,ω_v). The evaluation of the rate-determining $\{FC\}$ factor for many-mode systems is most easily carried out using saddle-point methods.[135]

This vibronic model has many advantages, including relative conceptual clarity, numerical adaptability, easy extension to multisite and multimode ET, and fairly simple extendability to include anharmonicity and frequency change. In mixed-valency, Piepho, Krausz, and Schatz have used[59] exactly this model to discuss very clearly and meaningfully delocalization and rate effects. For ET events, even in its simplest one-mode formulation the small-polaron scheme has been very widely used for interpetation of molecular ET in both solids and solutions. Jortner's formulation[144] of the problem in terms of three simple parameters (which really arise from the smallness parameters η_1–η_4, and are defined by $S \equiv \lambda/\hbar\omega$, $p = \Delta E^\circ/\hbar\omega$, and $2T_c = \hbar\omega/k_B$) has been particularly useful.

Vibronic ET theories of small-polaron type have been given by several workers;[6,8,16,104,109,110] in addition, two other ET theories are very closely related to the small-polaron work. Scher and Holstein have[145] presented a chemical-rate treatment of small-polaron hopping between inequivalent sites. It can handle both adiabatic and nonadiabatic transfer, and has been applied both to pair recombination in a Coulomb field and to ET rates in proteins. An analytic form can be derived for the transfer rate in either limit. This approach is a very compact and attractive one, but has not been extensively applied. Hopfield approached[15,147,148] the problem in a very different way, borrowing the same expression from the energy-transfer literature on which the Inokuti/Hirayama scheme[84] of section III is based. He can then write, in the nonadiabatic limit,

$$k_{ET} = \frac{2\pi}{\hbar} t^2 \int_0^\infty dE\, D_A(E) D_D(E) \tag{73}$$

where D_A and D_D are, respectively, distributions for

energy capture by the acceptor and energy loss by the donor ($D_A(E)$ dE is the possibility for electron capture at energies between E, $E + dE$). By making a Gaussian approximation to these distributions, Hopfield derives a form for the ET probability which is very similar to those arising from small-polaron theory, in the limiting case of a single vibrational mode. There are differences in these rate expressions, and both have been used to discuss ET in proteins, especially the T-dependence. One clear advantage of the Hopfield approach is that the Gaussian approximation can be avoided by using the experimental $D(E)$ shapes in (73), whereas polaron theories become quite clumsy when harmonic behavior cannot be assumed; one disadvantage involves the possible identity of the solvent modes around D and A.

There are, however, some major inadequacies of this simple small polaron picture. These include: the very approximate, almost schematic, treatment of the electronic structure; the ignoring of the dynamics, as opposed to merely the energetics, of nuclear motion; and the quite unspecified nature of the actual initial and final states involved in ET. Each of these aspects has been addressed recently, and we shall briefly summarize some of these theoretical advances.

B. Electronic Structure Effects, Including Electron Tunneling

The electronic structure of any atom, molecule, or solid is the solution of a many-body coulomb problem, constrained by the Pauli principle, and no exact solutions are known for any many-electron system; this simple fact is often forgotten in considerations of ET. The process of ET amounts to a change in the space distribution of electron density, and any proper description of the process must involve all of the relevant terms in the electronic hamiltonian; this is nearly always ignored in treatments of the electronic terms in ET. Part of the reason for this neglect is the difficulty of the problem, since ET involves open-shell wave functions on precursor and successor complexes of differing geometry. Another part is that the electronic terms will really matter only for nonadiabatic ET, and most reports on ET in solution are devoted to adiabatic ET. Finally, simple electronic perturbation theory or two-state electronic models offer the advantages of formal simplicity and comprehensibility. Thus unlike the closely related field of magnetism,[149] in which the intricacies of the coulombic hamiltonian are really essential for any understanding, the area of ET is nearly always studied in terms of effective, or model, one-electron hamiltonians.

If, then, two-site ET situations are considered, the electronic hamiltonian may be written formally as

$$H_{el} = \sum_{i,j=1,2} |i\rangle\langle i|H_{el}|j\rangle\langle j| \quad (74)$$

$$= \sum_{i,j=1,2} H_{ij}|i\rangle\langle j| \quad (75)$$

where 1,2 label the two electronic "states" of interest, which are usually taken to be single atomic or molecular orbitals. Then the effective electronic tunneling matrix element, denoted t in eq 5 and 59 is just H_{12} of (75). This term can be evaluated theoretically in several ways, as described by Newton and Sutin.[16] Experimentally t can also be deduced in several ways. For example, t can be determined from the intensity of the intervalence bands[45] for mixed-valency species, and several papers[142,150] have appeared in which comparisons of semiempirical electronic structure studies have been used to deduce the effective coupling between Ru sites in mixed-valency binuclear Ru complexes; the results compared rather well. A second approach is again based on the close formal analogy between ET and magnetic exchange, which has permitted t to be estimated from magnetic and spectroscopic data.[16,151,152] A third experimental approach is very similar to the most common theoretical technique for obtaining $H_{12} = t$; it is simply to note that the two-state electronic hamiltonian of (75) is formally the same as, say, the Hückel π-electron model for propene, consisting of two site energies $\epsilon_i = H_{ii}$ and a tunneling integral $t = H_{12}$. Then the energy eigenvalues are

$$E_\pm = \tfrac{1}{2}\{\epsilon_1 + \epsilon_2 \pm \sqrt{(\epsilon_1 - \epsilon_2)^2 + 4t^2}\} \quad (76)$$

and therefore a knowledge of any three of (ϵ_1, ϵ_2, t, E_+, E_-) will fix the other two. In particular, for dimeric species $\epsilon_1 = \epsilon_2$, and the splitting between E_+ and E_- is simply $2t$. For oxo-bridged silicon phthalocyanine dimers, this approach has been used[63] to obtain t from photoemission measurements of the dimer energy levels E_+ and E_- (Table I).

TABLE I. Dimer Splitting and Conduction Bandwidths in $[SiPcO]_n$[a]

method	bandwidth
dimer electronic structure calculation	0.76 eV
photoemission in dimer[b]	0.58 eV
Drude analysis[c]	0.60 eV

[a] Ciliberto, E.; Doris, K. A.; Pietro, W. J.; Reisner, G. M.; Ellis, D. E.; Fragalà, I.; Herbstein, F. H.; Ratner, M. A.; Marks, T. J. *J. Am. Chem. Soc.* **1984**, *106*, 7748. [b] Measurement on dimer. [c] Measurements in conductive polymer.

As already indicated, this calculation of the tunneling matrix element via calculation of the splitting of the eigenstates of (74) is a quite common way of estimating t. The calculations can be carried out at any chosen level of electronic structure theory, and such calculations have been reported using ab initio techniques,[30,103,153] local density methods,[51,52,56,165] extended Hückel models,[155-158] and the CNDO model;[101,159,160] comparable sorts of results are generally obtained for valence type interactions. For special cases, severe constraints must be fulfilled by the wave functions. For example, local-density calculations[51,53] on HOSiPcO-SiPcOH (Pc = phthalocyanine) have been carried out, for comparison[63] with the tunneling splitting observed via photoemission, the optical spectra, the bandwidth of the linear-chain Pc salts, and the temperature dependence of the conductivity (Figures 4 and 5). In this case, the π orbitals are on planar rings separated by roughly 3.20 Å, so that the effective overlap comes largely from the tails of the wave functions. In such cases, the basis sets used in semiempirical and standard ab initio studies are far too constrained (to be optimal in the valence region) to describe properly the coupling, but the numerical basis sets used[161] in the local-density study work quite well, as shown in Table I by the good agreement between splittings calculated and observed.

In an extensive series of ab initio calculations,[16,30,153] Newton and his collaborators have studied the elec-

tronic structure aspects of ET between solvated transition-metal ions, including the dependence of t on distance, orientation, and solvation. They find that the Fe^{II}–Fe^{III} transfer in aqueous solution is nonadiabatic; a t integral value of ~ 115 cm^{-1} for a face-to-face approach of the $Fe(H_2O)_6$ species is obtained. Thermal averaging gives good agreement with exchange experiments in aqueous solution. On the other hand, as Newton and Sutin point out,[16] projecting the electronic wave function onto a two-state representation as is done in eq 74, means that all factors responsible for mixing states (overlaps, kinetic energy, various exchange processes) are lumped together in t in a way which is quite difficult to disentangle. Kusunoki,[162] following an earlier suggestion of Igawa and Fukutome,[163] has presented an unrestricted-Hartree–Fock-based electronic structure description of the ET process, but for the most part the projection of eq 74 is the standard theoretical model used.

Halpern and Orgel[164] suggested that double exchange processes were responsible for efficient electron delocalization over conjugated π-type bridges, and there has been considerable recent use of McConnell's early suggestion[165] that effective coupling between centers without conjugated linkages could occur via superexchange through occupied σ-type orbitals of the intervening matter. This is closely analogous to the "through-bond" interactions which Hoffmann[166] has used for explaining many reactivity and electron density phenomena. Essentially, the idea of superexchange[167] is that even high-lying empty states of a linking-group between two redox sites (electron-type superexchange) or a convenient occupied level of the bridge (hole-type superexchange) can provide an amplified mixing compared[164,168] to a simple vacuum between the redox sites. That this might be so is fairly clear from simple perturbation theory. For an n-site bridge linking donor to acceptor, the effective tunneling integral may be written

$$t \cong -(t_D t_A/B)(-t_S/B)^{n-1} \qquad (77)$$

Here t_D, t_A, and t_S are the one-electron mixing integrals (Hückel-type resonance integrals) between the bridge and the donor, the bridge and the acceptor, and two subunits of the bridge, respectively; B is the energy level of the virtual states on each bridge subunit. The superexchange form (77) is physically suggestive: any bridge should provide more efficient nonadiabatic transfer if the required virtual states are not *too* high in energy (B not too large) and the bridge subunits have good electronic overlap both with each other (large t_S) and with the redox sites at the ends (t_D,t_A large).

The analytical approximation of eq 77 is useful for qualitative discussion of the superexchange process and its energy and distance dependence. For discussion of any specific ET species, numerical studies of the electronic structure may be more useful, in which case only $H_{12} = t$ itself (eq 75) will be found. Examples abound and some have been discussed by Newton and Sutin. One of the most complete efforts is the work[30,153] of Newton et al. on Fe^{II}/Fe^{III}, which has already been discussed. Larsson[152-158] used extended Hückel studies to investigate superexchange-type coupling through saturated hydrocarbons, and found substantial coupling even over many C–C bonds. Stein et al. used[159] semiempirical methods to examine transfer between Ru centers with dithiaspiro bridging ligands. Once again, they observe fairly strong interactions. Older work[169] using INDO models suggested that [2.2.2]bicyclooctane would provide only an inefficient "tunneling bridge" between donor and acceptor species of quite different redox potential, and used this observation to suggest the possible existence of a molecular rectifier; experimental studies on ET with such bridging ligands[34] are now being published. At a quite different level of sophistication, Ondrechen et al. have used[154] first-principles discrete-variation-method local density studies with a large basis set to calculate the extent of bridge-assisted mixing in the pyrazine-bridged Creutz–Taube ion **B**. They find strong mixing and are able to calculate accurately the frequency maximum of the intervalence band (error of 0.08 eV out of 0.89 eV). They discuss the transfer in terms of a three-site, rather than a two-site, picture.

The technique of using electronic-structure studies to deduce t from the two-site projection of eq 74 is a useful one, when the two-level approximation is valid. For molecular ET with exoergicity sufficiently small that no electronically-excited product states are available and with no important bridge localization, there really are only two relevant states, and the technique can indeed deduce an effective t, much like the superexchange-determined t of eq 77. The precision of these calculations should, of course, depend on how good the treatment of electronic structure is (basis set, model hamiltonian, correlation treatment), but the approach is an attractive one so long as the effective tunneling elements t are large enough that the calculations can be trusted. For smaller t, which are more relevant to the case of nonadiabatic electron transfer, these methods are probably of inadequate numerical precision.

To compute very small effective t integrals, analytic-type approximations are necessary. Probably the simplest, and one of the most attractive, such schemes involve WKB calculation[170] of the tunneling probability. This yields a form

$$t \propto \exp\left\{-r\sqrt{2m\ V_B}/\hbar\right\} \qquad (78)$$

where r is the width of the barrier through which the electron must tunnel and V_B is the barrier height. Using convenient units, this becomes, roughly

$$t \propto \exp\left\{-r(\text{Å})\sqrt{V_B(\text{ev})}/2\right\} \qquad (79)$$

Hopfield used[147] the form $t = (2.7/(20)^{1/2})\ \exp\{-0.72r\ (\text{Å})\}$, which corresponds to a barrier roughly 2 eV in height (the prefactor comes from some specific assumptions about carbon-bridged species). This general form $t^2 \sim \exp\{-r/a\}$, with a ~ 0.71 Å, has been found to fit ET rates for many long-distance transfers in many varied systems, for many of which the barrier height was certainly not 2 eV (compare section VI.A,B and Table II). This has been used to argue that the simple barrier-tunneling picture underlying (78) requires amplification, say by use of superexchange, (eq 77). Beitz and Miller[167] and others have fit the distance-dependence of *measured* ET rates to deduce values for the a in $t \sim N \exp(-r/2a)$. Some values are listed in Table II which shows that a is often quite close to 0.71 Å, but that many other values may be observed.

More elaborate treatments to obtain t have also been given. Beratan and Hopfield[160,171] have utilized the periodicity, which is required when a bridge consists of multiple subunits, to obtain estimates for the effects of bridge-assisted tunneling. This approach is quite elegant, as are all symmetry-based arguments, but it is not clear how useful it will be in the general case of an arbitrary bridge. Larsson has used the partitioning technique[156,172] to obtain reasonable approximations to the effective matrix elements for systems with quite specific bridges between acceptor and donor. Linderberg and Ratner[173] have analyzed the vibronic ET process in terms of three-site and four-site (corresponding to donor plus acceptor plus bridge) models. Several workers[164,168] have used simple perturbation theory to derive expressions much like (76) for arbitrary bridge-assisted transfer, and calculations involving different π bridges, based upon these perturbation-theoretic results and semiempirical MO theory, compare rather well with observed intervalence transfer band intensities in binuclear Ru complexes.[40,142] All of these studies share one virtue and one drawback: the virtue is that they can be used to calculate very small tunneling integrals t, while the two-site projections based on eq 75 often cannot, for numerical reasons (the splitting is far too small); the drawback is that all of them are implicitly based on one-electron model hamiltonians, and, as such, do not deal properly with many-electron effects. Nevertheless, the numerical electronic-structure approaches toward calculating t are useful in many situations of adiabatic and nonadiabatic ET.

C. Solvent Dynamics in Electron Transfer

1. Theory and Experiment in Liquid Solution

The reorganization energy for electron transfer consists of inner-sphere and outer-sphere contributions. As we have discussed both in section IV and in this section, these two terms are generally brought together as an energy-weighted Franck–Condon factor, which provides the nuclear part of the ET rate constant (eq 49). For nonadiabatic transfer, this form arises from the golden-rule (or correlation-function) formula for the rate constant, when the Condon approximation is made. That is, the expression for the rate constant is factored as a product of an electronic term (the t in (66)) and a vibrational overlap factor, and the latter is evaluated assuming simple vibrational equilibrium. Thus the dynamics, as opposed to the energetics, of the vibrations and of the solvent are ignored—the vibrational states are assumed to relax to equilibrium with no memory effects, and it is simply the changing of their equilibrium position due to the ET which causes the reorganization.

The Condon approximation, mathematically, amounts to writing

$$\langle A_{el}(r,Q)B_{vib}(Q)\rangle_Q \cong A_{el}(r,Q_0)\langle B_{vib}\rangle_Q \qquad (80)$$

where Q_0 is some fixed arbitrary value of Q. Here the average is over the vibrational coordinate Q, and the operators $A_{el}(r,Q)$ and $B_{vib}(Q)$ are electronic and vibrational operators; the product form A × B arises from the Born–Oppenheimer approximation. The ignoring of the Q-dependence of the electronic operator A is the Condon approximation, and is reasonable due to the parametric (slow) dependence of $T_{\alpha\beta}$ in (30). Nevertheless, it is an approximation, and there are situations in which it might be expected to fail.

Similar concerns arise if ET is considered in the adiabatic case. Here the original Marcus formulation[1] is closely related to activated complex theory, with a universal prefactor describing the passage over the free-energy barrier from reactant to product. Now the free-energy surface on which the system point moves is generally defined based upon an assumption of vibrational equilibrium for all bound vibrational states which are perpendicular to the reaction coordinate. In some reactions, especially in the vapor phase, kinetic energy effects[174] can result in the system point leaving this path and gaining vibrational energy due to couplings which actually vanish on the reaction coordinate itself. Condensed-phase difficulties can arise for a completely different reason: the system point can[28] "get lost" off the reaction path because vibrational energy which is present in one of the bound modes takes a finite amount of time to relax. This effect amounts to a sort of drag, or viscosity, or friction term, which substantially modifies the dynamics of the system.

Thus both adiabatic and nonadiabatic ET reactions can be substantially affected by generalized friction terms due to energy relaxation in the solvent modes.[28-33,175] Indeed, since those friction forces change the rate of passage of the system point over the barrier, they can change the classification of the transfer process; a transfer which appeared nonadiabatic because the electronic tunneling term did not permit state mixing when the system reached the "coincidence event" geometry or the configuration at which the Franck–Condon principle permits state change to occur, can become adiabatic because large friction keeps the nuclear configuration in the neighborhood of the saddle point for a larger time.[28] The first analysis of barrier-crossing problems in terms of friction effects was given by Kramers[177] in 1940, and within the past decade a good deal of theoretical work has been reported[28,178-180] in which a Kramers-like approach has been applied to many chemical processes, including ET.

Since our subject here is electron tunneling in solid-state ET processes, and since these frictional effects really relate to nuclear rather than electronic tunneling, these friction effects lie outside our strict purview. They might be quite important, however, in changing both the overall ET rate and its conceptual understanding.[28,182,183] The dominant effect is to change the so-called transmission coefficient (the κ_{el} in eq 56). In transition-state theory it is assumed that the system passes through the saddle point once on its route from reactant to product, and does so with characteristic thermal rate $\nu_{nuc} = k_B T h^{-1}$. One effect of friction is to cause the system to wander drunkenly back and forth in the region of the barrier top, so that the barrier is in fact crossed backwards and forwards many times. In the high-friction limit, the Kramers rate becomes proportional to η^{-1} (the inverse friction), since the behavior is overdamped; and no transfer will occur at infinite friction. In the low-friction limit, the rate is proportional to the friction, since increased friction will decrease both the probability of ballistic "bounceback" from product to reactant and the effectiveness of pulling the system back onto the reaction coordinate, through

vibrational energy flow.[28,177-180]

Calef and Wolynes have examined[28] the role of solvent dynamics on ET rates in liquid solution. For the rate of back-transfer after photoexcitation in the intramolecular system $Ru(NH_3)_5(pyz)Ru(edta)_2^+$ (pyz = pyrazine, edta = ethylenediaminetetraacetate) in solution at 25 °C, they found a rate constant of 3×10^{10} s^{-1}, compared to 8×10^9 from experiment,[184] 5×10^{11} using the absolute rate theory prefactor $k_BT/\hbar$, and 2×10^{12} from a nonadiabatic expression. The difference is due to the preexponential factor, that is, to the effects of entropy and of solvent dynamics.

The work of Wolynes and Calef,[28] as well as that of Garg et al.,[184a] is based on a Kramers-like model with frictional forces along the reaction coordinate. Hopfield and Agmon[184b] have considered the case in which the frictional behavior occurs along a laboratory coordinate that is the same as the reaction coordinate only right at this product and reactant geometries. For example, this coordinate might be a slow solvent libration. The numerical results of Agmon and Hopfield do not yield the correct behavior in all limits (their high-temperature activation barrier appears too high), but the physical model is quite appropriate, and merits further study.

Weaver and co-workers[185,186] have used these Kramers-type formulas to argue that substantial changes due to solvent friction can occur in the rates calculated for oxidation or reduction, both in homogeneous solution and at electrodes. For example, they analyzed[26] the rates of electron exchange involving a series of metallocenes in several solvents, and found that the differences between the standard activated complex theory formulas and ones which took account of solvent dynamics was less than a factor of 10, but that the latter expressions were more accurate. They conclude that "conventional transition-state theory may not apply to ET reactions where the free energy barrier is due chiefly to solvent reorganization, at least in "high-friction" media in which concerted solvent relaxation is slow." Further work on effects of solvent dynamics on solution-phase ET is progressing quite rapidly.

2. *Effects of Vibrational Dynamics on Solid-State Electron Transfer*

Vibrational and Librational Effects. Once again there has been far less work on vibrational dynamics in solid-state than in liquid-state ET. Most of what has been done is focused on orientational effects rather than on solvent dynamics.[187,188] It is intuitively clear that since electronic overlaps depend strongly not only on distance but also on orientation, any vibrational motion which changes the relative geometry of donor and acceptor may strongly influence ET rates. Indeed, the effects of allosteric behavior on ET in biological systems reflect the great sensitivity of rates to geometric change and such motion as a restricted rotation which completely alters the relative orientation of two planar aromatics will also modify very strongly the ET rate.[52,53,188-190] Situations may easily be imagined in which the ET rate depends solely on a geometric motion which aligns donor and acceptor into a geometry favorable for very rapid ET.

Theoretically, two approaches have been taken to discuss the role of orientation changes on ET. One centers on the vibrational dynamics per se and analyzes the role of orientation dependence by expanding the transfer integral t of eq 5 in a Taylor series around its value for the equilibrium orientation, and then uses small-polaron-type theory to calculate the additional temperature and frequency dependence which arise from the orientation changes.[187] The second set of studies is far more extensive[53] and concentrates on the changes in t itself due to changes in relative geometry. The most celebrated such geometric change is that in relative separation—this is discussed in section VI. Changes in t due to orientation have also been examined, particularly with respect to planar π-electron species.[53,188]

In linear-chain conductors, in which the conduction is due to π-electron bands, it was suggested by Gutfreund and Weger[189] that rotations of the planar subunits about the z-axis, which they referred to as librons, would lead to strong modulation in the bandwidth, and therefore to substantial contributions to the resistivity. Whangbo[155] carried out calculations at the extended-Huckel level which showed that the overlaps were indeed sensitive to such librational motion. Marcus and collaborators have given a lucid discussion of the role of orientation dependence in ET between ellipsoidal-shaped charge clouds.[168] The Northwestern group has reported more elaborate calculations[51-53] in which first-principles electronic structure calculations were used to calculate both bandwidths and electron/phonon and electron/libron coupling constants for phthalocyanine-based conductors. Figure 5 shows the resistivity of the molecular metal NipcI as calculated and observed. Note the substantial "libron" contributions, with resistivity quadratic in temperature, which is due to changes in π cloud orientation due to restricted molecular rotation about the z-axis. The actual calculated change in $\pi-\pi$ overlap of a phthalocyanine dimer is also shown in Figure 4, and again substantial orientation dependence is seen.

Effects of Environment Dynamics. Relaxation processes in solids, particularly molecular solids, are in general more complex than in liquids. One simple example is afforded by dipole relaxation: whereas in liquids a simple single-exponential form for the decay of an induced polarization P_0 is generally adequate (Debye relaxation), in polymers and glasses the relaxation process is more complicated, and a distribution of relaxation times may be observed.[191] Thus one can write, to a good approximation

$$P = P_0\exp\{-t/\tau_D\} \text{ (liquids)} \quad (81)$$

$$P = P_0\exp\{-(t/\tau_0)^\beta\} \text{ (amorphous solids)} \quad (82)$$

where τ_D is the Debye relaxation time, τ_0 is a typical solid-state relaxation time, and β is a parameter often found to be very close to 0.5 in value.[191,192] Numerically, relaxation processes in polymers and glasses can occur at rates varying from nanoseconds to many hours.[193]

We are not aware of detailed experimental or theoretical studies which analyze the effect of solvent dynamics on ET reactions in solids, as opposed to liquids, though some useful insights have been given[27] (cf. sections VI.A,C). One might expect, however, that the ET processes will be even more sensitive to configuration change, friction effects, and relaxation limitation in the solid than in liquid solutions. For proton transfer and for some other simple models (such as a two-level sys-

tem in a harmonic bath representing the environment), important dissipation effects on the dynamics of the fast system (such as the electrons) due to dynamic phenomena in the slow system (vibrations) have been calculated.[28-33,175-184] Extension to experimental and theoretical studies for real solid-state ET processes will be of interest.

D. Initial State Considerations and Electron-Transfer Processes: "Solitonic" States

All of our theoretical considerations thus far have been slightly cavalier in treating the details of the two electronic states between which transfer occurs. For example, in electronic-structure calculations of the effective tunneling integral $t = H_{12}$ based on eq 75, the geometries assumed for the donor/acceptor species are generally taken from crystallographic information on the equilibrium structures. An actual exoergic ET process, however, is in some senses an energy relaxation event, in which electronic energy is eventually degraded to heat. Therefore the initial state of such an ET is in fact not an equilibrium state, and any study of its evolution (electron transfer) rate to form products should take cognizance of this facet of state preparation. To be more explicit, consider the common experimental situation of ET quenching of fluorescence. The initial ground-state donor is photoexcited, and generally has time to undergo vibrational relaxation in the excited state before ET or fluorescence or nonradiative decay can occur—this statement is sometimes called Vavilov's law.[194] The vibrationally relaxed photoexcited state will have an electronic configuration which is, generally, different from the ground-state one, and we accordingly expect its geometry to differ. In any theoretical treatment of the ET from this state, therefore, the correct initial-state geometry and wave function should be used. Precisely the same considerations will apply when the donor is prepared by electron capture.

The statement that the initial state should be properly chosen is just common sense, but few actual calculations have chosen the correct state, which is not the closed-shell ground state. Analogous considerations apply to the (generally open-shell) final state. Davydov was one of the first to stress the importance of the geometric and electronic structure changes on forming the precursor complex for ET from the ground state.[195-197] Davydov concentrated on energy transfer, rather than ET, but the essential idea remained the same: the precursor state must be properly constructed before transfer rates might be calculated. Recent work by Davydov has extended these ideas to consider ET in a polymeric conductor,[198] while Fischer and his collaborators[199-202] have adopted the idea of a "solitonic" state, corresponding to a properly-selected initial state, to discuss bimolecular ET.

Fischer and Nussbaum have used[200] these ideas to examine bridge-assisted ET in two-site species. They start with a hamiltonian very similar to the two-site small-polaron model of eq 57–61, except that it contains one or more sites corresponding to bridge units. Then rather than simply choose the displaced-oscillator transformation to remove, formally, the linear electron-vibrational coupling term of eq 62, they use a variational procedure to choose the equilibrium positions, and therefore the precise form of the transformation. This yields a hamiltonian for the system, from which one can select donor and acceptor states. They find that so long as the system is far away from the abnormal regime, so that $|\Delta G°| < 2\lambda$ (where λ is the reorganization free-energy including inner- and outer-sphere), a "self-trapped" donor state may be defined, which corresponds precisely to the vibrationally-relaxed precursor which we have discussed. Then the effective transfer rate is given by a rather complex expression involving both standard Franck–Condon-type factors and a prefactor which includes both an electronic resonance term (similar to that of eq 66) and a contribution from the reorganization energy. When the abnormal regime is entered, they claim that the sort of initial state which we might expect for ET, in which the electron is in fact temporarily self-trapped on the donor site, can be stabilized only as an excited-charge-transfer state, which means that the electronic wave function has a node between donor and acceptor. These results imply that, as $\Delta G°$ becomes larger, the ET phenomenon changes from normal ET, to long-range transfer, to internal conversion with charge transfer, to vibrational relaxation with charge transfer.

There is a powerful logical argument underlying the work of Fischer and collaborators: the behavior in the abnormal regime should really be found starting from a correct structure, and the variational principle provides a reasonable estimate of that state. They find that that structure can include wave-function extension onto the bridge, substantially increasing transfer rates. When the abnormal regime is entered, the ET rate will indeed drop with increasing $|\Delta G°|$, but only because the initial state is a charge-transfer excited state, which will undergo decay with typical gap-law behavior ($k \sim e^{-|\Delta G°|/\text{const}}$).

Mikkelsen et al. have investigated[100] the notion of initial-state preparation in a slightly different fashion. They consider the actual evolution of the electronic structure as a function of time, starting out with some chosen initial electronic configuration of the donor and acceptor, and using a full hamiltonian describing the molecular subsystem, the solvent subsystem, and the dielectric interactions between the molecular and the solvent subsystem. The solvent is described using Glauber states,[203,204] determined by a variational procedure using unitary transformations. Inner-sphere reorganization effects are not included, but the electronic structure calculations include a hamiltonian term derived from the classical multipolar description of the solvent polarization. They then calculate by a Hartree–Fock method a basis set of molecular orbitals for donor and acceptor, symmetrically orthogonalize them, and calculate a probability $P(t)$ for ET during the interaction time t (using a nonlinear time-dependent Hartree–Fock method) as

$$P(t) = |\langle D,A^-|U(t)|D^-,A\rangle|^2 \qquad (83)$$

where $U(t)$ is the evolution operator and the two states involve electron localization on donor and acceptor sites, respectively. The overall density operator is taken as a product of the molecular subsystem density operator and the solvent subsystem density operator. An appropriate average of $P(t)$ over times and geometries will then yield the rate constant.

Mikkelsen et al. apply[100] this method to examine ET between monosubstituted benzenes, and extensions to

consider bridge-assisted ET are in progress.[205] There are two advantages to their approach: firstly, the electronic structure is properly considered: no semiempirical estimates are made, and use of a relatively good basis set should assure that both static and dynamic electronic structure changes, as well as different sorts of exchange and of orthogonality corrections, are properly taken into account. Secondly, the presence in the electronic hamiltonian of a term corresponding to polarization of the medium (the polaron-type interaction of the solvent) means that some of the non-Condon and relaxation effects in the medium and molecular vibrations can be included. So far, these studies have been restricted to liquid-solution studies and have not included inner-sphere terms, but extension to solids and the full vibronic coupling should be straightforward.

The conceptual basis for understanding ET in solids seems to be fairly well agreed upon, but the actual understanding of such systems at the same quantitative or semiquantitative level as is now found for solution-phase ET is not yet at hand. Some of the theoretical difficulties are quite formidable, and their actual working out will depend upon comparison with careful and precise experimental work. Such work is beginning to appear, and is the area to which we now turn.

VI. Experimental Studies of Molecular Electron Transfer in Solids

This section summarizes some distinct molecular ET in disordered or ordered solids. It considers intermolecular (sections A, B, C) and intramolecular (sections C, D, E) ET. Currently, preparation of the reactant species is done either by irradiation or by pulse radiolysis (sections A, B). The intramolecular discussion is divided into subsections discussing ET in low-temperature biological systems, mixed valency ET in solids, and ET in nonbiological systems placed in an ordered or disordered solid (sections C, D, E).

A. Intermolecular Electron Transfer in Photoexcited Solids

ET quenching experiments are quite common in liquids, and have been extensively investigated in solids by Miller's[206] group, who considered reactions such as

$$D + A^* \rightarrow D^+ + A^- \qquad (84)$$

where the acceptor is irradiated and the quenching of the fluorescence is assumed caused by ET from D to A. The hosts included solid *trans*-1,5-decalindiol (DD), ethanol (Et), and 2-methyltetrahydrofuran (MTHF). D and A are chosen so that the quencher D always has a substantially higher-lying excited state than A, so that quenching due to energy transfer may be neglected. The features expected for ET quenching in these hosts are as follows:

(i) The decrease of fluorescence should have an almost exponential dependence on quencher concentration.

(ii) The quenching efficiency should depend on $-\Delta G°$ and should be at a maximum when $-\Delta G° \sim \lambda \sim 0.5$–$1.0$ eV:

$$-\Delta G° = [(E(S_1) - E(D/D^+) + E(A/A^-)] + \frac{e^2}{\epsilon R} \qquad (85)$$

$E(S_1)$ is the singlet excitation energy of the irradiated molecule and $E(D/D^+)$ and $E(A/A^+)$ are the oxidation and reduction potentials. The last term is a correction for the coulomb energy changes associated with charge separation, and ϵ is the dielectric constant for the solid.

(iii) The observable value of the maximum quenching radius R_q should be ~ 15 Å.

(iv) The quenching efficiency of the donor should depend only weakly on the lifetime of the excited molecule.

(v) When $-\Delta G° = \lambda$, where λ is the total reorganization free energy, the quenching efficiency should be nearly temperature independent.

The quenching radius is defined following Perrin[207] by introducing a volume V surrounding each fluorescing molecule; only if the quencher lies within this volume will the fluorescence be quenched. The volume is usually approximated as a sphere, which gives for the quenching radius:

$$R_q = \left[\frac{3V}{4\pi} + R_0^3\right]^{1/3} \qquad (86)$$

where R_0 is defined as the distance between the center of the irradiated molecule and the center of the quenching molecule when the two molecules are in contact. Miller et al. used the semiempirical expression (87) for the ET rate,

$$k_{ET}(R) = \nu \exp[-(R-R_0)/a] \qquad (87)$$

and the fluorescence quenching model of Inokuti and Hirayama[84] plus an approximate expression for R_q (eq 88) to interpret fluorescence quenching by the ET mechanism

$$R_q = R_0 + a \ln(\nu\tau_f) \qquad (88)$$

τ_f is a fluorescence lifetime, and ν is expressed following Marcus[1,113] as

$$\nu = \nu_0 \exp[-(\Delta G° + \lambda)^2/4\lambda k_B T] \qquad (89)$$

where ν_0 is a rather complicated frequency function,[16] and a determines the range of the transfer and is usually found by experimental data fitting. It is found that the maximum value of quenching is observed for systems with $\Delta G° \approx -1.7$ eV. This value of $\Delta G°$ is based upon electrochemical measurements in polar fluids, and therefore is not really appropriate for these glasses; simple dielectric corrections yield an appropriate $\Delta G°$ in the glass of ~ -1.00 eV, in agreement with expectation (ii) above. The experimental data show little difference in quenching efficiency in DD($T \approx 295$ K) compared to Et/MTHF ($T \approx 77$ K), and little T-dependence was observed from room temperature to 90 °C for the reaction of 9-methylanthracene with a phenylenediamine in solid DD. The lack of temperature dependence for the quenching is not surprising since $\Delta G° \sim -\lambda$. It would be useful to obtain quenching data for a weakly exothermic reaction in the same kind of solid medium. The whole treatment neglects orientation effects and the dispersion of solvation energies of D and A.

Miller et al. also measured[208] the phosphorescence quenching in two different glassy matrices (MTHF at 77 K and triacetin–tributyrin at 196 K) for two types of ET reactions

$$D(T_1/S_1) + A \rightarrow D^+ + A^- \quad (90)$$

$$D + A(T_1/S_1) \rightarrow D^+ + A^- \quad (91)$$

In reaction 90 the donor compound is excited to the first triplet/singlet state and transfers an electron to the acceptor compound; in (91) the acceptor compound is excited and accepts an electron from the unexcited donor molecule. The decay of luminescence intensity I was found to be exponential in quencher concentration, and given as

$$I/I_0 = \exp[-(4/3)\pi R^3 C] \quad (92)$$

where C is the concentration of the quenching compounds (number per unit volume), R is the distance between acceptor and donor at which the quenching rate is equal to the unquenched decay rate. Miller et al. used eq 87 and 88 to discuss ET quenching. Other quenching mechanisms were ruled out by the design of the reaction systems and by the fact that phosphorescence is quenched far more than fluorescence, which is expected for the ET mechanism since the phosphorescence lifetime is so much longer. The quenching radius R is also larger (~29 Å vs. 17 Å) for triplets than for singlets, again due, probably, to the longer lifetime.

Sadovski and Kuzunin studied[209] the fluorescence quenching of aromatic compounds at 77 K in solid solutions of ethanol or toluene using electron acceptors. The measured fluorescence decay curve shows a nonexponential decay when the acceptor concentrations are above 1 M. They interpreted the experimental data as ET fluorescence quenching, with the decay expressed as

$$\frac{I(t)}{I(t=0)} = \exp[-k_0 t - (4\pi/3)Na^3 \ln^3 \nu t] \quad (93)$$

$$N = [Q] \times N_A \quad (94)$$

$$k_{ET} = \nu \exp(-r/a) \quad (95)$$

where (95) is the semiempirical expression for the rate constant and k_0 describes the decay in the absence of quencher, N_A is Avogadro's number, ν is the frequency factor, r is the transfer distance, and a is said to be "a parameter characterizing the electronic wave function". The validity of eq 93 is limited to $\ln(\nu t) \gg 1$, uniform distribution of quencher molecules, and concentration of quenchers much larger than of excited molecules. A parameter β_0 may be defined by

$$-\beta_0 \ln(t/t_0) = \ln \frac{I(t)}{I(t_0)} + k_0(t - t_0) \quad (96)$$

If the approximation of uniform distribution of the quencher molecule is reasonable, β_0 should depend linearly on the quencher concentration [Q]; this is found to hold quite well. Sadovski and Kuzunin state that the parameters a and ν, which determine the rate of ET transfer, depend differently on the properties of the system, with a rather insensitive and ν very sensitive to the details of the ET pair. They also consider, and reject, exciplex fluorescence as a major quenching pathway.

Namiki, Nakashima, and Yoshihara (NNY) studied[210] the fluorescence quenching of indole by chloromethanes in ethanol glass solutions at low temperatures (76, 93, 117 K). The lifetimes depend both on concentration and identity of the quencher. The data do not show any clear temperature dependence. NNY also indicated that the triplet state reactions did not occur under the experimental conditions and that complex formation in both ground and excited states is a less effective quenching mechanism. The temperature independence (within the experimental uncertainties) was explained by assuming the vibrational coupling of the electron with the low frequency phonons of the medium (outer-shell reorganization energy) to be small and without importance in the ET. They only considered the vibrational coupling of the electron with the high frequency intramolecular modes of the donor and acceptor.

Domingue and Fayer studied[83] ET in a system of randomly distributed pentacene donor and decaquinone acceptor in a sucrose octaacetate glass. The donor molecule is excited to its first singlet state S_1 by a picosecond optical pulse and the fluorescence of the excited donor was measured. They found that the Inokuti/Hirayama model[84] theory without orientational modifications gave a good description of the experimental data, with the value for the critical transfer distance R_0 = 14.3 Å and the value of the exponential decay rate a = 0.35 Å.

Fiksel, Parman, and Zamarev (FPZ) studied[211] the ET from the first singlet excited state of naphthalene (Nh) to CCl_4 in various matrices at low temperature. The decay kinetics was described by

$$Nh^* + CCl_4 \rightarrow Nh^+ + CCl_4^{\bullet -} \quad (97)$$

and the fluorescence decay was explained using a scheme similar to eq 93–95, assuming no orientation effects and uniform distribution of quencher. The glassy hosts were C_2H_5OH, CH_3OH, CD_3OH, and toluene at temperatures between 77–140 K. Both Nh and perdeuterionaphthalene (Nh-$d8$) were studied. The characteristic lifetimes τ_0 in the absence of quencher for Nh and Nh-$d8$ were respectively (240 ± 5 ns) and (275 ± 5 ns) at 77 K. The nonexponential curves of the decay in the presence of CCl_4 were analyzed using the determined values of τ_0, thereby giving the values for the quenching rate. FPZ also showed that neither change of τ^0 in the presence of CCl_4 nor complex formation had any effect on the quenching, which is caused by ET from the excited Nh to the randomly distributed CCl_4. For all concentrations of CCl_4 studied, the nonexponential decay was more rapid for Nh-$d8$ than for Nh. To interpret this inverse isotopic effect, FPZ assumed that the deuteriation of Nh only influenced the nuclear wave function, and therefore the observed increase in k_{ET} is related to the increase of the frequency factor ν. They used a small-polaron-type model of[104] Ulstrup and Jortner, including only the C–H/C–D stretch vibrations. The C–H frequency is about 3000 cm^{-1}, and therefore only the ground levels of these vibrational modes are populated in the initial state. They concluded that when the energy difference between the initial and final states exceeds the medium reorganization energy by only one or a few vibrational quanta, the inverse isotopic effect can be observed. FPZ also studied the influence of the medium on the rate of ET by using the four different glassy matrices. Within the experimental accuracy they concluded that the β_0 of eq 96 does not depend on the nature of the matrix.

Mori, Weri, and Wan studied[212] the primary ET process in the quenching of triplet quinones by orga-

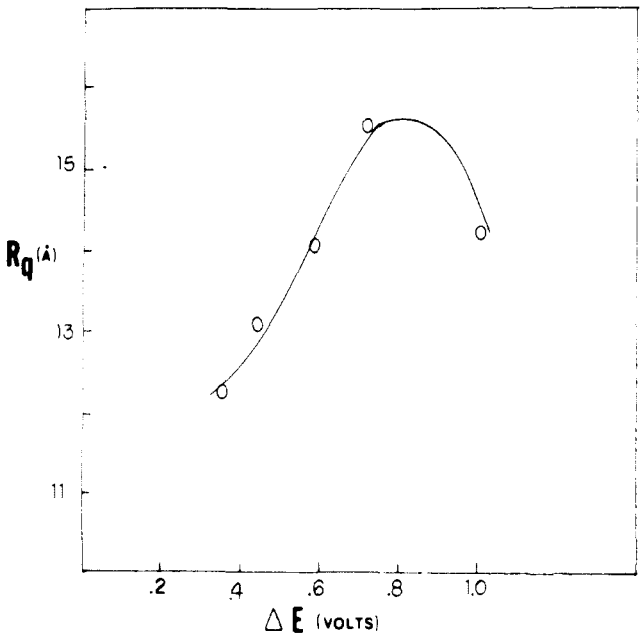

Figure 11. Plot of critical distance for electron transfer quenching of $(Ru_3^{2+})^*$ by methylviologen in rigid glycerol glass at $T \sim 260$ K. Abscissa is driving force, or exoergicity $\Delta G°$. The points correspond to different amine ligands L. R_q is the donor–acceptor distance at which the electron transfer quenching rate is the same as the inverse lifetime in the absence of quencher. Reprinted with permission from: Strauch, S.; McLendon, G.; McGuire, M.; Guarr, T. *J. Phys. Chem.* **1983**, *87*, 3579; *J. Am. Chem. Soc.* **1983**, *105*, 616.

notin initiated by photolysis of quinones in an organotin solid at 77 K. They added a small amount of quinone to a phenyltin compound (Ph_4Sn, Ph_3SnCl, $Ph_3SnCOOCH_3$) and studied the effect of irradiation of the sample by ESR, reporting values for the mean distance between the two radical ions within the primary ion pair. Brickenstein, Ivanov, Kozhushner, and Khairutdinov (BIKK) studied[213] the behavior of CCl_4 as electron acceptor in glassy matrices at 277 K, using zinc porphyrin (ZnP) as the electron donor. The matrices (CH_3OH, MTHF, C_2H_5OH) containing ZnP and CCl_4 at different concentrations were exposed to light which caused ET from ZnP to CCl_4, as concluded from the observation of an absorption band considered to belong to CCl_4^-. Without irradiation the ZnP is slowly regenerated, due to an ET recombination of photoseparated charges. BIKK also studied the charge recombination kinetics during irradiation of the absorption bands of ZnP^+ and CCl_4^-, and in this case the ZnP regeneration is observed to increase.

McLendon et al. studied[214] photoinduced ET in rigid glycerol solution. The electron donors were ruthenium pyridine homologues; the acceptor was N,N′-dimethyl-4,4-bipyridine (methyl viologen, MV^{2+}). The donor compound ($Ru(LL)_3^{2+}$) and the acceptor compound (MV^{2+}) were dissolved in glycerol and cooled to 248 K. The experimental timescale limited diffusion distances to be 2 Å or less. The experimental data were interpreted using the Inokuti–Hirayama model.[84] Figure 11 shows the effective quenching distance R_q corrected for the molecular volume, as a function of the exothermicity of the ET reactions. McLendon et al. also studied[215] the ET reaction

$$Ru(LL)_3^{2+} + D \rightarrow Ru(LL)_3^{+} + D^{+} \qquad (98)$$

where D is an organic reductant, and LL a ligand, in a Lexan (99) polyester film

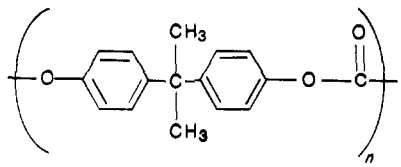

(99)

The donor compounds were a series of aromatic amines. They studied three reaction systems at $T = 77$ K,

$$Ru(ester)_3^{2+*} + TMPD \rightarrow Ru(ester)_3^{+} + TMPD^{+}$$
$$-\Delta G° = 0.88 \text{ V} \qquad (100)$$

$$Ru(Me_2phen)_3^{2+*} + TMPD \rightarrow Ru(Me_2phen)_3^{+} + TMPD^{+}$$
$$-\Delta G° = 0.13 \text{ V} \qquad (101)$$

$$Ru(5\text{-}Clphen)_3^{2+*} + TMPD \rightarrow Ru(5\text{-}Clphen)_3^{+} + TMPD^{+}$$
$$-\Delta G° = 0.49 \text{ V} \qquad (102)$$

and found a significant increase in rate on warming from 77 to 298 K.

Most recently, McGuire and McLendon have reported on ET from photoexcited $Ru(LL)_3^{2+}$ to methylviologen in glassy glycerol. They observed a strong temperature dependence in the rate, from 253 to 150 K. The rate is nearly of Arrhenius form, which they blame on solvent dynamical effects.

Thomas and Milosavljevic[215b] have examined ET from photoexcited $Ru(bpy)_3^{2+}$ to methylviologen in cellophane. They find that the dependence on concentration can be fit with a modified Inokuti/Hirayama formula,[216] that the rates are lower than in glycerol, and that the small-polaron description of Jortner[144] properly describes the temperature dependence (flat at low T, activated at higher T).

These experimental studies of ET quenching suggest certain regularities in strongly exergic electron-tunneling ET in solids: modified Hirayama/Inokuti-type models[84] seem adequate to characterize the ET rates; k_{ET} seems to drop exponentially with distance; nuclear tunneling behavior leads to very weak T-dependence at low T, but activated behavior is observed for higher T; the rates seem to maximize for $\lambda \cong \Delta G°$, as expected from Marcus theory;[1,16] and for this value, again as expected, k_{ET} is really T-independent.

B. Pulse Radiolysis Generated Intermolecular Electron Transfer in Solids

The problems associated with the reactions of trapped electrons are mainly due to the difficulty of assigning a redox potential to the trapped electron; in addition, the reactions are so exoergic that electronically excited states may easily be produced. We will only consider pulse generated intermolecular ET in glassy matrices. Miller et al. considered[27] reactions of the type

$$D^- + A \rightarrow D + A^- \qquad (103)$$

with MTHF as the solvent. They used relatively large concentrations of a low-electron-affinity molecule (0.15 M or 0.30 M) and a much lower concentration (0.025 M) of a higher electron-affinity species. The frozen solutions ($T = 77$ K) were exposed to 20-ns pulses of

15-MeV electrons; this pulse ionization creates a certain concentration ($\approx 10^{-4}$ M) of trapped electrons and radical cations of MTHF. The cations are rapidly trapped by transfer of a proton to a neighboring solvent molecule. The trapped electrons will be transferred rapidly to the solute molecules. The solute anion radicals are detected spectrophotometrically, and the decay of the donor anion radical is followed. The exothermicities are determined from experimental reduction potentials. The $\Delta G°$ values used are from experiments performed in polar solvents; these $\Delta G°$ values are expected to differ slightly from the $\Delta G°$ values in the solid matrix. Since a small error in $\Delta G°$ might be very critical for these weakly exothermic reactions, Miller et al. only used acceptor/donor pairs of similar size and nature.

They interpreted their experimental results using eq 66. The matrix element t was assumed to decay exponentially

$$t(r) = t(R_0) \exp(-[r - R_0]/2a) \quad (104)$$

as for free barrier tunneling (eq 78). The Franck–Condon factor {FC} of (66) was evaluated using the formulation of small-polaron theory given by Ulstrup and Jortner,[104] in which the rate constant at fixed distance is given by:

$$k(r) = \nu \exp[-(r - R_0)/a] \quad (105)$$

$$\nu = [\pi/(\hbar^2 \lambda_0 k_B T)]^{1/2}\, t(R_0)^2 F = \nu_0 F \quad (106)$$

$$F = \sum_{W=0} e^{-S} \frac{S^W}{W!} \exp\left[-\frac{(\Delta G° + \lambda_0 + W\hbar\omega)^2}{4\lambda_0 k_B T} \right] \quad (107)$$

Here λ_0 is the solvent (outer sphere) relaxation energy, which is treated classically. The factor S is described in section V.A, and is $\lambda_i/\hbar\omega_i$. Only one vibration is considered in the λ_i term. When $[D^-] \ll [A]$, the surviving fraction of electron donors at time t is given by

$$P(t) = \exp[-(4/3)\pi C(R^3 - R_0^3)] \quad (108)$$

where C is the acceptor concentration (number per unit volume) and $R(t)$ is interpreted as the average radius of a reaction volume $V(t)$, approximated as

$$R = R_0 + a \ln(\gamma \nu_0 F t) \quad (109)$$

where γ is a dimensionless constant determined to be 1.9, so that the $P(t)$ from (108) agrees with the modified Inokuti–Hirayama ET quenching[84,216] model; eq 107 does not take orientational effects into account.

From the observable surviving fraction $P(t)$ it is possible to determine the ET rate constant as a function of distance for the randomly distributed solid solutions. F is normally considered to be time independent, and therefore neglects the time dependent solvent relaxation which occurs in rigid media (section V.C). Miller et al. presented[27] a detailed study of the biphenyl radical anion $BPh^{\bullet -}$ as donor. They measured the time-dependent concentration of $BPh^{\bullet -}$ absorbance and plotted A/A_0 against time, where A_0 is the absorbance in a sample containing the same concentration of BPh but no acceptor. A/A_0 measures the surviving fraction of $BPh^{\bullet -}$ anion radicals. The corrected A/A_0 plots for the ET $BPh^{\bullet -}$ reactions with four different acceptors [triphenylene ($-\Delta G° = 0.14$ eV), pyrene ($-\Delta G° = 0.52$ eV), fluoranthene ($-\Delta G° = 0.82$ eV), and 2-methylnaphthoquinone ($-\Delta G° = 1.81$ eV)] showed that it was necessary to make F time-dependent to allow for the solvent relaxation. The measurements also showed that the ET rate was largest for the reactions with intermediate exothermicities. Miller et al. also plotted the time-dependent function $R(t)$ which they called the "tunnel-distance" or the "reaction radius"; it is related to $P(t)$ by eq 108. These plots should be linear with a slope of a ln 10 if the ET rate is exponential in distance. Miller et al. explained the deviation from linearity and the different slopes for different reactions as due to the time dependence of the F-factor. By use of eq 105–109, the plot also gives the ET rate constant as a function of r. By using methyl-p-benzoquinone as acceptor with five different donor anion radicals, Miller et al. showed that the behavior of $BPh^{\bullet -}$ was similar to the four other donor compounds. They discussed the important issue of how ET rates depend on distance and reaction exothermicity. They plotted the ET rate vs. reaction exothermicity $-\Delta G°$ at different times; Figure 12, parts a and b, are for the times 10^{-6} and 10^2 s. These two show different values of $-\Delta G°$ for maximum ET rate; the plots for the longer times were broader and the weakly exothermic reactions were dramatically slowed. Miller et al. suggested that this was due to increased solvent reorganization energy with increasing time intervals, and fitted the experimental data by increasing the value of λ and assuming that a was independent of $\Delta G°$. They concluded that

(i) The ET rate constant is maximized for intermediate exothermicity.

(ii) The exothermicity corresponding to the maximum ET rate increases with time from ≈ 0.8 eV at 10^{-6} s to ≈ 1.1 eV at 10^2 s.

(iii) The shift of the position of the max ET rate is due to an increase of the solvent reorganization energy λ_0. They also fitted each decay curve to eq 109 with both a and $\nu_0 F$ varied to obtain the best fit. They obtained a range parameter a which increased with exothermicity from 0.14 to 0.96 Å, when the parameters a and $\nu_0 F$ of eq 109 were permitted to vary simultaneously.

The distance dependence of λ_0 was studied using the dielectric continuum expression to correct the experimental data of $BPh^{\bullet -}$ with naphthalene. This reaction is very weakly exothermic and should be quite sensitive to changes in λ_0. By doing simulations which included or omitted the distance dependence of λ_0 Miller et al. showed that the experimental data lies between the two simulated curves. They used their experimental data and the assumption that a is constant for reactions involving a certain donor compound and several acceptors for determining the value of a, and found a value $a \approx 0.8$ Å. Miller also studied[217] the ET between biphenyl and triphenylethylene (TPhE) in rigid glassy ethanol at 77 K. By use of the pulse radiolysis technique, the frozen matrix was ionized, and the changes in concentration of donor and acceptor compounds were followed by absorbance measurements over the time range 10^{-6} to 10^2 s. The surviving fraction of $BPh^{\bullet -}$ was measured by the ratio A/A_0. The experiments were analyzed in terms of an ET through an energy barrier with a height equal to the electronic binding energy of $BPh^{\bullet -}$.

Miller and Beitz used[167] pulse radiolysis to study the following reaction in rigid 2-chlorobutane glass at 77 K.

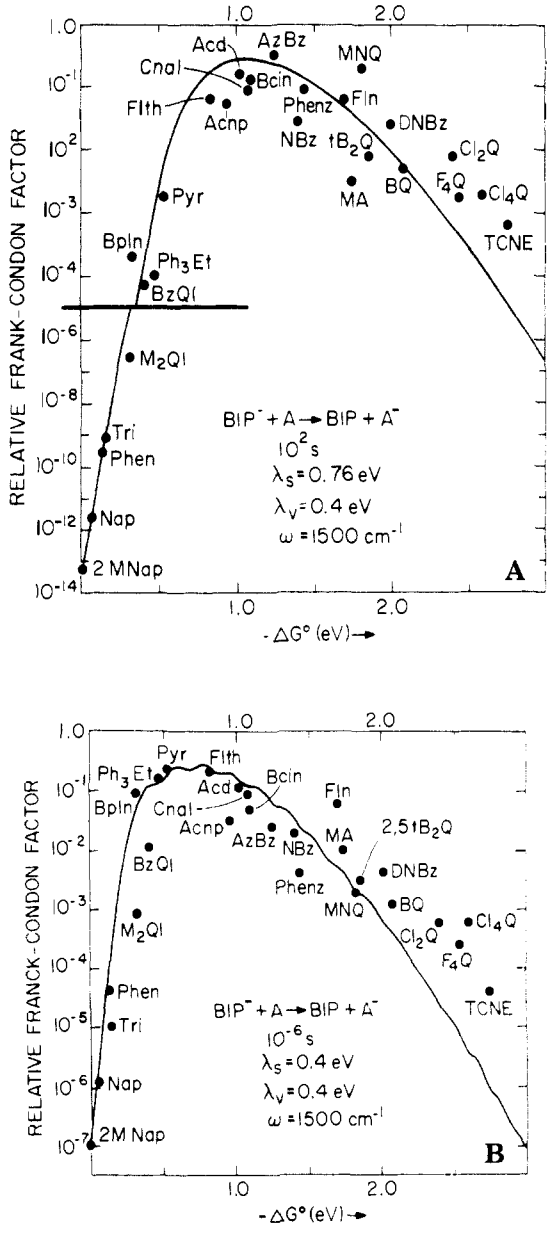

Figure 12. Relative rates for electron transfer from biphenyl anion at 77 K in methyltetrahydrofuran glass. The rate is expressed as a relative Franck–Condon factor, which is proportional to {FC} of eq 66. Allowing for experimental scatter and possible occurrence of excited states, the fit to a simple harmonic-oscillator form with one internal mode, as given by eq 107, is quite good (solid line); abnormal regime behavior (downward slope at the right of the curve) is clearly seen. Part A shows results at 10^{-6} s; Part B, at 100 s. Reprinted with permission from: Miller, J. R.; Beitz, J. V.; Huddleston, R. K. *J. Am. Chem. Soc.* **1984**, *106*, 5057. Copyright 1984, American Chemical Society. Compounds used as acceptors, given by the abbreviations in Figure 12a,b, and their $\Delta G°$ values[a] in eV: 2MNap = 2-methylnaphthalene (0.010), Nap = naphthalene (0.056), Phen = phenanthrene (0.13), Tri = triphenylene (0.14), M_2Q1 = 2,6-dimethylquinoline (0.31), Bpln = biphenylene (0.32), BzQ1 = 7,8-benzoquinoline (0.41), Ph_3Et = triphenylethene (0.47), Pyr = pyrene (0.52), Flth = fluoranthene (0.82), Acnp = acenaphthylene (0.95), Acd = acridine (1.02), Cnal = cinnamaldehyde (1.08), Bcin = benzocinnoline (1.09), AzBz = azobenzene (1.25), NBz = nitrobenzene (1.4), Phenz = phenazine (1.44), Fln = 9-fluorenone (~1.7), MA = maleic anhydride (1.74), MNQ = 2-methylnaphthoquinone (1.82), $tB_2Q/2,5tB_2Q$ = 2,5-di-*tert*-butyl-*p*-benzoquinone (1.85), DNBz = *p*-dinitrobenzene (2.00), BQ = *p*-benzoquinone (2.07), Cl_2Q = 2,5-dichlorobenzoquinone (2.40), F_4Q = tetrafluorobenzoquinone (2.54), Cl_4Q = tetrachlorobenzoquinone (2.59), TCNE = tetracyanoethylene (2.75). [a] *Free* energy change for ET from the biphenyl anion to the indicated acceptor.

$$BPh^+ + TMPD \rightarrow BPh + TMPD^+ \quad (110)$$

$$Py^+ + TEA \rightarrow Py + TEA^+ \quad (111)$$

$$Py^+ + TMPD \rightarrow Py + TMPD^+ \quad (112)$$

where Py = pyrene; BPh = biphenyl; TMPD = *N,N,N′,N′*-tetramethyl-*p*-phenylenediamine; TEA = triethylamine. The ratio A/A_0 is as before related to the survival ratio $P(t)$ of eq 78 and 104 for the cationic compounds (BPh^+,Py^+). The two reactions eq 110 and 112 were very fast, the decay was interpreted using eq 104. The range parameter a was determined from the experimental data to be 1.72 Å which corresponds to a donor electronic binding energy of ~1.3 eV when using the approximation in eq 78 and 104. This is not a reasonable value of the electronic binding energy since Bernas et al.[218] measured ionization potentials from TMPD in glassy 3-methylpentane 77 K as 5.75 eV and in glassy *n*-butanol (77 K) as 5.0 eV. When Miller and Beitz used more reasonable values for the electronic binding energy it was not possible to fit the experimental data using the simple tunnel model of eq 78. Instead they introduced the superexchange model (eq 77), and showed that this model was able to fit the experimental data when using reasonable values for the binding energies.

Kira et al. studied[219,220] ET from neutral donors (amines and aromatic hydrocarbons) to cationic acceptors in *sec*-butyl chloride (BuCl) glasses at 77 K. The cationic acceptors were generated by the irradiation of the sample by a 2-μs electron pulse.

$$D + A^+ \rightarrow D^+ + A \quad (113)$$

They used the theoretical survival ratio of the acceptors as given[84] by Inokuti and Hirayama, and assumed that the electronic interaction term was the same for reactions with a fixed donor and a variety of acceptors. Therefore any change in the survival ratio is assumed due to the FC factor. With this approach the survival ratio decay curves for a common donor and different acceptors should be related by a horizontal shift of the curves. The experimental data do not support this, since the curves seem to flatten as the exothermicity of the reaction decreases. According to the method of Kira et al., the {FC} factors for ET from trimethylamine (TEA) and *N,N*-dimethylaniline (DMA) to various solute cations as a function of the exothermicity of the reaction are plotted in Figure 13. The free energy difference is calculated by

$$\Delta G° = -(IP(A) - IP(D)) \quad (114)$$

where IP(A) and IP(D) are the gas phase ionization potentials for the acceptor and donor compound. These gas phase IP's should be corrected for the medium effects. Figure 13 shows that the {FC} factor increases until $-\Delta G° \sim 0.8$ eV and thereafter becomes clustered. According to Kira, excited electronic states would be unimportant due to the small exoergicity of these reactions.

The various experimental efforts using pulse radiolysis to prepare ET donors can, at least qualitatively, be explained using the nonadiabatic small-polaron-type ET theories of section V.A. Both solvent and inner-shell reorganization must generally be included. Both some of the special effects described in Chapter V (solvent relaxation dynamics and electronic structure effects) as

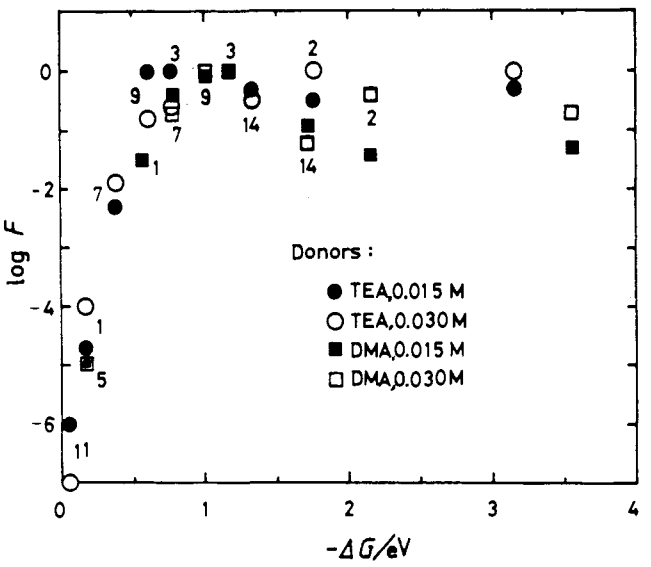

Figure 13. Franck–Condon factors for electron transfer from amines to cationic acceptors. The measurements were made in *sec*-butyl chloride glass at 77 K. The four points to the extreme right are for transfer to a trapped hole. There may be some slowdown in the rate in the abnormal region ($|\Delta G°| > 1.0$ eV). From: Kira, A.; Nosaka, Y.; Imamura, M. *J. Phys. Chem.* **1980**, *84*, 1882. Kira, A. *J. Phys. Chem.* **1981**, *85*, 3647. Compounds used as acceptors, given by numbers in Figure 13, and their ionization potentials in eV: (1) acenaphthene (7.66), (2) benzene (9.25), (3) biphenyl (8.27), (4) *N,N*-dimethylaniline (7.10), (5) diphenylamine (7.25), (6) durene (8.03), (7) fluorene (7.78), (8) hexamethylbenzene (7.90), (9) naphthalene (8.10), (10) phenanthrene (7.93), (11) pyrene (7.55), (12) triethylamine (7.50), (13) 1,2,4-trimethylbenzene (8.27), (14) toluene (8.82).

expected for nonadiabatic ET in solids and the strong dependence of k_{ET} on exoergicity $\Delta E°$, with a rate maximum near $-\Delta G° = \lambda$, are observed. A great deal remains to be done both in experiment and in interpretation.

C. Electron Transfer in Biologically Related Systems at Low Temperature

Low-temperature studies of ET in biological systems comprise one of the clearest examples of ET in solids, since the biological systems can be studied as frozen systems similar to the glassy matrices just discussed. Since the area of biological ET has been reviewed recently[13-15] we emphasize here more recent work. Experiments in this area began with the pioneering study by DeVault and Chance[221] on the reaction center in the photosynthetic bacterium *C. vinosum*. They studied the photon excitation of the bacteriochlorophyll dimer $(BCh)_2$ from room temperature to liquid helium temperature using a pulsed laser with fast scan spectrophotometric detection. They found that when $(BCh)_2$ was photooxidized, an electron was transferred to $(BCh)^+$ from one of the surrounding cytochromes, and by observing the oxidized cytochrome they were able to measure the ET rate of the reaction. They also observed that the activation energy for the process changed from 3.3 kcal/mol for temperatures above 130 K to less than 4 cal/mol for temperatures less than 100 K. They explained the experimental data in terms of an electron-tunneling mechanism. As a followup of this study, Kihara and Chance studied[222] 15 different photosynthetic bacteria at liquid nitrogen temperature and found that most of these were able to photooxidize the cytochrome in a manner similar to that in *C. vinosum*.

More recently, Hoffman et al.[223-227] have described ET between donor (D) and acceptor (A) sites with crystallographically known distances and orientations. They used a mixed-metal hemoglobin hybrid. The hemoglobin consists of two identical bimetallic subunits α and β. They are here denoted $\alpha_1,\alpha_2,\beta_1,\beta_2$ and form a complex with very specified geometry. The mixed-metal [Zn,Fe] hybrid hemoglobin was prepared by substituting both chains of one type (either α or β) with a zinc(II) porphyrin ($Zn^{II}P$); both chains of the other type contain the ferriheme group. In this structure the closest redox centers are the α_1 and β_2 subunits, with a Zn(II)–Fe(III) distance of approximately 25 Å. The distance between the redox centers for the α_1 and β_1 subunits is about 35 Å which led Hoffman et al. to neglect ET between them, leaving only the reaction between the redox centers for the α_1 and β_2 subunits. They used flash photoexcitation for initiating the reaction, thereby favoring the longlived ZnP triplet state. This triplet state may either decay to the ground state or transfer an electron to the $Fe^{III}P$ group

$$^3ZnP + Fe^{III}P \xrightarrow{k_{ET}} (ZnP)^+ + Fe^{II}P \qquad (115)$$

The reduction potential of reaction 115 is about 0.8–0.9 V.

The observable rate constant for the decay of the triplet state (^3ZnP) is a sum of an intrinsic triplet decay rate constant for the decay to the ground state of ZnP and a rate constant for the ET reaction in eq 115. The ET rate constant was determined by subtracting the rate constant for the decay of the triplet from the observable rate constant. The intrinsic triplet decay rate constant was measured by doing similar experiments with the hybrid hemoglobin containing Fe^{II} instead of Fe^{III}, thereby not allowing decay via ET. The products formed by reaction 115 will react by ET from $Fe^{II}P$ to $(ZnP)^+$:

$$(ZnP)^+ + Fe^{II}P \xrightarrow{k_{GET}} ZnP + Fe^{III}P \qquad (116)$$

The reduction potential for the reaction 116 is about 0.85–1.0 V. The rate constant associated with reaction 116, k_{GET}, is much larger than k_{ET} and has not been accurately measured. For the $[\alpha(Zn),\beta(Fe^{III}H_2O)]$ hybrid as for the *C. vinosum* system,[221] the k_{ET} changes smoothly from being activated at high temperature to being temperature independent below 77 K (Figure 1). From a study of the temperature response of the $[\alpha(Zn),\beta(Fe^{III}H_2O)]$ optical spectrum, it was concluded that the ligation state of the ferriheme remains invariant upon cooling. Therefore k_{ET} seen in Figure 1a is the rate constant for the ET from $^3ZnP(\alpha_1)$ to $Fe^{III}(H_2O)(\beta_2)$. The $[\alpha(Fe^{III}),\beta(Zn)]$ hybrid shows different temperature response for k_{ET}, since there is a plateau in the temperature interval 230 to 270 K (Figure 1b); this effect has apparently nothing to do with the properties of the solvent, since it occurs above the freezing point and does not occur for the other hybrid. Hoffman et al. explained this in terms of replacement of the ferriheme axial ligands ($H_2O \rightarrow$ imidazole). For the low temperature region, the ET rate constant is measured to be about 9 s^{-1} for the two different complexes, even though they have different ferriheme axial ligands in this region. These long-range ET have been explained in terms of the small-polaron-type models described in sections III, IV, V. At low temperatures,

the reaction involves both electron tunneling (nonadiabaticity) and nuclear tunneling through the barrier ($\eta_1 \ll 1$, $\eta_3 \ll 1$, $\eta_2 \ll 1$ in Chart II of section V). At higher temperature, η_3 becomes larger and activated behavior is observed. The very small rate constants, of order 10^2 s^{-1}, arise because both the electronic factors and {FC} factors of eq 66 are unfavorable for these transfers.

Wasielewski et al.[228] studied the photoinduced ET reactions in a chlorophyllide–pheophorlide cyclophane which was chosen for modeling the primary donor–acceptor pair in the green plant photosystem. They measured among other things the temperature dependence of the fluorescence decay in butyronitrile and concluded that below the freezing point the ET could not occur. Above the freezing point they observed decreasing ET quenching with decreasing temperature. They related this to the inability of the solvent to relax and stabilize the ion pair on the formation of a new conformation at low temperatures.

Bolton et al. studied[229] the photoinduced ET in porphyrin–quinone complexes with a diamide bridge where n = 2,3,4 (PAnAQ) is the number of CH_2 groups between the two amides. They irradiated the PAnAQ compounds and observed the EPR signals corresponding to formation of the linked radical ion pair $P^{\bullet+}$-$AnAQ^{\bullet-}$. For the low-temperature region they used 10 different frozen solvents as media for the intramolecular ET. The quantum yields for the appearance of $P^{\bullet+}$-$AnAQ^{\bullet-}$ were measured using EPR. They found that quantum yields for production of $P^{\bullet+}AnAQ^{\bullet-}$ increase with temperature in solid matrices and indicated that this might be due to restrictions on the vibrational motion. They stated from spectroscopic analysis that these linked molecules seemed to exist in two types of conformation. One of these is denoted "complexed" and seems to be folded in such a way that the porphyrin and the quinone are sufficiently close for their π-electron systems to interact directly. The other type is denoted "extended" and here the porphyrin and the quinone do not interact directly in any significant manner. Bolton et al. explained the decrease of ET quenching with decreasing temperature in the glassy matrices as arising from restriction in the thermal fluctuation and vibration (for example, rotation around the amide link), thereby limiting the number of PAnAQ complexes having the optimum configuration for ET.

Loach et al. have studied[230,231] the photoinduced fluorescence decay of bridged zinc porphyrin–quinone complexes at low temperatures (77 K) using EPR measurements. This work pioneered the synthesis of models for the primary photochemical sequences in bacterial photosynthesis. They were the first to prepare a porphyrin/quinone moiety covalently linked together by a diester. More recently, this work was extended to study fast ET (nanoseconds) in liquids.[232] In addition, in liquid solution there has been very elegant and exciting recent work by Gray,[233] Isied,[234] McLendon,[235] and their collaborators on intramolecular ET in biologically-related species (modified cytochromes, peptides, azurin, etc.). These experiments have not yet been extended to solids.

D. Intramolecular Electron Transfer in Non-Biological Compounds in the Solid State

Kinoshita et al. have studied[236] thermally induced intramolecular ET in solids for complexes with the formulas Co^{III}(SALEN)L where SALEN is *N,N'*-ethylenebis(salicylideneaminato) and L is a series of four different 2,4-pentanedionates. ET from the L ligand to the Co^{III} ion occurred upon heating the solid Co^{III}(SALEN)L. The ET rate constant increased in the following order acetylacetonato < propynylacetonato < *n*-butyrylacetonato < *n*-caproylacetonato. From their kinetic analysis they concluded that the ET rates seemed to be dominated by entropy effects since the activation enthalpy *decreased* in the above order. Ihara et al.[237] also studied the ET of Co^{III} complexes in the solid phase. The Co^{III} complexes had the form *trans*-$[Co(A_2)(phbgH)_2]X_3 \cdot nH_2O$, where A denotes volatile ligands as NH_3, CH_3NH_2, and C_5H_5N, and phbgH denotes 1-phenylbiguanide. X denotes either Cl^- or Br^- and n = 2, 3. They observed ET reactions by heating the solid Co^{III} complexes, and found the following order of reactivity:

(i) $$NH_3 < CH_3NH_2 < C_5H_5N$$

(ii) $$Br^- < Cl^-$$

They argued that the liberation of the coordinated A is part of the rate-determining step (the strength of the ligand field shows the opposite order of that in (i)). The differences between the halides was explained in terms of the anation (halide/H_2O ligand exchange) and addition to the phbgH group.

Leland et al. studied[34] linked porphyrin quinone systems A and A1 using picosecond-fluorescence experiments. ET occurs between a quinone and zinc mesophenyloctaalkylporphyrins; the linking part of the compound was one (A) or two (A1) bicyclo[2.2.2]octyl spacers. Their experiments make it possible to discuss the effect of distance between the ET centers since the driving force, the solvent, the orientation, and the type of linker are unchanged. A2 was used as a reference compound for the non-ET decay of the excited state of the porphyrin part. For A and A1 they observed a decrease of the fluorescence lifetimes compared to A2. They assumed this decrease to be due to ET quenching, and obtained the ET rate constants in the usual way from

$$k_{ET} = \frac{1}{\tau_{obsd}(i)} - \frac{1}{\tau_0}$$

where $\tau_{obsd}(i)$ is the experimentally-determined fluorescence lifetime for compound i (i = A,A1) and τ_0 is the observed fluorescence lifetime of A2. They determined k_{ET} for compound A to be $5.0 \times 10^9 - 1.5 \times 10^{10}$ s^{-1}, depending on the solvent at 298 K, with k_{ET} for A1 $\leq 10^7$ s^{-1}. This difference was related to different linkers and therefore to the different distances between the porphyrin and the quinone. They estimated (Table II) the range parameter a in the ET matrix element expressed as in eq 104, since {FC} was assumed the same for A1. The ET rate for A decreases when the polarity of the solvent is increased. To compare the ET reactions they performed similar experiments at low temperature in a MTHF glass, finding that the fluorescence decay for A could be explained by an ET quenching, taking account of the angular orientation of the por-

TABLE II. Experimental Values of *a* from the Literature

system[a]	*a*, Å	experiment	ref
Al/fa/Hg,Al,Au	0.67	conduction	*c*
Al/fa/Mg	1.0	conduction	*c*
Al/fa/Al	1.3[b]	conduction; multilayer structure	*d*
Al/fa,dye/L	2.0–0.3	photoconduction; multilayer structure	*e*
dye/fa/acceptor	3.3	fluorescence quenching	*f*
Al/fa/anthracene crystal	2.2	photoconduction	*g*
Al/fa/chloranil crystal	1.25	photoconduction	*g*
biphenyl–triphenylethylene	0.9–1.0	pulse radiolysis in frozen ethanol, 77 K	*h*
biphenyl–several aromatics	0.83	pulse radiolysis in frozen TMHF, 77 K	*i*
biphenyl–tetramethylphenylenediamine	0.86	pulse radiolysis in frozen 2-chlorobutane, 77 K	*j*
pyrene–tetramethylphenylenediamine	0.86	pulse radiolysis in frozen 2-chlorobutane, 77 K	*j*
derivatives of the cytochrome *c*/cytochromato complex	0.67	pulse radiolysis in solution (room temperature(?))	*k*
aromatic donors and acceptors	0.75	fluorescence quenching in TMHF ethanol, *trans*-1,5-decalindiol at different temperatures	*l*
naphthalene and CCl_4	0.5	fluorescence quenching in ethanol at 77 and 140 K	*m*
pentacene and duroquinone	0.35	fluorescence quenching in sucrose octaacetate glass at room temperature	*n*
ruthenium compounds and methylviologen	0.75	fluorescence quenching in glycerol	*o*
ruthenium compounds and organic reductants	0.78–1.00	fluorescence quenching in polymeric film	*p*
porphyrins linked to quinones	≤0.71	fluorescence quenching	*q*
indole and chlorinated methanes	0.52	fluorescence quenching in ethanol glass, 76, 93, 117 K	*r*

[a] Fit of electron transfer rate constant to $k_{ET} \propto \exp\{-r/a\}$. Al/fa/contact layer describe a capacitor with a medium consisting of a monolayer of fatty acids (fa) {often with added dye} in between an Al plate and another contact layer. [b] The fit is poor. [c] Mann, B.; Kuhn, H. *J. Appl. Phys.* **1971**, 42, 4398. Polymeropoulos, E. E. *J. Appl. Phys.* **1977**, 48, 2404. [d] Sugi, M.; Fukui, T.; Iizima, S. *Appl. Phys. Lett.* **1975**, *27*, 559. [e] Sugi, M.; Nembach, K.; Möbius, D.; Kuhn, H. *Solid State Commun.* **1974**, *15*, 1867. [f] Kuhn, H. *J. Photochem.* **1979**, *10*, 111. [g] Killesreiter, H.; Baessler, H. *Chem. Phys. Lett.* **1971**, *11*, 411; *Phys. Status Solidi* B **1972**, 51, 657. [h] Miller, J. R. *Science* **1975**, *189*, 221. Alexandrov, I. V.; Khairutdinov, R. F.; Zamaraev, K. I. *Chem. Phys.* **1978**, *32*, 123. [i] Miller, J. R.; Beitz, J. V.; Huddleston, R. K. *J. Am. Chem. Soc.* **1984**, *106*, 5057. Miller, J. R.; Bertz, J. *J. Chem. Phys.* **1981**, *74*, 6746. [k] Miller, J. R.; McLendon, G. *J. Am. Chem. Soc.* **1985**, *107*, 7811. [l] Miller, J. R.; Peeples, J. A.; Schmitt, M. J.; Closs, G. L. *J. Am. Chem. Dokl.* **1982**, *104*, 6488. [m] Khairutdinov, R. F.; Sadovski, N. A.; Parmon, V. N.; Kuz'min, M. G.; Zamaraev, K. I. *Dokl. Akad. Nauk. SSSR* 1975, *220*, 888. [n] Domingue, R. P.; Fayer, M. D. *J. Chem. Phys.* **1985**, *83*, 2242. [o] Guarr, T.; McGuire, M.; Strauch, S.; McLendon, G. *J. Am. Chem. Soc.* **1983**, *105*, 616. [p] Guarr, T.; McGuire, M.; McLendon, G. *J. Am. Chem. Soc.* **1985**, *107*, 5104. [q] Leland, B. A.; Joran, A. D.; Felker, P. M.; Hopfield, J. J.; Zewail, A. H.; Dervan, P. B. *J. Phys. Chem.* **1985**, 89, 5571. [r] Naimiki, A.; Nakashima, N.; Yoshihara, K. *J. Chem. Phys.* **1979**, *71*, 925.

phyrin and quinone parts of the compound. From this they calculated an ET rate constant approximately equal to the room temperature ET rate constant in MTHF and therefore concluded that the ET reaction for A is temperature-independent within a factor of two.

Very recent work by Miller and collaborators[237a] involves ET between aromatic substituents in adiabatic fused ring systems at room temperature. These reactions were carried out in liquid MTHF, and therefore strictly fall outside our scope, but the results are of real interest with regard to the electronic structure arguments of section V. They observe quite different rates dependent on the isomers (axially or equitorially substituted). This dependence is a particularly striking example of nonadiabatic ET with strong matrix element effects on the rate.

Michel-Beyerle et al.[238] have synthesized four compounds with linked donor and acceptor parts. They used dimethylaniline as the donor part and pyrene or anthracene as the acceptor part. The linkage was either a $-CH_2-(C_6H_4)-CH_2-$ bridge or a 4,4′-dimethylbiphenyl bridge. They excited the acceptor part and measured the fluorescence lifetimes for the four acceptor bridge–donor compounds and two reference compounds. All their experiments were done at room temperature and in liquid solvents. Similarly, Hush et al.[239] have examined ET in photoexcited intramolecular systems comprising an acceptor quinone and a photoexcited donor linked by rigid fused norbornyl bridge (C). They observe ET rate constants of $>5.10^{10}$ s^{-1} for C in water at 298 K, and also find that the rate drops by a factor of at least 3 on extending the length of the bridge from three to four norbornyl units. The work of the Sydney and Munich groups, like that from Pasadena and Argonne, involves elegant synthesis and spectroscopy. Extension of their measurements into the solid state should shed further light upon just what mechanisms in fact mediate bridge-assisted ET tunneling in solids; the norbornyl groups in particular are very attractive species, since length of bridge and orientation angle may be controllably varied.

E. Mixed-Valence Electron-Transfer Reactions in Solids

Since mixed-valence ET reactions have been reviewed recently,[11,21,23,240] we consider here only more recent experiments on mixed-valence ET in solids. Rosseinsky et al.[241] examined mixed valence (Robin/Day II) potassium manganate–permanganate $K_3(MnO_4)_2$, a MnO_4^-–MnO_4^{2-} mixed-valence solid. Their experimental observations were used for testing the diffusive hopping conductivity expression

$$\sigma = n\, e^2\, a^2\, \nu_{ET}/6k_BT \qquad (117)$$

where σ is the dc conductivity, n is the number density of charge carriers, and a is the distance between transfer sites; ν_{ET} is the hop frequency for ET between the transfer sites. They performed dielectric measurements for the dc conductivity and determined the ET frequency ν_{ET} from dielectric relaxometry. They compared the values of σ calculated from eq 117 and the measured ν_{ET} with the observed values of the dc conductivity σ_{obsd} and found agreement within the experimental error; therefore in this situation the simple diffusive hopping expression (117) seems adequate. They also studied the temperature dependence of both ν_{ET} and σ_{obsd} and determined activation energies, which were compared to

those for the solution reaction:

$$MnO_4^- + MnO_4^{2-} \rightarrow MnO_4^{2-} + MnO_4^- \quad (118)$$

E_A for the solution reaction was corrected for the work terms needed for assembling the precursor. They found that all three activation energies (for σ_{obsd}, ν_{ET} in the solid, and k_{ET} in solution) were identical within experimental error. These experimental observations suggest a similar mechanism (site-to-site transfer) for the MnO_4^-–MnO_4^{2-} reaction in liquid and solid. This work represents a particularly nice example of the similarities and differences between solid-state and liquid-state ET discussed in section II.

Hendrickson et al. have studied[242-245] intramolecular ET in mixed-valence dialkylbiferrocenium salts and in trinuclear oxo-centered mixed-valence iron acetates. For both series of compounds they observed that the rate of intramolecular ET is affected by dynamics in the solid state. For the mixed-valence biferrocenium they suggested that the position of the anion I_3^- largely determines the intramolecular ET between the two metal centers, and they related the observed temperature dependence in the Mossbauer spectra to a phase transition involving motions of the I_3^- ions. The rate of intramolecular ET in the solid state of mixed valence trinuclear iron acetate complexes was observed to be partly determined by the dynamics of the coordinated ligands or solvate molecules. They prepared a series of trinuclear iron acetates which differed only with respect to the solvate molecules $[Fe_3O(O_2CCH_3)_6(py)_3]$-(solvate), where solvate is pyridine, benzene, or nothing. The mixed-valence compound without solvate molecule did not show any change in intramolecular ET when changing the temperature from 120 to 315 K. For the pyridine–solvate mixed-valence compound, they observed an increase in the intramolecular ET rate as the temperature was increased and for temperatures larger than 200 K they reported an ET rate greater than 10^8 s^{-1}. The compound having benzene as solvate showed a different temperature dependence. For the mixed-valence compound $[Fe_3O(O_2(CH_3)_6(4\text{-Et-py})_3](4\text{-Et-py})$, where 4-Et-py is 4-ethylpyridine, they suggested the intramolecular ET in the solid was related to the motion of one of the three ligands 4-Et-py as the temperature was increased.

The dependence of k_{ET}, and indeed of Robin/Day classification,[24] of mixed-valency species upon counterion and upon solvent is not at all unexpected. The nature of the electronic state as localized or delocalized is determined, for symmetric species, largely by η_1, of section V.A—that is, by the competition between electronic delocalization energy and polarization terms describing reorganization of the intramolecular and solvent coordinates. Increased solvent polarity or polarizability should increase the solvent reorganization energy, thereby favoring localized (Robin/Day II) valency. For unsymmetric species in which $\Delta E^\circ \neq 0$, there will be an additional localization effect arising simply from the different potentials at different sites in the molecule. Very much the same behavior can be caused by strong ion pairing with a small counterion or even by a strain field due to the environment. All of these terms cause the electronic hamiltonian of eq 59 to become asymmetric (that is, they cause $\epsilon_l \neq \epsilon_r$) and can lead to localization. In the theory of the Jahn–Teller effect,[246,247] these terms[248] are generally lumped together as strain effects, and can cause very large changes in the electronic properties and in spectroscopic (EPR, optical, vibrational) and even structural properties. The celebrated Creutz–Taube ion B is structurally symmetric in frozen aqueous solution with a chloride counterion, but asymmetric, with a difference of .015 Å in Ru–*trans*-NH_3 distance, with a tosylate counterion.[141] Recently, Hendrickson and co-workers[249] have examined intramolecular ET in dihalobiferricinium salts. They find that the dichloro compound is valence-localized, with specific Fe^{+2} and Fe^{+3} cations, while the diiodo compound shows crystallographically equivalent metals. They conclude that this difference is due neither to differences in electronic nor in vibronic coupling, but rather to "differences in the symmetry of the solid-state environment." That is precisely the generalized "strain" effect which we have just discussed.

In an attempt to understand the role of solvent dynamics, Meyer and Schanze studied[250] ligand-bridged osmium dimers of the type

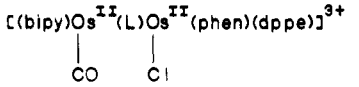

where bipy is 2,2′-bipyridine, dppe is *cis*-$Ph_2PCH{=}CHPPh_2$, phen is 1,10-*o*-phenanthroline, and L is 4,4′-bipyridyl or related bridges. Excitation of the dimers in the MLCT band caused appearance of excited-state $Os^{III}(phen^{\bullet-})$ whose decay lifetime in frozen ethanol–methanol at 77 K was studied. They related the quenching of the photochemically prepared mixed-valence dimer to an intramolecular ET ($Os^{II} \rightarrow Os^{III}$) process. For the decay of $[(bipy^{\bullet-})(CO)Os^{III}(L)Os^{II}$-$(phen)(dppe)Cl]^+$ they found the intramolecular mixed-valence ET rate constant k to be temperature independent for 77–120 K ($k \sim 2.2\ 10^7\ s^{-1}$) and temperature dependent for temperatures larger than 130 K ($k \sim 4.8\ 10^7\ s^{-1}$ for 160 K). Indeed, "once the glass-to-fluid transition transition is reached, there is a marked decrease in lifetime." This interesting observation confirms the intuitive suggestion (section III) that the more rapid relaxation processes and higher fluidity (lower viscosity) in liquid as opposed to solid hosts should significantly change (generally increase) ET tunneling processes. This should occur because upon melting there is a shift of vibrational state density toward lower frequency, which will cause stronger damping.[251] More work along these lines would be of real value in further illuminating these differences.

VII. Remarks

Solid-state electron transfer reactions can occur on time scales running over at least 13 orders of magnitude, from the very fast resonant tunneling transfer through heterostructures (section III) to long-distance highly exoergic tunneling in matrices (section VI). From a mechanistic viewpoint, the essential small polaron requirement for occurrence of a "coincidence event", in which the geometry of donor and acceptor sites has fluctuated until electron tunneling or delocalization can occur following Franck–Condon conditions (no change in electronic energy or in nuclear position or momentum) seems correct both intuitively and, so far as the data permit interpretation, experimentally. The ori-

ginal analysis of Marcus in terms of activated-complex theory is, in fact, essentially equivalent conceptually to the polaron picture, though there are differences in the actual treatment of the vibrational motions. Despite the fundamental value of this approach, there remain a host of unresolved questions which make tunneling in solid-state ET reactions an area of great current interest. These include

(1) The proper description of the initial and final states for ET—to what extent is the electron localized, and how do changes in the electronic structure of these states change the ET rate? Recent theoretical work involving variational selection of reaction-state geometries (section V.D) indicates that major mechanistic and rate constant changes can occur depending on actual geometric and electronic structure of the initial states; in some cases, substantial delocalization of the electronic wave function in the initial state can provide both enhanced ET rates and exquisite sensitivity to modifications in electronic structure due to bridges or substituents. In a larger sense, it is certainly more appropriate to begin the discussion of ET processes using the full electron–nucleus hamiltonian, rather than simple two-site representations. Such full description will be especially useful in situations of long-range and facilitated ET.

(2) The physical geometry of the solid in which ET occurs. Clearly, motions which are permitted in liquids can be frozen out in the solid state, and therefore certain ET pathways can be very much reduced in efficiency. For example, intermolecular transfer in a diamide-linked porphyrin/quinone species was observed[229] by Bolton et al. to occur in solution via two pathways, one involving transfer through the bridge, the other arising from diffusive motions allowing direct contact of porphyrin acceptor and quinone donor. In a solid, the latter pathway would be foreclosed if the structure was extended, and dominant if the structure placed the quinone close to the porphyrin. Thus actual structural details, which are strongly history-dependent and will not be "washed out" in the solid as they are in solution, should be considered in discussion of ET rates. These effects will be less important as temperature increases, and some diffusion begins to occur in the solid.

(3) The role of solvent dynamics in affecting the rate. The generalized friction models first introduced[177] by Kramers represent an extension of activated complex theory which takes cognizance of finite relaxation-time effects in the nuclear motions which accompany ET. Both formal study (section V.C) and some experimental comparisons (section VI.A,B) have indicated that these frictional effects can change the numerical value of k_{ET} and even the mechanism: apparently nonadiabatic transfers (in which electron tunneling appears as the preexponential in k_{ET}) can become adiabatic (independent of electron tunneling) if the slow relaxation processes keep the system in the vicinity of the coincidence event, or saddle point, geometry for a long enough time. Proper microscopic understanding of the friction, as well as detailed experimental study of the frictional effects on the solid-state ET rate and on its temperature dependence, are still lacking.

(4) The dependence of the ET rate on the nuclear motions of the medium in which ET occurs. There has been extensive work[185] on corrections to the continuum electrostatic description of the outer-shell vibrational contributions to the rate, but effects of disorder or phonon dispersion or impurities or librational/orientational dynamics on the rate remain largely unexplored. In addition, the possibility of "triggering" events, in which an ET process becomes permitted only when a particular geometric constraint is relaxed by nuclear motion, is a fascinating but largely undocumented one. The allosteric control of many biological rate processes, including ET, represents one type of triggering phenomenon; the abrupt change in k_{ET} seen near 250 K in Figure 1b is most simply interpreted as due to such a triggering phenomenon arising from change in the axial ligands of the metalloporphyrin. Finally, the actual electron/nuclear coupling (Born–Oppenheimer breakdown) is usually oversimplified; proper calculation of the rate should consider all effects of the nuclear kinetic energy operator.

(5) The dependence of the rate on the electronic structure of the material which intervenes between donor and acceptor. Many theoretical models have been put forward to explain the dependence of the electron tunneling amplitude H_{12} (eq 74) or t (eq 66) on the electronic structure of the "bridge" species between A and D. The superexchange model (eq 77) and the barrier tunneling picture (eq 78) are the simplest semianalytic forms to use for calculating the contributions of bridge or medium electronic states to k_{ET}. Perturbation–theoretic arguments also lead to superexchange type formulas, and permit use of local electronic structure information (one-electron energies and overlaps) to evaluate effective t or H_{12} values. Alternatively, the electronic structure of the entire D/bridge/A structure can be studied and the splitting of D,A states used to evaluate H_{12} (section V.3). Such evaluation puts very stringent precision requirements on the electronic structure study, since typical nonadiabatic t or H_{12} values are generally less than 0.1 eV. Dynamical propagator studies[100] (eq 83) or direct evaluation of the matrix elements[100,102,103] are probably more promising, but not enough has yet been done using dynamical evolution with realistic, as opposed to highly idealized, electronic structure problems.

There are important generalities concerning the electronic structure effects on tunneling ET. For example, resonant tunneling is greatly faster than nonresonant (theoretically this is because even very small perturbations will mix degenerate levels; experimentally, it is best observed in mixed valency situations or in heterostructure ET such as that shown in Figures 8 and 9). More precise experimental study of the dependence of k_{ET} upon exoergicity in the near resonance case of very small exoergicity will be of real interest in examining how energy is in fact conserved in ET (is resonance with the pure electronic state really required?). At the other end of the gap, although the inverted behavior (rate decreasing with $|\Delta E^\circ|$ for $|\Delta E^\circ|/\lambda > 1$) has now been seen in several experimental studies, its final understanding awaits even more clear experimental verification, especially with truly molecular systems, than is now available: both time-resolved and carefully energy-resolved values of k_{ET} are needed.

Finally, the distance dependence of k_{ET} is still not properly understood: it is nearly always fit to an ex-

ponential as in eq 87, which is justified either by the barrier tunneling idea of eq 88 or by the fact that the direct overlap of electronic wave functions decreases exponentially at long distances. Exponential behavior can also be derived, for a repeating bridge, from the superexchange form of eq 77 [$H_{12} \sim (t_s/B)^n = (e^{-c})^n = e^{-cr/d}$, where n is the number of bridging sites and c,d are constants]. Experimentally, exponential behavior has been invoked in many cases, and some of the demonstrations, as with tunneling through Langmuir–Blodgett films of fatty acid, are convincing. But several unsolved problems remain. One involves the distance threshold for exponential behavior: adiabatic ET should be roughly distance independent, and the minimum distance beyond which k_{ET} should decay as in eq 89 has not been established (it must depend on the four smallness parameters η_1–η_4 of section V.A). A second involves actual data analysis—in fitting observed data to k_{ET} expressions such as eq 87, dispersion in the data is generally ignored. In the absence of such analysis, the fitted data are much less useful. A third centers on some recent theoretical ideas about distance dependence, one involving a suggestion[252] that the Franck–Condon principle is invalid for long-distance ET, another a statement[253,254] that at long range, k_{ET} should go like $\exp\{-\alpha r - \beta r^2\}$. Both of these are, at this point, ingenious but speculative ideas which have generated a great deal of discussion and disagreement:[255,256] the field is a very lively one.

A final issue involves the actual facilitating role of the medium between redox centers: is it always either superexchange (as has been argued in molecular ET in glasses) or actual stepwise transfer (as in photosynthetic ET pathways), or can other mechanisms occur? One might suspect that coherent (bandlike, delocalized) electronic states are important for ET events like the resonant transfers responsible for the peaks in Figures 8 and 9. Clearly there is a relationship among exoergicity, temperature, vibronic coupling, and electron tunneling, as expressed in η_1–η_4, and more experimental investigation of ET mechanisms in the parameter space of η_1–η_4 is needed. Particularly promising experimental approaches to such studies include modified protein centers in which $\Delta E°$ can be made close to zero, artificial structures such as Langmuir–Blodgett films and the heterostructures discussed in section III.B.3, and intramolecular ET systems with rigid bridges of variable length and orientation, as discussed in V.D,E. For any or all of these, measurement of k_{ET} should be carried out as the exoergicity, temperature, and geometry are varied.

It has now been a bit more than three decades since careful experimental and theoretical research began on liquid-state ET reactions. That research area has been one of the most fruitful and rewarding ones in physical, inorganic, and biological chemistry. Very recent experimental and theoretical advances have made solid-state ET a very exciting and fast-moving research area; both its intrinsic interest and its widespread application indicate that this field will continue to be a centerpiece area of chemical research.

Note Added in Proof. A recent issue of *The Journal of Physical Chemistry* (1986, Vol. 90, No. 16) contains a number of important contributions concerning solid state ET reactions.

Acknowledgments. We are grateful to P. D. Hale, F. Lewis, B. M. Hoffman, K. G. Spears, R. P. Van Duyne, N. S. Hush, R. C. Hughes, S. F. Fischer, E. Dalgaard, J. Eriksen, J. R. Miller, R. Zwanzig, and M. J. Weaver for helpful remarks. We thank the Chemistry Division of NSF and the Gas Research Institute and Statens Naturvidenskabelig Forskningsraad [Denmark] for partial support of this research.

References

(1) Marcus, R. A. *Ann. Revs. Phys. Chem.* **1965**, *16*, 155.
(2) Reynolds, W. L.; Lumry, R. W. *Mechanisms of Electron Transfer*; Ronald: New York, 1966.
(3) Levich, V. G. *Adv. Electrochem. Electrochem. Eng.* **1966**, *4*, 249.
(4) Levich, V. G. In *Physical Chemistry, an Advanced Treatise*; Eyring, H., Henderson, D., Jost, W., Ed.; Academic: Orlando, FL, 1976.
(5) Dogonadze, R. R. In *Reactions of Molecules at Electrodes*; Hush, N. S., Ed.; Wiley: New York, 1971.
(6) Dogonadze, R. R.; Kuznetsov, A. M.; Maragishvili, T. A. *Electrochim. Acta* **1980**, *25*, 1–28.
(7) Schmidt, P. P. *Electrochemistry* **1975**, *5*, 21–131; **1978**, *6*, 128–241.
(8) Ulstrup, J. *Charge Transfer Processes in Condensed Media*; Springer: New York, 1979.
(9) Cannon, R. D. *Electron Transfer Reactions*; Butterworths: London, 1980.
(10) *Faraday Discuss. Chem. Soc.* **1982**, *74*.
(11) Prog. Inorg. Chem. **1983**, *30*.
(12) Jortner, J. *Biochim. Biophys. Acta* **1980**, *594*, 193.
(13) Guarr, T.; McLendon, G. *Coord. Chem. Rev.* **1985**, *68*, 1.
(14) Marcus, R. A.; Sutin, N. *Biochim. Biophys. Acta* **1985**, *811*, 265.
(15) DeVault, D. *Quantum-Mechanical Tunneling in Biological Systems*; Cambridge University: New York, 1984.
(16) Newton, M. D.; Sutin, N. *Ann. Rev. Phys. Chem.* **1984**, *35*, 437.
(17) Cristov, S. G. *Collision Theory and Statistical Theory of Chemical Reactions*; Springer: New York, 1980.
(18) *Tunneling in Biological Systems*; Chance, B., DeVault, D. C., Frauenfelder, H., Marcus, R. A., Schrieffer, J. R., Sutin, N., Eds.; Academic: New York, 1979.
(19) Sutin, N. In *Inorganic Biochemistry*; Eichhorn, G. L., Ed.; American Elsevier: New York, 1979; Vol. 2, p 611.
(20) Basolo, F.; Pearson, R. G. *Mechanisms of Inorganic Reactions*; Wiley: New York, 1967.
(21) Taube, H. *Electron Transfer Reactions in Solution*; Academic: New York, 1970. Richardson, D. E.; Taube, H. *Coord. Chem. Rev.* **1984**, *60*, 107.
(22) Pauling, L. In *Quantum Theory of Atoms, Molecules, and the Solid State*; Löwdin, P.-O., Ed.; Academic: New York, 1966.
(23) Brown, D. B. *Mixed-Valence Compounds*; Reidel: Dordrecht, 1980.
(24) Robin, M. B.; Day, P. *Adv. Inorg. Chem. Radiochem.* **1967**, *10*, 247.
(25) Cf., e.g.: Mott, N. *Metal–Insulator Transitions*; Taylor and Francis: London, 1974.
(26) Gennett, T.; Milner, D. F.; Weaver, M. J. *J. Phys. Chem.* **1985**, *29*, 2787.
(27) Miller, J. R.; Beitz, J. V.; Huddleston, R. K. *J. Am. Chem. Soc.* **1984**, *106*, 5057.
(28) Calef, D. F.; Wolynes, P. G. *J. Phys. Chem.* **1983**, *87*, 3387; *J. Chem. Phys.* **1983**, *78*, 470.
(29) Zusman, L. D. *Chem. Phys.* **1980**, *49*, 295.
(30) Tembe, B. L.; Friedman, H. L.; Newton, M. D. *J. Chem. Phys.* **1982**, *76*, 1490. Friedman, H. L.; Newton, M. D. *Faraday Discuss. Chem. Soc.* **1982**, *74*, 73.
(31) van der Zwan, G.; Hynes, J. T. *J. Chem. Phys.* **1982**, *76*, 2993.
(32) Bixon, M. *Faraday Discuss. Chem. Soc.* **1982**, *74*, 103.
(33) Alexandrov, I. V. *Chem. Phys.* **1980**, *51*, 449.
(34) Leland, B. A.; Joran, A. P.; Felker, P. M.; Hopfield, J. J.; Zewail, A. H.; Dervan, P. B. *J. Phys. Chem.* **1985**, *89*, 5571.
(35) Meyer, T. J. *Acc. Chem. Res.* **1978**, *11*, 94.
(36) Van Duyne, R. P., personal communication. Creutz, C.; Sutin, N. *J. Am. Chem. Soc.* **1977**, *99*, 241.
(37) Beitz, J. V.; Miller, J. R. *J. Chem. Phys.* **1979**, *71*, 4579.
(38) Huddleston, R. K.; Miller, J. R. *J. Phys. Chem.* **1981**, *85*, 2292.
(39) Beitz, J. V.; Miller, J. R. *Radiation Research, Proceedings International Congress, 6th*; Okada, S., Ed.; Toppan: Japan; 1979, p 301.
(40) Taube, H. In *Bioinorganic Chemistry II*; Raymond, K. N., Ed.; American Chemical Society: Washington, DC, 1976. Taube, H. *Pure Appl. Chem.* **1975**, *44*, 25. Isied, S.; Taube,

H. *J. Am. Chem. Soc.* **1973**, *95*, 8198. Richardson, D. E.; Taube, H. *J. Am. Chem. Soc.* **1983**, *105*, 40.
(41) Krogh-Jespersen, K.; Ratner, M. A. *Theoret. Chim. Acta* **1978**, *47*, 283.
(42) Linderberg, J.; Öhrn, Y. *Propagators in Quantum Chemistry*; Academic: London, 1973.
(43) Cf., e.g.: Heeger, A. J. In *Highly Conducting One-Dimensional Solids*; Devreese, J. T., Evrard, R. P., van Doren, V. E., Eds.; Plenum: New York, 1978.
(44) Stynes, H. C.; Ibers, J. A. *Inorg. Chem.* **1971**, *10*, 2304.
(45) Hush, N. S. *Prog. Inorg. Chem.* **1967**, *8*, 391.
(46) Siders, P.; Marcus, R. A. *J. Phys. Chem.* **1982**, *86*, 622; *J. Am. Chem. Soc.* **1981**, *103*, 741, 748.
(47) *Extended Linear Chain Compounds*; Miller, J. S., Ed.; Plenum: New York; Vol. 1–3.
(48) Schramm, C. J.; Stojakovic, D. R.; Hoffman, B. M.; Marks, T. J. *Science* **1978**, *200*, 47.
(49) Martinsen, J.; Palmer, S. M.; Tanaka, J.; Greene, R. C.; Hoffman, B. M. *Phys. Rev. B: Condens. Matter* **1984**, *B30*, 6259.
(50) Schramm, C. J.; Scaringe, R. P.; Stojakovic, D. R.; Hoffman, B. M.; Ibers, J. A.; Marks, T. J. *J. Am. Chem. Soc.* **1980**, *102*, 6702.
(51) Pietro, W. J.; Ellis, D. E.; Marks, T. J.; Ratner, M. A. *Mol. Cryst. Liq. Cryst.* **1984**, *105*, 273.
(52) Pietro, W. J.; Marks, T. J.; Ratner, M. A. *J. Am. Chem. Soc.* **1985**, *107*, 5387.
(53) Hale, P. D.; Ratner, M. A. *J. Chem. Phys.* **1985**, *83*, 5277.
(54) Hush, N. S. In *Mixed-Valence Compounds*; Brown, D. B., Ed.; Reidel: Dordrecht, **1980**; p 115.
(55) Wong, K. Y.; Schatz, P. N. *Prog. Inorg. Chem.* **1981**, *28*, 370.
(56) Ko, J.; Ondrechen, M. J. *Chem. Phys. Lett.* **1985**, *112*, 507.
(57) Hale, P. D.; Ratner, M. A.; Hofacker, G. L. *Chem. Phys. Lett.* **1985**, *119*, 264.
(58) Ratner, M. A. *Int. J. Quantum Chem.* **1978**, *14*, 675.
(59) Piepho, S. B.; Krausz, E. R.; Schatz, P. N. *J. Am. Chem. Soc.* **1979**, *101*, 2793.
(60) Libby, W. E. *J. Phys. Chem.* **1952**, *56*, 863.
(61) Ashcroft, N. W.; Mermin, N. D. *Solid State Physics*; Saunders College: Philadelphia, 1976.
(62) Cf., e.g.: *Mol. Cryst. Liq. Cryst.* **1985**, *118*(1–14).
(63) Ciliberto, E.; Doris, K. A.; Pietro, W. J.; Reisner, G. M.; Ellis, D. E.; Fragalà, I.; Herbstein, F. H.; Ratner, M. A.; Marks, T. J. *J. Am. Chem. Soc.* **1984**, *106*, 7748.
(64) Cheung, A. S.; Hush, N. S. *Chem. Phys. Lett.* **1977**, *47*, 1.
(65) Pople, J. A.; Walmsley, J. H. *Mol. Phys.* **1962**, *5*, 16.
(66) Su, W. P.; Schrieffer, J. R.; Heeger, A. J. *Phys. Rev. Lett.* **1979**, *42*, 1698.
(67) Bredas, J. L.; Street, G. B. *Acc. Chem. Res.* **1985**, *18*, 309, and references therein.
(68) Fincher, C. R.; Chen, C. E.; Heeger, A. J.; McDiarmid, A. G.; Hastings, J. G. *Phys. Rev. Lett.* **1982**, *48*, 102. Yannoni, C. S.; Clarke, T. C. *Phys. Rev. Lett.* **1983**, *51*, 1191. Boudeaux, D. S.; Chance, R. R.; Bredas, J. L.; Silbey, R. *Phys. Rev. B: Condens. Matter B28*, 6927. Thomann, H.; Dalton, L. R.; Tomkiewicz, Y.; Shiren, N. S.; Clarke, J. C. *Phys. Rev. Lett.* **1983**, *50*, 533.
(69) Landau, L. D. *Phys. Z. Sowjetunion* **1933**, 644. Landau, L. D.; Pekar, S. *Zh. Exp. Theor. Fiz.* **1946**, *16*, 341.
(70) Kuper, C. G.; Whitfield, G. D. *Polarons and Excitons*; Plenum: New York, 1963.
(71) Holstein, T. *Ann. Phys. (N.Y.)* **1959**, *8*, 325, 343.
(72) General references include: Gratzel, M. *Energy Resources Through Photochemistry and Catalysis*; Academic: New York, 1983. Fendler, J. H. *J. Phys. Chem.* **1985**, *89*, 2730, and references therein.
(73) For example: Morrison, S. R. *The Chemical Physics of Surfaces*; Plenum: New York, 1977.
(74) For example: Alkaitis, S. A.; Beck, G.; Gratzel, M. *J. Am. Chem. Soc.* **1975**, *97*, 5723.
(75) For example: Fox, M. A. *Acc. Chem. Res.* **1983**, *16*, 314.
(76) For example: Govindjee. *Bioenergetics of Photosynthesis*; Academic: New York, 1975. Sutin, N. *Prog. Inorg. Chem.* **1983**, *30*, 441.
(77) West, R.; Carberry, E. *Science* **1975**, *185*, 179. Wadsworth, C. L.; West, R.; Nagai, Y.; Watanabe, H. *Organometallics* **1985**, *4*, 1659. Berkovitch-Yellin, Z.; Ellis, D. E.; Ratner, M. A. *Chem. Phys.* **1981**, *62*, 21. Pitts, C. G. In *Homoatomic Rings, Chains and Macromolecules of Main-Group Elements*; Reingold, A., Ed.; Elsevier: Amsterdam, 1977. Ernst, C.; Allred, A. L.; Ratner, M. A. Ibid.
(78) For example: Emin, D. *J. Solid State Chem.* **1975**, *12*, 246. Spear, W. E. *Adv. Phys.* **1974**, *23*, 523. Emin, D. *Adv. Phys.* **1975**, *24*, 305.
(79) For example: Murray, R. W. *Annu. Rev. Mater. Sci.* **1984**, *14*, 145. Chidsey, C. E. D.; Murray, R. W. *Science* **1986**, *231*, 25, and references therein.
(80) For example: Wrighton, M. S. *Science* **1986**, *231*, 32, and references therein.
(81) Heller, A. *Science* **1984**, *223*, 1141.
(82) *Handbook of Conducting Polymers*; Skotheim, T., Ed.; Dekker: New York, in press.
(83) Domingue, R. P.; Fayer, M. D. *J. Chem. Phys.* **1985**, *83*, 2242.
(84) Inokuti, M.; Hirayama, F. *J. Chem. Phys.* **1965**, *43*, 1978.
(85) Dexter, D. C. *J. Chem. Phys.* **1953**, *21*, 836.
(86) Förster, T. *Naturwissenschaften* **1946**, *33*, 166; *Z. Naturforsch.* **1949**, *49*, 321.
(87) Chang, L. L.; Esaki, L.; Tsu, R. *Appl. Phys. Lett.* **1974**, *24*, 593.
(88) Sollner, T. C. L. G.; Tannewald, P. E.; Peck, D. D.; Goodhue, W. D. *Appl. Phys. Lett.* **1984**, *45*, 1319. Sollner, T. C. L. G.; Goodhue, W. D.; Tannewald, P. E.; Parker, C. D.; Peck, D. C. *Appl. Phys. Lett.* **1984**, *43*, 580.
(89) Capasso, F.; Mohammed, K.; Cho, A. Y. *I.E.D. Meeting of IEEE*, IEEE: Washington, DC, 1985; p 764. (a) Reed, M. A.; Lee, J. W.; Aldert, R. K.; Wetsel, A. E. *J. Mater. Res.* **1986**, *1*, 337.
(90) Rehm, D.; Weller, A. *Isr. J. Chem.* **1970**, *6*, 259. Fox, M.-A. *Adv. Photochem.* **1986**, *13*, 237.
(91) For example: *Tunneling Spectroscopy: Capabilities, Applications and New Techniques*; Hansma, P. K., Ed.; Plenum: New York, 1982. Wolf, E. D. *Principles of Electron Tunneling Spectroscopy*; Oxford: Oxford, 1985.
(92) Jaklevic, R. C.; Lambe, J. *Phys. Rev. Lett.* **1966**, *17*, 1139.
(93) Binnig, G.; Rohrer, H. *Physica B+C* **1984**, *127B*, 37. Binnig, G.; Rohrer, H. *Helv. Phys. Acta* **1982**, *55*, 726.
(94) Robinson, A. L. *Science*, **1981**, *229*, 1074. Golovchenko, J. A. *Science* **1986**, *232*, 48.
(95) Coleman, R. V.; Drake, B.; Hansma, P. K.; Slough, G. *Phys. Rev. Lett.* **1986**, *55*, 394.
(96) Feenstra, R. M.; Thomson, W. A.; Fein, A. P. cited in ref 94. Feenstra, R. M.; Oerlein, G. S. *Phys. Rev. B: Condens. Matter* **1985**, *B32*, 1394.
(97) Noufi, R.; Frank, A. J.; Nozik, A. J. *J. Am. Chem. Soc.* **1981**, *103*, 1849. Noufi, R.; Tench, D.; Warren, L. F. *J. Electrochem. Soc.* **1980**, *125*, 2310. Skotheim, T.; Lundstrom, I.; Prejza, J. *J. Electrochem. Soc.* **1981**, *128*, 1625. Fan, F. R. F.; Wheeler, B.; Bard, A. J. *J. Electrochem. Soc.* **1981**, *128*, 2042.
(98) Feldman, B. J.; Burgmeyer, P.; Murray, R. W. *J. Am. Chem. Soc.* **1985**, *107*, 872. Kittelsen, G. P.; White, H. S.; Wrighton, M. S. *J. Am. Chem. Soc.* **1984**, *106*, 7389. Simon, R. A.; Ricco, A. J.; Wrighton, M. S. *J. Am. Chem. Soc.* **1982**, *104*, 203.
(99) Diaz, A. *Chem. Scripta* **1981**, *17*, 145.
(100) Mikkelsen, K. V. Thesis, Århus University, 1985. Mikkelsen, K. V.; Dalgaard, E.; Swanstrøm, P., manuscript in preparation.
(101) Dolin, S. P.; Dogonadze, R. R.; German, E. D. *J. Chem. Soc., Faraday Trans. 1* **1977**, *73*, 649.
(102) Newton, M. D. *ACS Symp. Ser.* **1982**, *189*, 254.
(103) Newton, M. D. *Int. J. Quantum Chem. Symp.* **1980**, *14*, 363.
(104) Ulstrup, J.; Jortner, J. *J. Chem. Phys.* **1975**, *63*, 4358.
(105) Kestner, N. R.; Logan, J.; Jortner, J. *J. Phys. Chem.* **1974**, *78*, 2148.
(106) Brocklehurst, B. *J. Phys. Chem.* **1979**, *83*, 536.
(107) Sutin, N. *Prog. Inorg. Chem.* **1983**, *30*, 441.
(108) Sutin, N.; Brunschwig, B. S. *ACS Symp. Ser.* **1982**, *198*, 255.
(109) Van Duyne, R. P.; Fischer, S. F. *Chem. Phys.* **1974**, *5*, 183; *Chem. Phys.* **1977**, *26*, 9.
(110) Schmidt, P. P. *J. Chem. Soc., Faraday 2* **1973**, *69*, 1104. Duke, C. B.; Meyer, R. J. *Phys. Rev. B: Condens. Matter* **1981**, *B23*, 2118.
(111) Kirkwood, J. G. *J. Chem. Phys.* **1934**, *2*, 351.
(112) Kirkwood, J. G.; Westheimer, F. H. *J. Chem. Phys.* **1938**, *6*, 506.
(113) Marcus, R. A. *J. Chem. Phys.* **1956**, *24*, 966, 979; **1965**, *43*, 679.
(114) Rataczak, H.; Orville-Thomas, W. J. *Molecular Interactions*; Wiley: New York, 1982.
(115) *Quantum Theory of Chemical Reactivity*; Daudel, R., Salem, L., Pullman, B., Veillard, A., Eds.; Reidel: Dordrecht, 1980; Vol. 2.
(116) Dogonadze, R. R.; Kornishev, A. A. *Phys. Status Solidi B* **1972**, *B53*, 439; *J. Chem. Soc., Faraday 2* **1974**, *70*, 1121.
(117) Salem, L. *Electrons in Chemical Reactions: First Principles*; Wiley: New York, 1982.
(118) Levich, V. G.; Dogonadze, R. R. *Collect. Czech. Chem. Commun.* **1961**, *26*, 193.
(119) Hush, N. S. In *Mixed-Valence Compounds*; Brown, D. B., Ed.; Reidel: Dordrecht, 1980; p 151.
(120) Löwdin, P. O. *J. Chem. Phys.* **1950**, *18*, 365.
(121) Hush, N. S. *Trans. Faraday Soc.* **1961**, *57*, 557; *Electrochim. Acta* **1968**, *13*, 1005.
(122) Sutin, N. *Annu. Rev. Nucl. Sci.* **1962**, *12*, 285.
(123) Brunschwig, B. S.; Logan, J.; Newton, M. D.; Sutin, N. *J. Am. Chem. Soc.* **1980**, *102*, 5798.
(124) Reitz, J. R.; Milfod, F. J.; Christy, R. W. *Foundations of Electromagnetic Theory*; Addison-Wesley: Reading, 1979. Jackson, J. D. *Classical Electrodynamics*; Wiley: New York, 1964.

(125) Dogonadze, R. R.; Kuznetsov, A. M. *Elektrokhimiya*, **1967**, *2*, 1324.
(126) Dogonadze, R. R.; Kuznetsov, A. M.; Levich, V. G. *Electrochim. Acta* **1968**, *13*, 1025.
(127) Vorotyntsev, M. A.; Dogonadze, R. R.; Kuznetsov, A. M. *Dokl. Akad. Nauk SSSR* **1970**, *195*, 1135.
(128) Webman, I.; Kestner, N. R. *J. Phys. Chem.* **1979**, *83*, 451.
(129) Kuznetsov, A. M. *Nouv. J. Chim.* **1981**, *5*, 427; *Elektrokhimiya* **1982**, *18*, 594, 598, 736.
(130) Kuznetsov, A. M.; Ulstrup, *J. Phys. Status Solidi B* **1982**, *114*, 673.
(131) Hornburger, H.; Kono, H.; Lin, S. H. *J. Chem. Phys.* **1984**, *81*, 3554.
(132) Kudinov, E. K.; Firsov, T. A. *Sov. Phys. Solid State* **1965**, *7*, 435.
(133) Zener, C. *Proc. Roy. Soc. London* **1932**, *A137*, 696. Stueckelberg, E. G. *Helv. Phys. Acta* **1932**, *5*, 370. Landau, L. D. *Phys. Zeits. Sowjetunion* **1932**, *1*, 88.
(134) Nikitin, E. E. *Theory of Elementary Atomic and Molecular Processes in Gases*; Clarendon: Oxford, 1974; pp 99–178.
(135) Fischer, S. F. *J. Chem. Phys.* **1970**, *53*, 3195.
(136) Schlag, E. W.; Schneider, S.; Fischer, S. F. *Annu. Rev. Phys. Chem.* **1971**, *22*, 465.
(137) Lax, M. *J. Chem. Phys.* **1952**, *20*, 1752. O'Rourke, R. C. *Phys. Rev.* **1953**, *91*, 265.
(138) Sewell, G. L. *Phys. Rev.* **1963**, *129*, 597.
(139) Lee, T. D.; Low, F.; Pines, D. *Phys. Rev.* **1953**, *90*, 297.
(140) Creutz, C.; Taube, H. *J. Am. Chem. Soc.* **1969**, *91*, 3988; *J. Am. Chem. Soc.* **1973**, *95*, 1086.
(141) Fürholz, U.; Burgi, H. B.; Wasner, F. E.; Stabler, A.; Ammeter, J. H.; Krausz, E.; Clark, R. J. H.; Stead, M. J.; Ludi, A. *J. Am. Chem. Soc.* **1984**, *106*, 121.
(142) Hale, P. D.; Ratner, M. A. *Int. J. Quant. Chem. Symp.* **1984**, *18*, 195.
(143) Goodenough, J. *J. Appl. Phys.* **1966**, *37*, 1415.
(144) Jortner, J. *J. Chem. Phys.* **1976**, *64*, 4860.
(145) Scher, H.; Holstein, T. *Philos.* Mag. *B* **1981**, *B44*, 343. Holstein, T. *Philos. Mag. B* **1978**, *B37*, 49.
(146) Rackovski, S.; Scher, H. *Biochim. Biophys. Acta* **1982**, *681*, 152.
(147) Hopfield, J. J. *Proc. Natl. Acad. Sci. U.S.A.* **1974**, *71*, 3640.
(148) Redi, M.; Hopfield, J. J. *J. Chem. Phys.* **1980**, *82*, 6651.
(149) For example: Herring, C. *Magnetism*; Rado, G. T., Suhl, H., Eds.; Academic: New York, 1966; Vol. 4.
(150) Richardson, D. E.; Taube, H. *J. Am. Chem. Soc.* **1983**, *105*, 40.
(151) Haberkorn, R.; Michel-Beyerle, M. E.; Marcus, R. A. *Proc. Natl. Acad. Sci. U.S.A.* **1979**, *76*, 4185.
(152) Okamura, M. Y.; Fredkin, D. R.; Isaacson, R. A.; Feher, G., in ref 18, p 729.
(153) Logan, J.; Newton, M. D. *J. Chem. Phys.* **1983**, *78*, 4086.
(154) Ondrechen, M. J.; Ratner, M. A.; Ellis, D. E. *Chem. Phys. Lett.* **1984**, *109*, 50.
(155) Whangbo, M.-H. In *Extended Linear Chain Compounds*; Miller, J. S., Ed.; Plenum: New York, 1982, Vol. 2, p 127. Böhm, M. C. *Solid State Commun.* **1983**, *45*, 117. Whangbo, M.-H.; Stewart, K. R. *Isr. J. Chem.* **1983**, *23*, 133. Canadell, E.; Alvarez, S. *Inorg. Chem.* **1984**, *73*, 573.
(156) Larsson, S. *J. Am. Chem. Soc.* **1981**, *103*, 4034. Larsson, S. *J. Phys. Chem.* **1984**, *88*, 1321.
(157) Larsson, S. *Chem. Phys. Lett.* **1982**, *90*, 136.
(158) Larsson, S. *J. Chem. Soc., Faraday Trans. 2* **1983**, *79*, 1375.
(159) Stein, C. A.; Lewis, N. W.; Seitz, G.; Baker, A. D. *Inorg. Chem.* **1983**, *22*, 1124.
(160) Beratan, D. N.; Hopfield, J. J. *J. Am. Chem. Soc.* **1984**, *106*, 1584.
(161) Delley, B.; Ellis, D. E. *J. Chem. Phys.* **1982**, *76*, 1749.
(162) Kusunoki, M., submitted for publication in *J. Chem. Phys.*
(163) Igawa, A.; Fukutome, H. *Prog. Theor. Phys.* **1980**, *64*, 1980.
(164) Halpern, J.; Orgel, L. E. *Discuss. Faraday Soc.* **1960**, *29*, 32.
(165) McConnell, H. M. *J. Chem. Phys.* **1961**, *35*, 508.
(166) Hoffmann, R. *Acc. Chem. Res.* **1973**, *4*, 1.
(167) Miller, J. R.; Beitz, J. V. *J. Chem. Phys.* **1981**, *74*, 6746.
(168) Ratner, M. A.; Ondrechen, M. J. *Mol. Phys.* **1976**, *32*, 1223.
(169) Aviram, A.; Ratner, M. A. *Chem. Phys. Lett.* **1974**, *29*, 277.
(170) For example: Schiff, L. I. *Quantum Mechanics*; McGraw-Hill: New York, 1981; Chap. 8.
(171) Beratan, D. N., submitted for publication in *J. Am. Chem. Soc.*
(172) Löwdin, P.-O. *J. Math. Phys.* **1962**, *3*, 969; *J. Mol. Spectros.* **1963**, *10*, 12.
(173) Linderberg, J.; Ratner, M. A. *J. Am. Chem. Soc.* **1981**, *103*, 3265.
(174) Marcus, R. A. *J. Chem. Phys.* **1966**, *45*, 4493. Hofacker, G. L.; Levine, R. D. *Chem. Phys. Lett.* **1971**, *9*, 617. Fischer, S. F.; Ratner, M. A. *J. Chem. Phys.* **1972**, *57*, 276–279.
(175) Efrima, S.; Bixon, M. *J. Chem. Phys.* **1979**, *70*, 3531.
(176) Helman, A. B. *Chem. Phys.* **1983**, *79*, 235.
(177) Kramers, H. A. *Physica* **1940**, *7*, 284.
(178) Carmeli, B.; Nitzan, A. *J. Chem. Phys.* **1984**, *80*, 3596.
(179) Grote, R. F.; Hynes, J. T. *J. Chem. Phys.* **1980**, *73*, 2715.
(180) Montgomery, J. A.; Chandler, D.; Berne, B. J. *J. Chem. Phys.* **1979**, *70*, 6056.
(181) Matkowsky, B. J.; Schuss, Z.; Ben-Jacob *SIAM J. Appl. Math.* **1982**, *42*, 835.
(182) Allinger, K.; Carmeli, B.; Chandler, D. E. *J. Chem. Phys.* **1986**, *84*, 1724.
(183) Allinger, K.; Ratner, M. A., manuscript in preparation.
(184) Creutz, C.; Kroger, A.; Matsubara, T.; Netzel, T. L.; Sutin, N. *J. Am. Chem. Soc.* **1979**, *101*, 5442. (a) Garg, A.; Onuchic, J. N.; Ambegaokar, V. *J. Chem. Phys.* **1985**, *83*, 4491. (b) Agmon, N.; Hopfield, J. J. *J. Chem. Phys.* **1983**, *78*, 6947; **1983**, *79*, 2042.
(185) Hupp, J. T.; Weaver, M. J. *J. Phys. Chem.* **1985**, *89*, 1601, 2795.
(186) Weaver, M. J.; Gennett, T. *Chem. Phys. Lett.* **1985**, *113*, 213.
(187) Ratner, M. A.; Madhukar, A. *Chem. Phys.* **1978**, *30*, 201.
(188) Siders, P.; Cave, R. T.; Marcus, R. A. *J. Chem. Phys.* **1984**, *81*, 563.
(189) Gutfreund, H.; Weger, M. *Phys. Rev. B: Solid State* **1978**, *16*, 1753.
(190) Conwell, E. M. *Phys. Rev. B: Condens. Matter* **1980**, *B22*, 1761.
(191) Williams, G.; Watts, D. C. *Trans. Faraday Soc.* **1970**, *66*, 80.
(192) Shore, J. E.; Zwanzig, R. *J. Chem. Phys.* **1975**, *63*, 5445. Skinner, J. E. *J. Chem. Phys.* **1983**, *79*, 1955.
(193) Brawer, S. A. *J. Chem. Phys.* **1984**, *80*, 954.
(194) Birks, J. B. *Photophysics of Aromatic Molecules*; Wiley: New York, 1970.
(195) Davydov, A. S. *Physica* **1981**, *30*, 1.
(196) Davydov, A. S.; Zolotariuk, A. V. *Phys. Scr.* **1984**, *30*, 426.
(197) Davydov, A. S. *Solitons in Molecular Systems*; Reidel: Dordrecht, 1985.
(198) Davydov, A. S.; Gaididei, Yu. B. *Phys. Status Solidi* **1985**, *B132*, 189.
(199) Fischer, S. F.; Venzl, G. In *Photoreaktive Festkörper*; Sixl, H., Ed.; M. Wahl Verlag: Karlsruhe, 1984; p 723. Fischer, S. F.; Heiden, N. **1985**, preprint.
(200) Fischer, S. F.; Nussbaum, I.; Scherer, P. O. J. In *Antennas and Reaction Centers of Photosynthetic Bacteria*; Michel-Beyerle, M. E., Ed.; Springer: Berlin; p 256.
(201) Scherer, P. O. J.; Knapp, E. V.; Fischer, S. F. *Chem. Phys. Lett.* **1984**, *106*, 191.
(202) Venzl, G.; Fischer, S. F. *J. Chem. Phys.* **1984**, *81*, 6090.
(203) Glauber, R. *Phys. Rev.* **1963**, *137*, 2766.
(204) Dalgaard, E. *J. Phys.* **1976**, *B9*, 2573.
(205) Mikkelsen, K. V.; Ratner, M. A., work in progress.
(206) Miller, J. R.; Peeples, J. A.; Schmidt, M. J.; Closs, G. L. *J. Am. Chem. Soc.* **1982**, *104*, 6488.
(207) Perrin, F. *C. R. Hebd. Seances Acad. Sci.* **1924**, *178*, 1978.
(208) Miller, J. R.; Hartman, K. W.; Abrash, S. *J. Am. Chem. Soc.* **1982**, *104*, 4296.
(209) Sadovski, N. A.; Kuzunin, M. G. *Dokl Phys. Chem.* (*Engl. Transl.*) **1975**, *222*, 643.
(210) Namiki, A.; Nakashima, N.; Yoshihara, K. *J. Chem. Phys.* **1979**, *71*, 925.
(211) Fiksel, A. I.; Parmon, V. N.; Zamaraev, K. I. *Chem. Phys.* **1982**, *69*, 135.
(212) Emori, S.; Weri, D.; Wan, J. K. S. *Chem. Phys. Lett.* **1981**, *84*, 512.
(213) Brickenstein, E. Kh.; Ivanov, G. K.; Kozhushner, M. A.; Khairutdirov, R. F. *Chem. Phys.* **1984**, *91*, 133.
(214) Strauch, S.; McLendon, G.; McGuire, M.; Guarr, T. *J. Phys. Chem.* **1983**, *87*, 3579; *J. Am. Chem. Soc.* **1983**, *105*, 616.
(215) Guarr, T.; McGuire, M. E.; McLendon, G. *J. Am. Chem. Soc.* **1985**, *107*, 5104. (a) McGuire, M.; McLendon, G. *J. Phys. Chem.* **1986**, *90*, 2549. (b) Milosavljevic, B. H.; Thomas, J. K. *J. Am. Chem. Soc.* **1986**, *108*, 2513.
(216) Tachiya, M.; Mozumder, A. *Chem. Phys. Lett.* **1974**, *28*, 87.
(217) Miller, J. R. *Science* **1975**, *189*, 221.
(218) Grand, D.; Bernas, A. *J. Phys. Chem.* **1977**, *81*, 1209.
(219) Kira, A.; Nosaka, Y.; Imamura, M. *J. Phys. Chem.* **1980**, *84*, 1882.
(220) Kira, A. *J. Phys. Chem.* **1981**, *85*, 3647.
(221) DeVault, D.; Chance, B. *Biophys. J.* **1966**, *6*, 825.
(222) Kihara, T.; Chance, B. *Biochim. Biophys. Acta* **1969**, *189*, 116.
(223) McGourty, J. L.; Blough, N. V.; Hoffman, B. M. *J. Am. Chem. Soc.* **1983**, *105*, 4470.
(224) Peterson-Kennedy, S. E.; McGourty, J. L.; Hoffman, B. M. *J. Am. Chem. Soc.* **1984**, *106*, 5010.

(225) Peterson-Kennedy, S. E.; McGourty, J. L.; Ho, P. S.; Sutoris, C. J.; Liang, N.; Zemel, H.; Blough, N. Y.; Margoliash, E.; Hoffman, B. M. *Coord. Chem. Rev.* **1985**, *64*, 125.
(226) Peterson-Kennedy, S. E.; McGourty, J. L.; Kalweit, J. A.; Hoffman, B. M. *J. Am. Chem. Soc.* **1986**, *108*, 1739.
(227) Liang, N.; Kang, C. H.; Margoliash, E.; Ho, P.-S.; Hoffman, B. M. *J. Am. Chem. Soc.* **1986**, *108*, 4665.
(228) Overfield, R. E.; Scherz, A.; Kaufman, K. J.; Wasielewski, M. R. *J. Am. Chem. Soc.* **1983**, *105*, 5747.
(229) Siemiarczuk, A.; McIntosh, A. R.; Ho, T.-F.; Stillman, M. J.; Roach, K.; Weedon, A. C.; Bolton, J. R.; Connolly, J. S. *J. Am. Chem. Soc.* **1983**, *105*, 7224.
(230) Kong, J. L. Y.; Spears, K. G.; Loach, P. A. *Photochem. Photobiol.* **1982**, *35*, 545.
(231) Kong, J. L. Y.; Loach, P. A. *J. Heterocycl. Chem.* **1980**, *17*, 737.
(232) Loach, P. A.; Runquist, J. A.; Kong, J. L. Y.; Dannhauser, T. J.; Spears, K. G. *Adv. Chem. Ser.* **1982**, *201*, 515.
(233) For example: Nocera, D. G.; Winkler, J. R.; Yocom, K. M.; Bordignon, E.; Gray, H. B. *J. Am. Chem. Soc.* **1984**, *106*, 5145. Crutchley, R. J.; Ellis, W. R.; Gray, H. B. *J. Am. Chem. Soc.* **1985**, *107*, 5092.
(234) For example: Isied, S. S.; Kuehn, C.; Worsila, G. *J. Am. Chem. Soc.* **1984**, *106*, 1722.
(235) McLendon, G.; Miller, J. R. *J. Am. Chem. Soc.* **1985**, *107*, 2811.
(236) Kinoshita, S.; Miyokawa, K.; Wakita, H.; Masuda, I. *Polyhedron* **1983**, *2*, 125.
(237) Ihara, Y.; Uehara, A.; Tsuchiya, R.; Kyuno, E. *Bull. Chem. Soc. Jpn.* **1978**, *51*, 2578. (a) Closs, C. L.; Calcaterra, L. T.; Green, N. J.; Penfield, K. W.; Miller, J. R. *J. Phys. Chem.* **1986**, *90*, 3673.
(238) Heitele, H.; Michel-Beyerle, M. E. *J. Am. Chem. Soc.* **1985**, *107*, 8286.
(239) Hush, N. S.; Paddon-Row, M. N.; Cotsaris, E.; Oevering, H.; Verhoeven, J. W.; Heppener, M. *Chem. Phys. Lett.* **1985**, *117*, 8.
(240) Day, P. *Int. Rev. Phys. Chem.* **1981**, *1*, 149.
(241) Rosseinsky, D. R.; Tonge, J. S. *J. Chem. Soc., Faraday Trans. 1* **1982**, *78*, 3595.
(242) Oh, S. M.; Hendrickson, D. N.; Hassett, K. L.; Davis, R. E. *J. Am. Chem. Soc.* **1984**, *106*, 7984.
(243) Oh, S. M.; Kambara, T.; Hendrickson, D. N.; Sorai, M.; Kaji, K.; Woehler, S. E.; Wittebort, R. J. *J. Am. Chem. Soc.* **1985**, *107*, 5540.
(244) Dong, T. Y.; Hendrickson, D. N.; Iwai, K.; Cohn, M. J.; Geib, S. J.; Rheingold, A. L.; Sano, H.; Motoyama, I.; Nakashima, S. *J. Am. Chem. Soc.* **1985**, *107*, 7996.
(245) Oh, S. M.; Hendrickson, D. N.; Hasset, K. L.; Davis, R. E. *J. Am. Chem. Soc.* **1985**, *107*, 8009. Woehler, S. E.; Wittebort, R. J.; Oh, S. M.; Hendrickson, D. N.; Inniss, D.; Strouse, C. E. *J. Am. Chem. Soc.* **1986**, *108*, 2938.
(246) Ham, F. S. In *Electron Paramagnetic Resonance*; Geschwind, S., Ed.; Plenum: New York, 1972; p 1.
(247) Sturge, M. D. *Solid State Phys.* **1967**, *20*, 91.
(248) Hoffman, B. M.; Ratner, M. A. *Mol. Phys.* **1978**, *35*, 901.
(249) Dong, T. Y.; Hendrickson, R. N.; Pierpont, C. G.; Moore, M. F. *J. Am. Chem. Soc.* **1986**, *108*, 963.
(250) Meyer, T. J.; Schanze, K. S. *Inorg. Chem.* **1986**, *24*, 2123.
(251) Zwanzig, R., 1986, personal communication. Zwanzig, R., 1986, work in progress.
(252) Beratan, D. N.; Hopfield, J. J. *J. Chem. Phys.* **1984**, *81*, 5753.
(253) Phillips, P. *J. Chem. Phys.* **1986**, *84*, 986.
(254) Phillips, P.; Silbey, R., submitted for publication in *J. Chem. Phys.*
(255) Objections to the arguments of ref 252 have been raised by Freed [Freed, K. F. *J. Chem. Phys.* **1986**, *84*, 2108]. Freed argues that the hamiltonian of ref 252 is oversimplified with too simple a description (one mode) of the vibrational manifold. It is also true that the classically based energy conservation arguments of ref 252 must be treated very cautiously in a multimode quantum system.
(256) The hamiltonian used in ref 252, 253 is a generalization of one used previously [by: Harris, R. A.; Silbey, R. *J. Chem. Phys.* **1983**, *78*, 7330] for protonic motions. The extension to electronic behavior is problematic however partly because it involves [Phillips, P., 1986, personal communication] a continuous coordinate representation of the electron, partly because the application of the Leggett–Caldeira scheme to this problem is not straightforward; there is no experimental evidence, as yet, for the predicted $\exp\{-\alpha r - \beta r^2\}$ behavior of the transfer.
(257) When $\Delta E^\circ = 0$, $E_A = \lambda/4$; λ itself is the optical,[121] not the thermal, activation energy.